



US011203569B2

(12) **United States Patent**
Almarsson et al.

(10) **Patent No.: US 11,203,569 B2**
(45) **Date of Patent: Dec. 21, 2021**

(54) **CRYSTAL FORMS OF AMINO LIPIDS**

(71) Applicant: **ModernaTX, Inc.**, Cambridge, MA (US)

(72) Inventors: **Orn Almarsson**, Cambridge, MA (US);
Eugene Cheung, Cambridge, MA (US)

(73) Assignee: **ModernaTX, Inc.**, Cambridge, MA (US)

(*) Notice: Subject to any disclaimer, the term of this patent is extended or adjusted under 35 U.S.C. 154(b) by 60 days.

(21) Appl. No.: **16/493,789**

(22) PCT Filed: **Mar. 15, 2018**

(86) PCT No.: **PCT/US2018/022740**

§ 371 (c)(1),

(2) Date: **Sep. 13, 2019**

(87) PCT Pub. No.: **WO2018/170322**

PCT Pub. Date: **Sep. 20, 2018**

(65) **Prior Publication Data**

US 2020/0131116 A1 Apr. 30, 2020

Related U.S. Application Data

(60) Provisional application No. 62/471,908, filed on Mar. 15, 2017.

(51) **Int. Cl.**

C07C 229/24 (2006.01)

C07C 55/07 (2006.01)

C07C 65/03 (2006.01)

C07C 227/16 (2006.01)

C07C 229/12 (2006.01)

(52) **U.S. Cl.**

CPC **C07C 229/24** (2013.01); **C07C 55/07** (2013.01); **C07C 65/03** (2013.01); **C07C 227/16** (2013.01); **C07C 229/12** (2013.01); **C07B 2200/13** (2013.01)

(58) **Field of Classification Search**

CPC combination set(s) only.

See application file for complete search history.

(56) **References Cited**

U.S. PATENT DOCUMENTS

3,872,171 A 3/1975 Cronin et al.
4,125,544 A 11/1978 Dygos
4,957,735 A 9/1990 Huang
5,807,861 A 9/1998 Klein et al.
6,143,276 A 11/2000 Unger
6,303,378 B1 10/2001 Bridenbaugh et al.
6,395,253 B2 5/2002 Levy et al.
6,652,886 B2 11/2003 Ahn et al.
6,696,038 B1 2/2004 Mahato et al.
7,268,120 B1 9/2007 Horton et al.
7,371,404 B2 5/2008 Panzner et al.
7,943,168 B2 5/2011 Schlesinger et al.
8,058,069 B2 11/2011 Yaworski et al.

8,158,601 B2 4/2012 Chen et al.
8,420,123 B2 4/2013 Troiano et al.
8,440,614 B2 5/2013 Castor
8,449,916 B1 5/2013 Bellaire et al.
8,450,298 B2 5/2013 Mahon et al.
8,460,696 B2 6/2013 Slobodkin et al.
8,460,709 B2 6/2013 Ausborn et al.
8,563,041 B2 10/2013 Grayson et al.
8,568,784 B2 10/2013 Lillard et al.
8,569,256 B2 10/2013 Heyes et al.
8,580,297 B2 11/2013 Essler et al.
8,603,499 B2 12/2013 Zale et al.
8,603,500 B2 12/2013 Zale et al.
8,603,501 B2 12/2013 Zale et al.
8,603,534 B2 12/2013 Zale et al.
8,603,535 B2 12/2013 Troiano et al.
8,609,142 B2 12/2013 Troiano et al.
8,613,951 B2 12/2013 Zale et al.
8,613,954 B2 12/2013 Zale et al.
8,617,608 B2 12/2013 Zale et al.
8,618,240 B2 12/2013 Podobinski et al.
8,637,083 B2 1/2014 Troiano et al.
8,642,076 B2 2/2014 Manoharan et al.

(Continued)

FOREIGN PATENT DOCUMENTS

AU 652831 B2 9/1994
CN 102068701 A 5/2011

(Continued)

OTHER PUBLICATIONS

Dong et al., "Lipopeptide nanoparticles for potent and selective siRNA delivery in rodents and nonhuman primates," PNAS, Mar. 2014, vol. 111, No. 11, 3955-3960; 5753-5754.

Hashiba et al., "pH-labile PEGylation of siRNA-loaded lipid nanoparticle improves active targeting and gene silencing activity in hepatocytes," Journal of Controlled Release (2017) vol. 262, 239-246.

Jaiswal et al., "Nanostructured lipid carriers and their current application in targeted drug delivery," Artificial Cells, Nanomedicine, and Biotechnology (2016) 44: 27-40.

Mohtar et al., "Solid Lipid Nanoparticles of Atovaquone Based on 24 Full-Factorial Design," Iranian Journal of Pharmaceutical Research (2015) 14(4): 989-1000.

Ramteke, K. H. et al., "Solid Lipid Nanoparticle: A Review," IOSR Journal of Pharmacy, Nov.-Dec. 2012, 2(60): 34-44.

(Continued)

Primary Examiner — Heidi Reese

(74) *Attorney, Agent, or Firm* — Cooley LLP; Heidi A. Erlacher; Christine C. Pemberton

(57) **ABSTRACT**

Provided herein are novel solid forms of each of four compounds: (1) heptadecan-9-yl 8-((2-hydroxyethyl)amino) octanoate ("Compound 1"), (2) heptadecan-9-yl 8-((2-hydroxyethyl)(6-oxo-6-(undecyloxy)hexyl)amino)octanoate ("Compound 2"), (3) heptadecan-9-yl 8-((2-hydroxyethyl)(8-(nonyloxy)-8-oxooctyl)amino)octanoate ("Compound 3"), and (6Z,9Z,28Z,31Z)-heptatriaconta-6,9,28,31-tetraen-19-yl 4-(dimethylamino)butanoate ("MC3"), and related compositions and methods.

20 Claims, 31 Drawing Sheets

(56)

References Cited

U.S. PATENT DOCUMENTS

8,652,487	B2	2/2014	Maldonado	2013/0183375	A1	7/2013	Schutt et al.
8,652,528	B2	2/2014	Troiano et al.	2013/0189351	A1	7/2013	Geall
8,663,599	B1	3/2014	Sung et al.	2013/0195759	A1	8/2013	Mirkin et al.
8,663,700	B2	3/2014	Troiano et al.	2013/0195765	A1	8/2013	Gho et al.
8,668,926	B1	3/2014	Mousa et al.	2013/0195967	A1	8/2013	Guild et al.
8,685,368	B2	4/2014	Reineke	2013/0195968	A1	8/2013	Geall et al.
8,691,750	B2	4/2014	Constein et al.	2013/0195969	A1	8/2013	Geall et al.
8,697,098	B2	4/2014	Perumal et al.	2013/0202684	A1	8/2013	Geall et al.
8,703,204	B2	4/2014	Bloom et al.	2013/0236500	A1	9/2013	Zale et al.
8,709,483	B2	4/2014	Farokhzad et al.	2013/0236533	A1	9/2013	Von Andrian et al.
8,715,736	B2	5/2014	Sachdeva et al.	2013/0236550	A1	9/2013	Ausborn et al.
8,715,741	B2	5/2014	Maitra et al.	2013/0243827	A1	9/2013	Troiano et al.
8,728,527	B2	5/2014	Singh	2013/0243848	A1	9/2013	Lobovkina et al.
8,734,832	B2	5/2014	O'Hagan et al.	2013/0243867	A1	9/2013	Mohapatra et al.
8,734,846	B2	5/2014	Ali et al.	2013/0251766	A1	9/2013	Zale et al.
8,734,853	B2	5/2014	Sood et al.	2013/0251816	A1	9/2013	Zale et al.
8,802,644	B2	8/2014	Chen et al.	2013/0251817	A1	9/2013	Zale et al.
9,006,487	B2	4/2015	Anderson et al.	2013/0266617	A1	10/2013	Mirosevich et al.
9,029,590	B2	5/2015	Colletti et al.	2013/0273117	A1	10/2013	Podobinski et al.
9,394,234	B2	7/2016	Chen et al.	2013/0274504	A1	10/2013	Colletti et al.
9,717,690	B2	8/2017	Guild et al.	2013/0274523	A1	10/2013	Bawiec, III et al.
9,738,593	B2	8/2017	Ansell et al.	2013/0280334	A1	10/2013	Karp et al.
9,867,888	B2	1/2018	Benenato	2013/0280339	A1	10/2013	Zale et al.
9,868,691	B2*	1/2018	Benenato A61K 38/1725	2013/0295183	A1	11/2013	Troiano et al.
9,868,692	B2	1/2018	Benenato	2013/0295191	A1	11/2013	Troiano et al.
9,868,693	B2	1/2018	Benenato	2013/0302432	A1	11/2013	Zale et al.
10,106,490	B2	10/2018	Du	2013/0302433	A1	11/2013	Troiano et al.
10,166,298	B2	1/2019	Ansell et al.	2013/0315831	A1	11/2013	Shi et al.
10,392,341	B2	8/2019	Benenato et al.	2013/0330401	A1	12/2013	Payne et al.
10,799,463	B2	10/2020	Benenato et al.	2013/0338210	A1	12/2013	Manoharan et al.
10,857,105	B2	12/2020	Benenato et al.	2013/0344158	A1	12/2013	Zale et al.
2003/0073619	A1	4/2003	Mahato et al.	2014/0017327	A1	1/2014	Cheng et al.
2003/0092653	A1	5/2003	Kisich et al.	2014/0017329	A1	1/2014	Mousa
2004/0142474	A1	7/2004	Mahato et al.	2014/0037573	A1	2/2014	Eliasof et al.
2005/0222064	A1	10/2005	Vargeese et al.	2014/0037660	A1	2/2014	Folin-Mleczek et al.
2006/0008910	A1	1/2006	Maclachlan et al.	2014/0037714	A1	2/2014	Quay et al.
2006/0083780	A1	4/2006	Heyes et al.	2014/0039032	A1	2/2014	Kumboyama et al.
2006/0172003	A1	8/2006	Meers et al.	2014/0044772	A1	2/2014	Maclachlan et al.
2006/0204566	A1	9/2006	Smyth-Templeton et al.	2014/0044791	A1	2/2014	Basilion et al.
2007/0252295	A1	11/2007	Panzner et al.	2014/0045913	A1	2/2014	Kumboyama et al.
2009/0042825	A1	2/2009	Matar et al.	2014/0050775	A1	2/2014	Slobodkin et al.
2009/0042829	A1	2/2009	Matar et al.	2014/0057109	A1	2/2014	Mechen et al.
2011/0009641	A1	1/2011	Anderson et al.	2014/0065172	A1	3/2014	Echeverri et al.
2011/0200582	A1	8/2011	Baryza et al.	2014/0065204	A1	3/2014	Hayes et al.
2011/0244026	A1	10/2011	Guild et al.	2014/0065228	A1	3/2014	Yarowoski et al.
2012/0136073	A1	5/2012	Yang et al.	2014/0079774	A1	3/2014	Brinker et al.
2012/0177724	A1	7/2012	Irvine et al.	2014/0093575	A1	4/2014	Hammond et al.
2012/0178702	A1	7/2012	Huang	2014/0093579	A1	4/2014	Zale et al.
2012/0226085	A1	9/2012	Ishihara et al.	2014/0113137	A1	4/2014	Podobinski et al.
2012/0295832	A1	11/2012	Constien et al.	2014/0121263	A1	5/2014	Fitzgerald et al.
2013/0017223	A1	1/2013	Hope et al.	2014/0121393	A1	5/2014	Manoharan et al.
2013/0064894	A1	3/2013	Martin et al.	2014/0134260	A1	5/2014	Heyes et al.
2013/0065942	A1	3/2013	Matar et al.	2014/0141070	A1	5/2014	Geall et al.
2013/0090372	A1	4/2013	Budzik et al.	2014/0141089	A1	5/2014	Liang
2013/0108685	A1	5/2013	Kuboyama et al.	2014/0141483	A1	5/2014	Bossard et al.
2013/0115273	A1	5/2013	Yang et al.	2014/0142165	A1	5/2014	Grayson et al.
2013/0115274	A1	5/2013	Knopov et al.	2014/0142254	A1	5/2014	Fonnum et al.
2013/0116307	A1	5/2013	Heyes et al.	2014/0161830	A1	6/2014	Anderson et al.
2013/0122104	A1	5/2013	Yaworski et al.	2014/0308304	A1	10/2014	Manoharan et al.
2013/0123338	A1	5/2013	Heyes et al.	2015/0174260	A1	6/2015	Yang et al.
2013/0129785	A1	5/2013	Manoharan et al.	2015/0174261	A1	6/2015	Kuboyama et al.
2013/0130348	A1	5/2013	Gu et al.	2015/0239926	A1	8/2015	Payne et al.
2013/0142868	A1	6/2013	Hoekman et al.	2015/0284317	A1	10/2015	Colletti et al.
2013/0142876	A1	6/2013	Howard et al.	2015/0343062	A1	12/2015	Kuboyama et al.
2013/0150625	A1	6/2013	Budzik et al.	2015/0376115	A1	12/2015	Ansell et al.
2013/0156845	A1	6/2013	Manoharan et al.	2016/0002178	A1	1/2016	Fenton et al.
2013/0156849	A1	6/2013	de Fougerolles et al.	2016/0009657	A1	1/2016	Anderson et al.
2013/0164400	A1	6/2013	Knopov et al.	2016/0151284	A1	6/2016	Heyes et al.
2013/0171241	A1	7/2013	Geall	2017/0119904	A1	5/2017	Ansell et al.
2013/0172406	A1	7/2013	Zale et al.	2018/0201572	A1	7/2018	Benenato
2013/0178541	A1	7/2013	Stanton et al.	2018/0273467	A1	9/2018	Benenato
2013/0183244	A1	7/2013	Hanes et al.	2018/0303925	A1	10/2018	Weissman et al.
2013/0183355	A1	7/2013	Jain et al.	2018/0333366	A1	11/2018	Benenato et al.
2013/0183372	A1	7/2013	Schutt et al.	2018/0369419	A1	12/2018	Benenato et al.
2013/0183373	A1	7/2013	Schutt et al.	2019/0016669	A1	1/2019	Benenato et al.
				2019/0314292	A1	10/2019	Benenato et al.
				2019/0314524	A1	10/2019	Ansell et al.
				2019/0336452	A1	11/2019	Brader et al.

(56)

References Cited

U.S. PATENT DOCUMENTS

2020/0069599 A1 3/2020 Smith et al.
 2020/0129445 A1 4/2020 Patel
 2021/0087135 A1 3/2021 Benenato et al.

FOREIGN PATENT DOCUMENTS

CN 102204920 A 10/2011
 CN 102813929 A 12/2012
 CN 104644555 A 5/2015
 EP 737750 10/1996
 EP 1404860 B1 5/2002
 EP 2073848 B1 8/2013
 JP 2000-169864 A 6/2000
 WO WO 1993/014778 8/1993
 WO WO 1999/014346 A2 3/1999
 WO WO 1999/052503 10/1999
 WO WO 1999/54344 A1 10/1999
 WO WO 2003/086280 10/2003
 WO WO 2005/034979 A2 4/2005
 WO WO 2006/063249 A2 6/2006
 WO WO 2008/042973 A2 4/2008
 WO WO 2009/024599 2/2009
 WO WO 2009/053686 A1 4/2009
 WO WO 2009/086558 A1 7/2009
 WO WO 2009/127060 A1 10/2009
 WO WO 2009/129385 A1 10/2009
 WO WO 2009/129395 A1 10/2009
 WO WO 2010/030739 A1 3/2010
 WO WO 2010/042877 A1 4/2010
 WO WO 2010/053572 A2 5/2010
 WO WO 2010/054406 A1 5/2010
 WO WO 2010/088537 A2 8/2010
 WO WO 2010/129709 A1 11/2010
 WO WO 2011/058990 A1 5/2011
 WO WO 2011/068810 A1 6/2011
 WO WO 2011/127255 A1 10/2011
 WO WO 2012/000104 A1 1/2012
 WO WO 2012/006376 A2 1/2012
 WO WO 2012/006378 A1 1/2012
 WO WO 2012/030901 A1 3/2012
 WO WO 2012/031043 A1 3/2012
 WO WO 2012/031046 A2 3/2012
 WO WO 2012/054365 A2 4/2012
 WO WO 2012/129483 A1 9/2012
 WO WO 2012/149252 A2 11/2012
 WO WO 2012/149255 A2 11/2012
 WO WO 2012/149265 A2 11/2012
 WO WO 2012/149282 A2 11/2012
 WO WO 2012/149301 A2 11/2012
 WO WO 2012/149376 A2 11/2012
 WO WO 2012/149393 A2 11/2012
 WO WO 2012/153338 A2 11/2012
 WO WO 2012/170889 A1 12/2012
 WO WO 2012/170930 A1 12/2012
 WO WO 2013/006825 A1 1/2013
 WO WO 2013/006834 A1 1/2013
 WO WO 2013/006837 A1 1/2013
 WO WO 2013/006838 A1 1/2013
 WO WO 2013/006842 A2 1/2013
 WO WO 2013/016058 A1 1/2013
 WO WO 2013/033438 A2 3/2013
 WO WO 2013/033563 A1 3/2013
 WO WO 2013/036835 A1 3/2013
 WO WO 2013/049328 A1 4/2013
 WO WO 2013/052167 A2 4/2013
 WO WO 2013/056132 A2 4/2013
 WO WO 2013/057715 A1 4/2013
 WO WO 2013/059496 A1 4/2013
 WO WO 2013/059922 A1 5/2013
 WO WO 2013/064911 A2 5/2013
 WO WO 2013/066903 A1 5/2013
 WO WO 2013/067537 A1 5/2013
 WO WO 2013/070872 A2 5/2013
 WO WO 2013/072929 A2 5/2013
 WO WO 2013/086322 A1 6/2013

WO WO 2013/086354 A1 6/2013
 WO WO 2013/086373 A1 6/2013
 WO WO 2013/086526 A1 6/2013
 WO WO 2013/087083 A1 6/2013
 WO WO 2013/087791 A1 6/2013
 WO WO 2013/093648 A2 6/2013
 WO WO 2013/135359 A1 9/2013
 WO WO 2013/143555 A1 10/2013
 WO WO 2013/143683 A1 10/2013
 WO WO 2013/148186 A1 10/2013
 WO WO 2013/148541 A1 10/2013
 WO WO 2013/149141 A1 10/2013
 WO WO 2013/151650 A1 10/2013
 WO WO 2013/155487 A1 10/2013
 WO WO 2013/155493 A9 10/2013
 WO WO 2013/158127 A1 10/2013
 WO WO 2013/158579 A1 10/2013
 WO WO 2013/166498 A1 11/2013
 WO WO 2013/173693 A1 11/2013
 WO WO 2013/177419 A2 11/2013
 WO WO 2013/177421 A2 11/2013
 WO WO 2013/185069 A1 12/2013
 WO WO 2014/007398 A1 1/2014
 WO WO 2014/008334 A1 1/2014
 WO WO 2014/026284 A1 2/2014
 WO WO 2014/028487 A1 2/2014
 WO WO 2014/028763 A1 2/2014
 WO WO 2014/047649 A1 3/2014
 WO WO 2014/052634 A1 4/2014
 WO WO 2014/054026 A1 4/2014
 WO WO 2014/071072 A2 5/2014
 WO WO 2014/072997 A1 5/2014
 WO WO 2014/089486 A1 6/2014
 WO WO 2014/144196 A1 9/2014
 WO WO 2014/160243 A1 10/2014
 WO WO 2014/172045 A1 10/2014
 WO WO 2011/136368 A1 11/2014
 WO WO 2014/182661 A2 11/2014
 WO WO 2014/210356 A1 12/2014
 WO WO 2015/011633 A1 1/2015
 WO WO 2015/130584 A2 9/2015
 WO WO 2015/154002 A1 10/2015
 WO WO 2015/199952 A1 12/2015
 WO WO 2016/004202 A1 1/2016
 WO WO 2016/004318 A1 1/2016
 WO WO 2016/118697 A1 7/2016
 WO WO 2016/118724 A1 7/2016
 WO WO 2016/176330 A1 11/2016
 WO WO 2017/015630 A2 1/2017
 WO WO 2017/031232 A1 2/2017
 WO WO 2017/049245 A2 3/2017
 WO WO 2017/070616 A2 4/2017
 WO WO 2017/070626 A1 4/2017
 WO WO 2017/075531 A1 5/2017
 WO WO 2017/099823 A1 6/2017
 WO WO 2017/100744 A1 6/2017
 WO WO 2017/112865 A1 6/2017
 WO WO 2017/127750 A1 7/2017
 WO WO 2017/180917 A2 10/2017
 WO WO 2017/192470 A1 11/2017
 WO WO 2017/201317 A1 11/2017
 WO WO 2017/201325 A1 11/2017
 WO WO 2017/201328 A1 11/2017
 WO WO 2017/201332 A1 11/2017
 WO WO 2017/201333 A1 11/2017
 WO WO 2017/201340 A2 11/2017
 WO WO 2017/201342 A1 11/2017
 WO WO 2017/201346 A1 11/2017
 WO WO 2017/201347 A1 11/2017
 WO WO 2017/201348 A1 11/2017
 WO WO 2017/201349 A1 11/2017
 WO WO 2017/201350 A1 11/2017
 WO WO 2017/201352 A1 11/2017
 WO WO 2017/218704 A1 12/2017
 WO WO 2018/078053 A1 5/2018
 WO WO 2018/081480 A1 5/2018
 WO WO 2018/081638 A1 5/2018
 WO WO 2018/089540 A1 5/2018
 WO WO 2018/170260 A1 9/2018

(56)

References Cited

FOREIGN PATENT DOCUMENTS

WO	WO 2018/170270	A1	9/2018
WO	WO 2018/170306	A1	9/2018
WO	WO 2018/170336	A1	9/2018
WO	WO 2018/191719	A1	10/2018
WO	WO 2018/232120	A1	12/2018
WO	WO 2019/046809	A1	3/2019
WO	WO 2019/089828	A1	5/2019
WO	WO 2019/152557	A1	8/2019
WO	WO 2019/193183	A2	10/2019
WO	WO 2019/202035	A1	10/2019
WO	WO 2020/002525	A1	1/2020
WO	WO 2020/061457	A1	3/2020
WO	WO 2020/123300	A2	6/2020

OTHER PUBLICATIONS

Sabnis et al., "A Novel Amino Lipid Series for mRNA Delivery: Improved Endosomal Escape and Sustained Pharmacology and Safety in Non-human Primates," *Molecular Therapy*, Jun. 2018, vol. 26, No. 6, pp. 1509-1519.

Yadava, P. et al., "Effect of Lyophilization and Freeze-thawing on the Stability of siRNA-liposome Complexes," *AAPS PharmSciTech*, Jun. 2008, 9(2): 335-341.

Abdelwahed et al., "Freeze-drying of nanoparticles: Formulation, process and storage considerations," *Advanced Drug Delivery Reviews* 58 (2006) 1688-1713.

Akinc et al., Development of Lipidoid-siRNA Formulations for Systemic Delivery to the Liver, *Molecular Therapy*, May 2009, vol. 17, No. 5, pp. 872-879.

Akinc et al., Targeted Delivery of RNAi Therapeutics With Endogenous and Exogenous Ligand-Based Mechanisms, *Mol Ther.* 2010 18(7):1357-1364.

Anderson, D.M. et al., Stability of mRNA/cationic lipid lipoplexes in human and rat cerebrospinal fluid: methods and evidence for nonviral mRNA gene delivery to the central nervous system. *Hum Gene Ther.* Feb. 10, 2003;14(3):191-202.

Andries, O., et al., Comparison of the gene transfer efficiency of mRNA/GL67 and pDNA/GL67 complexes in respiratory cells. *Mol Pharmaceutics.* 2012; 9: 2136-2145.

Ashizawa et al., "Liposomal delivery of nucleic acid-based anti-cancer therapeutics: BP-100-1.01," *Expert Opin. Drug Deliv.*, (2014) 12(7):1107-1120.

Bag, J., Recovery of normal protein synthesis in heat-shocked chicken myotubes by liposome-mediated transfer of mRNAs. *Can. J. Biochem. Cell Biol.* 1985; 63(3): 231-235.

Belliveau, N.M., et al., Microfluidic synthesis of highly potent limit-size lipid nanoparticles for in vivo delivery of siRNA. *Mol Ther Nucleic Acids.* Aug. 2012; 1(8): e37.

Bettinger, T. et al., Peptide-mediated RNA delivery: a novel approach for enhanced transfection of primary and post-mitotic cells. *Nucleic Acids Res.* Sep. 15, 2001;29(18):3882-91.

Bolhassani A., et al., Improvement of Different Vaccine Delivery Systems For Cancer Therapy, *Molecular Cancer, Biomed Central*, London, GB, 2011, vol. 10, No. 3, pp. 1-20.

Bonehill, A., et al., Single-step antigen loading and activation of dendritic cells by mRNA electroporation for the purpose of therapeutic vaccination in melanoma patients. *Clin Cancer Res.* May 2009; 15(10): 3366-3375.

Boussein, N.F., et al., Structure and gene silencing activities of monovalent and pentavalent cationic lipid vectors complexed with siRNA. *Biochem.* 2007; 46(16): 4785-4792.

Chen, D., et al., Rapid discovery of potent siRNA-containing lipid nanoparticles enabled by controlled microfluidic formulation. *J Am Chem Soc.* 2012; 134: 6948-6951.

Chen, S. et al., "Development of lipid nanoparticle formulations of siRNA for hepatocyte gene silencing following subcutaneous administration," *J Control Release*, 2014, 196, 106-112.

Cun, Dongmei, et al., Preparation and characterization of poly(DL-lactide-co-glycolide) nanoparticles for siRNA delivery. *International Journal of Pharmaceutics* 390 (2010) 70-75.

Dahlman, James E. et al., In vivo endothelial siRNA delivery using polymeric nanoparticles with low molecular weight, *Nature Nanotechnology*, 2014, No. vol.#, pp. 1-8.

Delehanty, James B., Peptides for Specific Intracellular Delivery and Targeting of Nanoparticles: Implications for Developing Nanoparticle-Mediated Drug Delivery, *Future Science, Therapeutic Delivery*, 2010, vol. 1, No. 3, pp. 411-433.

El Ouahabi, A., et al., Double long-chain amidine liposome-mediated self replicating RNA transfection. *FEBS Letters.* Feb. 1996; 380(1-2): 108-112.

Felgner, PL Cationic lipid/polynucleotide condensates for in vitro and in vivo polynucleotide delivery—the cytofectins. *J. of Liposome Research.* 1993; 3(1): 3-16.

Felgner, PL Particulate systems and polymers for in vitro and in vivo delivery of polynucleotides. *Adv. Drug Delivery Rev.* 1990; 5(3): 163-187.

Felgner, PL, et al., Lipofection: a highly efficient, lipid-mediated DNA-transfection procedure. *Proc Natl Acad Sci U SA.* Nov. 1987;84(21):7413-7.

Gao, X. et al., Nonviral gene delivery: what we know and what is next. *AAPS J.* Mar. 23, 2007;9(1):E92-104.

Geall et al., Nonviral delivery of self-amplifying RNA vaccines. *Proc Natl Acad Sci U S A.* Sep. 4, 2012;109(36):14604-9. doi:10.1073/pnas.1209367109. Epub Aug. 20, 2012.

He, K. et al., Synthesis and Separation of Diastereomers of Ribonucleoside 5'-(alpha-P-Borano)triphosphates. *J Org Chem.* Aug. 21, 1998;63(17):5769-5773.

Hecker, J.G. et al., Non-Viral DNA and mRNA Gene Delivery to the CNS Pre-Operatively for Neuroprotection and Following Neurotrauma. *Molecular Therapy.* 2004; 9, S258-S258.

Hoerr, I. et al., In vivo application of RNA leads to induction of specific cytotoxic T lymphocytes and antibodies. *EurJ Immunol.* Jan. 2000;30(1):1-7.

Jayaraman et al., "Maximizing the Potency of siRNA Lipid Nanoparticles for Hepatic Gene Silencing In Vivo," *Angew. Chem. Int. Ed.* 2012, 51, 8529-8533.

Juliano, R.L., et al., Cell-targeting and cell-penetrating peptides for delivery of therapeutic and imaging agents. *Wiley Interdisciplinary Reviews: Nanomedicine and Nanobiotechnology.* May/June. 2009; 1(3): 324-335.

Kang, Hyunmin, Inhibition of MDR1 Gene Expression by Chimeric HNA Antisense Oligonucleotides, *Nucleic Acids Research*, 2004, vol. 32, No. 14, pp. 4411-4419.

Kariko et al., Phosphate-enhanced transfection of cationic lipid-complexed mRNA and plasmid DNA. *Biochimica et Biophysica Acta.* 1998. 1369:320-34.

Kariko, K., et al., In vivo protein expression from mRNA delivered into adult rat brain. *J. of Neuroscience Methods.* Jan. 2001; 105(1): 77-86.

Kariko, K., et al., Incorporation of pseudouridine into mRNA yields superior nonimmunogenic vector with increased translational capacity and biological stability, *Molecular Therapy, Nature Publishing Group, GB*, vol. 16, No. 11, Nov. 1, 2008 (Nov. 1, 2008), pp. 1833-1840.

Keown, Wa, et al., Methods for Introducing DNA into Mammalian Cells. *Methods in Enzymology*, 1990, 185:527-37.

Kirpotin, D.B., et al., Antibody targeting of long-circulating lipidic nanoparticles does not increase tumor localization but does increase internalization in animal models. *Cancer Res.* 2006; 66: 6732-6740.

Kozielski, Kristen L. et al., Bioreducible Cationic Polymer-Based Nanoparticles for Efficient and Environmentally Triggered Cytoplasmic siRNA Delivery to Primary Human Brain Cancer Cells, *ACS Nano*, 2014, vol. 8, No. 4, pp. 3232-3241.

Lai, S.K., et al., Mucus-penetrating nanoparticles for drug and gene delivery to mucosal tissues. *Adv Drug Deliv Rev.* Feb. 27, 2009; 61(2): 158-171.

Lai, S.K., et al., Rapid transport of large polymeric nanoparticles in fresh undiluted human mucus. *PNAS.* Jan. 30, 2007; 104(5): 1482-1487.

(56)

References Cited

OTHER PUBLICATIONS

- Lee, Justin B. et al., Lipid Nanoparticle siRNA Systems for Silencing The Androgen Receptor In Human Prostate Cancer in Vivo, *International Journal of Cancer*, 2012, vol. 131, pp. 781-790.
- Lehto, T., et al., Cell-penetrating peptides for the delivery of nucleic acids. *Expert Opin. Drug Deliv.* Jul. 2012; 9(7): 823-836.
- Leung et al., "Lipid Nanoparticles for Short Interfering RNA Delivery", *Advances in Genetics*, vol. 88, Chapter 4, pp. 71-110.
- Lewis, David, Dynamic Polyconjugates (DPC) Technology: An elegant solution to the siRNA delivery problem. Arrowhead Research Corp (NASDAQ: ARWR). Nov. 2011.
- Lewis, R., et al., "Studies of the Thermotropic Phase Behavior of Phosphatidylcholines Containing 2-Alkyl Substituted Fatty Alkyl Chains: A New Class of Phosphatidylcholines Forming Inverted Nonlamellar Phases," *Biophysical Journal*, Apr. 1994, vol. 66, pp. 1088-1103.
- Li, L. et al., Overcoming obstacles to develop effective and safe siRNA therapeutics. *Expert Opin Biol Ther.* May 2009; 9(5): 609-19.
- Li, L. et al., Preparation and gene delivery of alkaline amino acids-based cationic liposomes. *Arch Pharm Res.* Jul. 2008;31(7):924-31. Epub Aug. 14, 2008.
- Lian, T. et al., Trends and developments in liposome drug delivery systems. *J Pharm Sci.* Jun. 2001;90(6):667-80.
- Lopez-Berestein, G. et al., Treatment of systemic fungal infections with liposomal amphotericin B. *Arch Intern Med.* Nov. 1989;149(11):2533-6.
- Love et al., Lipid-like materials for low-dose, in vivo gene silencing, *PNAS* vol. 107 No. 5, pp. 1864-1869, Feb. 2, 2010.
- M. Kanapathipillai, et al., Nanoparticle targeting of anti-cancer drugs that alter intracellular signaling or influence the tumor microenvironment, *Adv. Drug Deliv. Rev.* (2014), , pp. 1-12.
- Magee, W. E. et al., Marked stimulation of lymphocyte-mediated attack on tumor cells by target-directed liposomes containing immune RNA, *Cancer Res.*, 1978, 38(4):1173-6.
- Malone, R.W. et al., Cationic liposome-mediated RNA transfection. *Proc Natl Acad Sci U S A.* Aug. 1989;86 (16):6077-81.
- Martinon, F. et al., Induction of virus-specific cytotoxic T lymphocytes in vivo by liposome-entrapped mRNA. *Eur J Immunol.* Jul. 1993;23(7):1719-22.
- Maskarinec et al., "Direct Observation of Poloxamer 188 Insertion into Lipid Monolayers," *Biophys J.*, Mar. 2002, vol. 82, 1453-1459.
- Maurer, N., et al., Spontaneous entrapment of polynucleotides upon electrostatic interaction with ethanol-destabilized cationic liposomes. *Biophys J.* May 2001; 80(5): 2310-2326.
- Midoux et al., Lipid-based mRNA vaccine delivery systems. *Expert Rev Vaccines.* Feb. 2015;14(2):221-34. doi: 10.1586/14760584.2015.986104. Epub Dec. 26, 2014. Review.
- Mishra, R.K. et al., Improved leishmanicidal effect of phosphorothioate antisense oligonucleotides by LDL-mediated delivery. *Biochim Biophys Acta.* Nov. 7, 1995;1264(2):229-37.
- Mockey et al., mRNA-based cancer vaccine: prevention of B16 melanoma progression and metastasis by systemic injection of MART1 mRNA histidylated lipopolyplexes, *Cancer Gene Therapy*, 2007, 14, pp. 802-814.
- Morissette et al., "High-throughput crystallization: polymorphs, salts, co-crystals and solvates of pharmaceutical solids," *Advanced Drug Delivery Reviews* 56 (2004) 275-300.
- Müller et al., "Solid lipid nanoparticles (SLN) for controlled drug delivery—a review of the state of the art," *European Journal of Pharmaceutics and Biopharmaceutics*, 50 (2000) 161-177.
- Nair, S. et al., Soluble proteins delivered to dendritic cells via pH-sensitive liposomes induce primary cytotoxic T lymphocyte responses in vitro. *J Exp Med.* Feb. 1, 1992;175(2):609-12.
- Okumura, K., et al., Bax mRNA therapy using cationic liposomes for human malignant melanoma. *J Gene Med.* 2008; 10: 910-917.
- Oster, C.G., et al. Comparative study of DNA encapsulation into PLGA microparticles using modified double emulsion methods and spray drying techniques. *Journal of Microencapsulation*, May 2005; 22(3): 235-244.
- Parker et al., Targeting of Polyelectrolyte RNA Complexes to Cell Surface Integrins as an Efficient, Cytoplasmic Transfection Mechanism, *Journal of Bioactive and Compatible Polymers*, Jul. 2002, pp. 1-10.
- Pollard, C., et al., Type I IFN counteracts the induction of antigen-specific immune responses by lipid-based delivery of mRNA vaccines. *Mol Ther.* Jan. 2013; 21(1): 251-259.
- Pulford, B., et al., Liposome-siRNA-peptide complexes cross the blood-brain barrier and significantly decrease PrP^C on neuronal cells and PrP^{RES} in infected cell cultures. *PLoS ONE.* 2010; 5(6): e11085.
- Sahay, G. et al., "Efficiency of siRNA delivery by lipid nanoparticles is limited by endocytic recycling," *Nat Biotechnol.* Jul. 2013 ; 31(7): 653-658.
- Saito, R., et al., Distribution of liposomes into brain and rat brain tumor models by convection-enhanced delivery monitored with magnetic resonance imaging. *Cancer Res.* Apr. 2004; 64: 2572-2579.
- Sakuma, S. et al., Mucoadhesion of polystyrene nanoparticles having surface hydrophilic polymeric chains in the gastrointestinal tract. *Int J Pharm.* Jan. 25, 1999;177(2):161-72.
- Schott, J.W., et al., Viral and non-viral approaches for transient delivery of mRNA and proteins. *Current Gene Ther.* 2011; 11 (5): 382-398.
- Semple, S.C., et al., Efficient encapsulation of antisense oligonucleotides in lipid vesicles using ionizable aminolipids: formation of novel small multilamellar vesicle structures. *Biochim Biophys Acta.* Feb. 9, 2001; 1510(1-2): 152-166.
- Shah et al., "Lipid Nanoparticles: Production, Characterization and Stability," Springer International Publishing, 2014, 23 pages.
- Shea, R.G. et al., Synthesis, hybridization properties and antiviral activity of lipid-oligodeoxynucleotide conjugates. *Nucleic Acids Res.* Jul. 11, 1990;18(13):3777-83.
- Strobel, I. et al., Human dendritic cells transfected with either RNA or DNA encoding influenza matrix protein M1 differ in their ability to stimulate cytotoxic T lymphocytes. *Gene Ther.* Dec. 2000; 7(23): 2028-2035.
- Svinarchuk, F.P. et al., Inhibition of HIV proliferation in MT-4 cells by antisense oligonucleotide conjugated to lipophilic groups. *Biochimie.* 1993;75(1-2):49-54.
- Tam et al., "Advances in Lipid Nanoparticles for siRNA Delivery," *Pharmaceutics* 2013, 5, 498-507; doi:10.3390/pharmaceutics5030498.
- Tavernier, G., et al., mRNA as gene therapeutic: How to control protein expression. *J. of Controlled Release.* Mar. 2011; 150(3): 238-247.
- Thess et al., Sequence-engineered mRNA Without Chemical Nucleoside Modifications Enables an Effective Protein Therapy in Large Animals. *Mol Ther.* Sep. 2015;23(9):1456-64. doi: 10.1038/mt.2015.103. Epub Jun. 8, 2015.
- Torchilin, Vladimir et al., Multifunctional and Stimuli-Sensitive Pharmaceutical Nanocarriers, *Eur J. Pharm Biopharm*, 2009, vol. 71, No. 3, pp. 431-444.
- Tracy, M., "Progress in the Development of LNP Delivery for siRNA Advancing LNPs to the Clinic," *International Liposome Research Days Meeting*, Vancouver, Canada. Aug. 2010, pp. 1-52.
- Treat, J. et al., in *Liposomes in the Therapy of Infectious Disease and Cancer*, Lopez-Berestein and Fidler (eds.), Liss, New York, 1989. 353-65.
- Uzgun, S., et al., PEGylation improves nanoparticle formation and transfection efficiency of messenger RNA. *Pharm Res.* Sep. 2011; 28(9); 2223-2232.
- Van Tendeloo, V.F. et al., Highly efficient gene delivery by mRNA electroporation in human hematopoietic cells: superiority to lipofection and passive pulsing of mRNA and to electroporation of plasmid cDNA for tumor antigen loading of dendritic cells. *Blood.* Jul. 1, 2001;98(1):49-56.
- Wan et al., Lipid nanoparticle delivery systems for siRNA-based therapeutics. *Drug Deliv Transl Res.* Feb. 2014;4(1):74-83. doi:10.1007/s13346-013-0161-z.
- Wang et al., Systemic delivery of modified mRNA encoding herpes simplex virus 1 thymidine kinase for targeted cancer gene therapy. *Mol Ther.* Feb. 2013;21(2):358-67. doi: 10.1038/mt.2012.250. Epub Dec. 11, 2012.

(56)

References Cited

OTHER PUBLICATIONS

Weilhammer et al., The use of nanolipoprotein particles to enhance the immunostimulatory properties of innate immune agonists against lethal influenza challenge. *Biomaterials*. Dec. 2013;34(38):10305-18. doi: 10.1016/j.biomaterials.2013.09.038. Epub Sep. 27, 2013.

Yamamoto et al., Current prospects for mRNA gene delivery, *European Journal of Pharmaceutics and Biopharmaceutics* 71 (2009) 484-489.

Zhang et al., "A novel cationic cardiolipin analogue for gene delivery," *Pharmazie*, 2006, 61: 10-14).

Zhigaltsev, I.V., et al., Bottom-Up design and synthesis of limit size lipid nanoparticle systems with aqueous and triglyceride cores using millisecond microfluidic mixing. *Langmuir*. Feb. 21, 2012; 28(7): 3633-3640.

Zimmermann, E. et al., Electrolyte- and pH-stabilities of aqueous solid lipid nanoparticle (SLN™) dispersions in artificial gastrointestinal media. *Eur J Pharm Biopharm*. Sep. 2001;52(2):203-10.

Zohra, F.T., et al., Drastic effect of nanoapatite particles on liposome-mediated mRNA delivery to mammalian cells. *Analytical Biochem*. Oct. 2005; 345(1): 164-166.

Zohra, F.T., et al., Effective delivery with enhanced translational activity synergistically accelerates mRNA-based transfection. *Biochem Biophys Res Comm*. Jun. 2007; 358(1): 373-378.

* cited by examiner

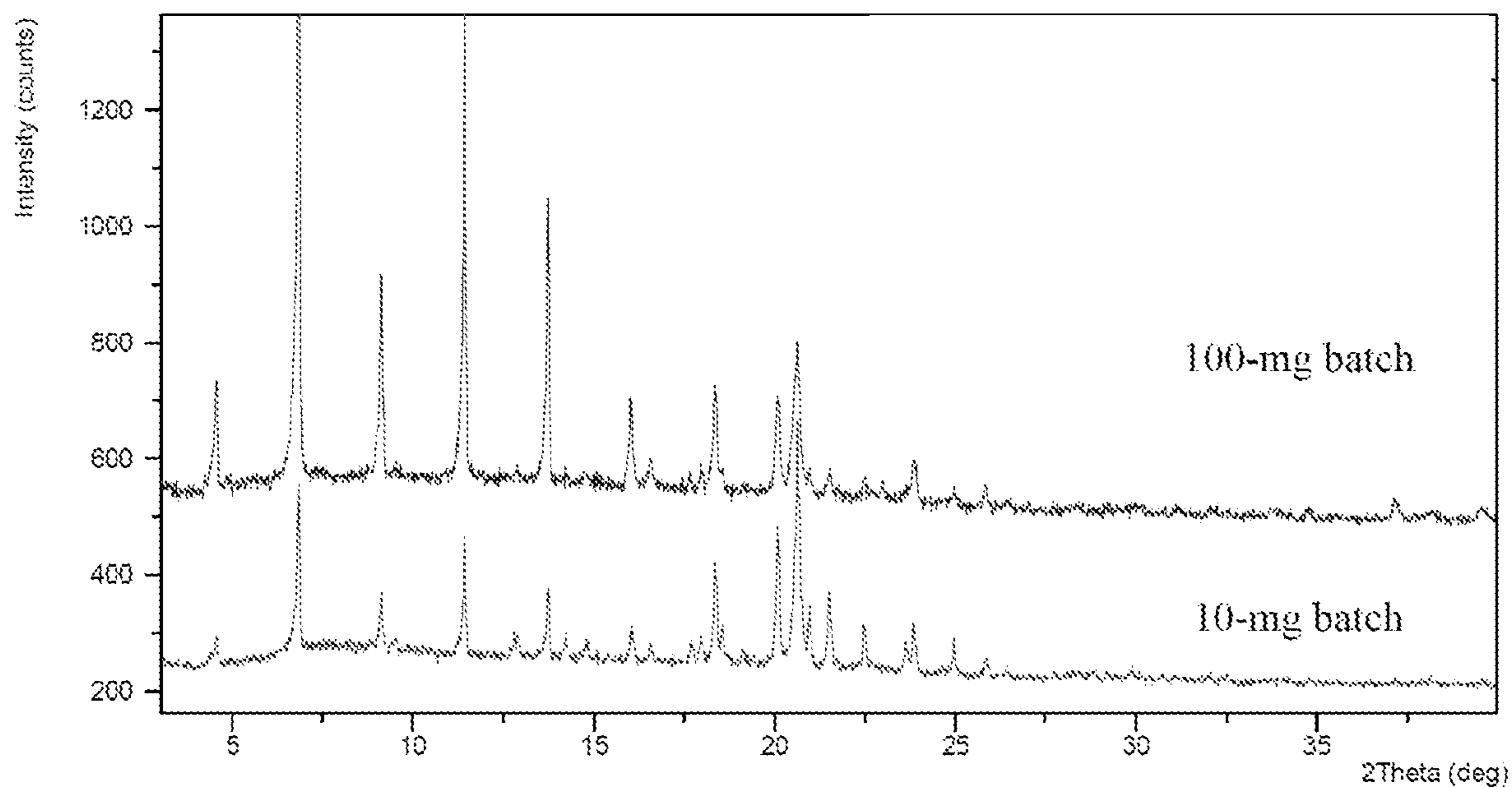


Figure 1

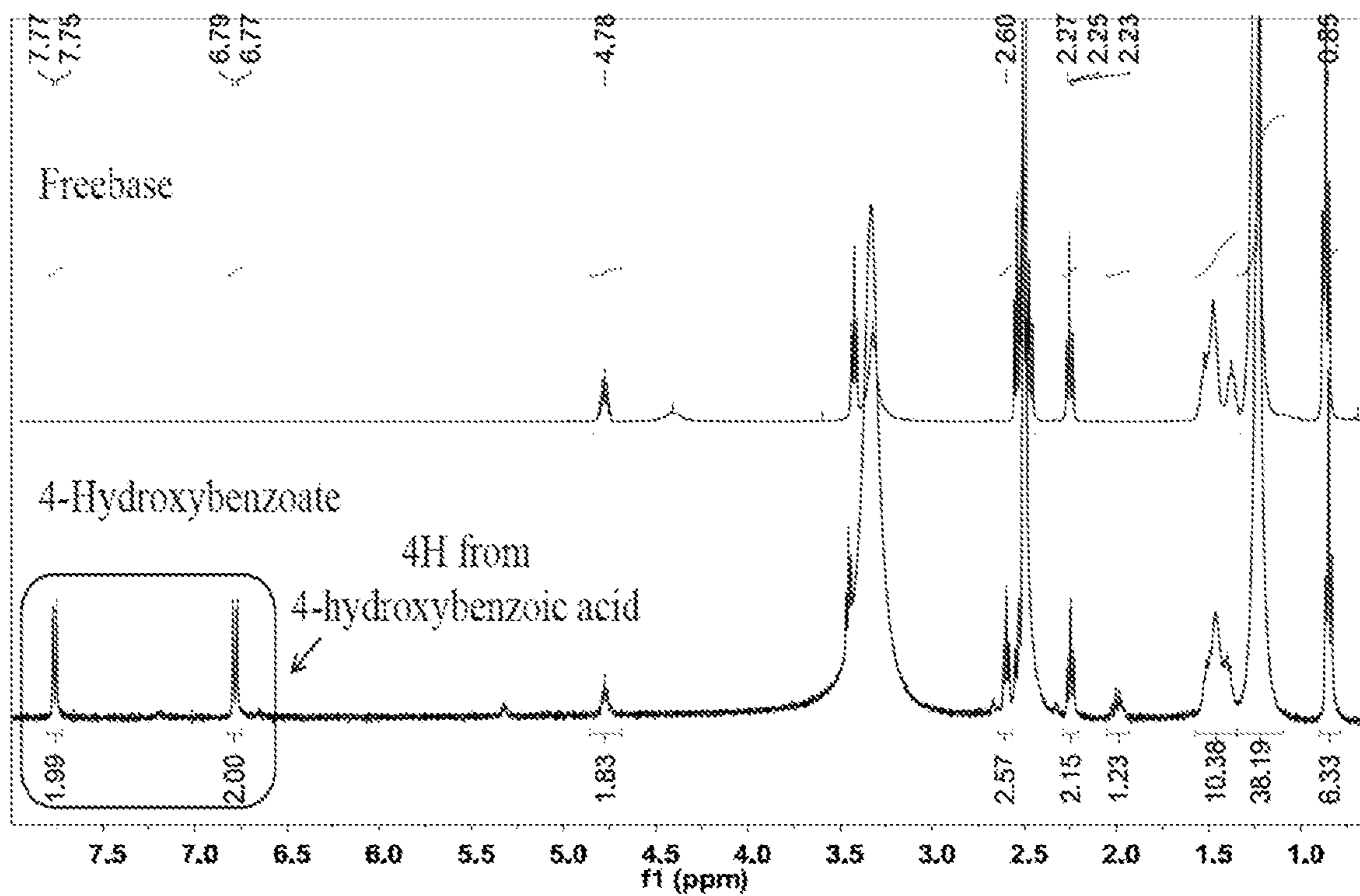


Figure 2

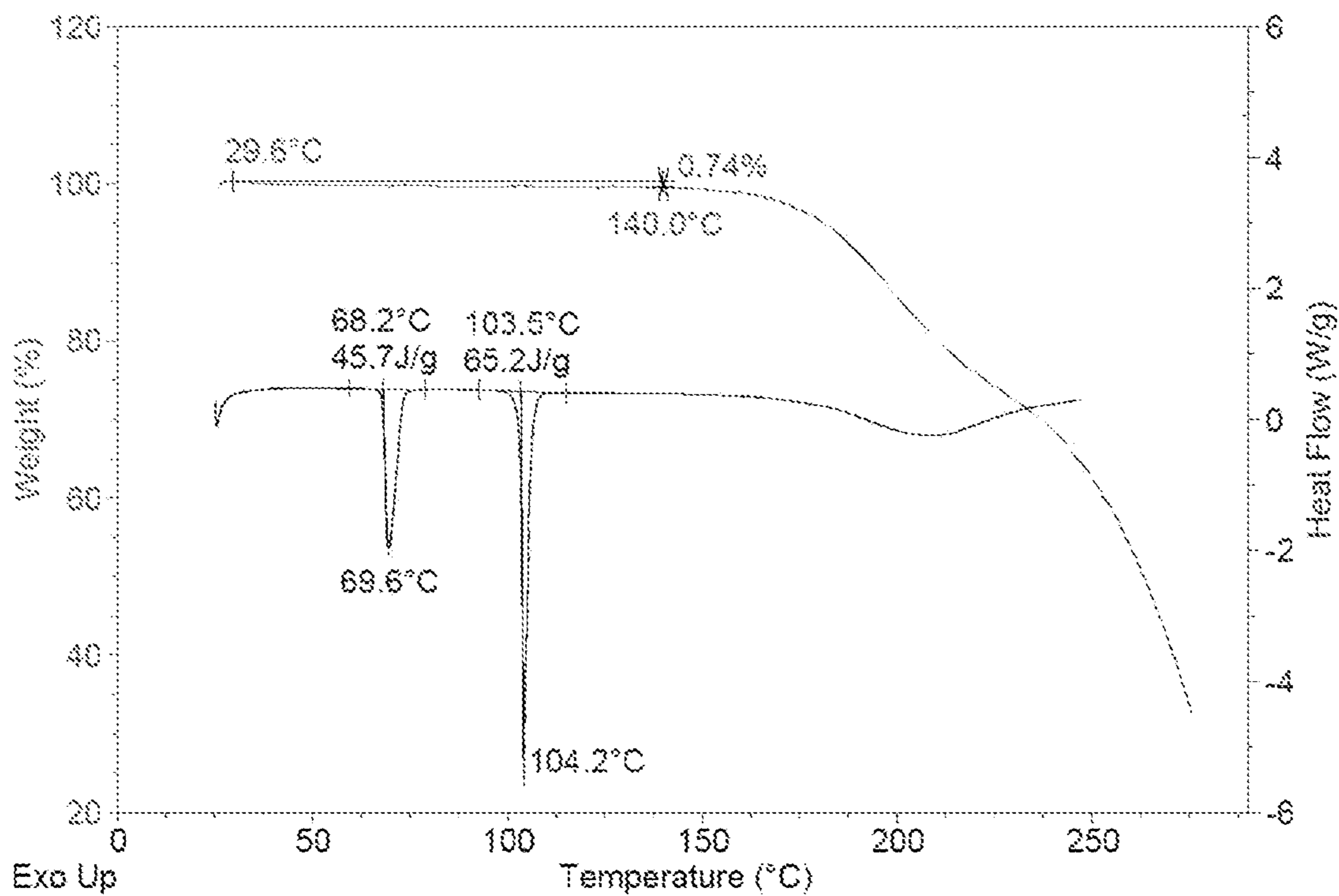


Figure 3

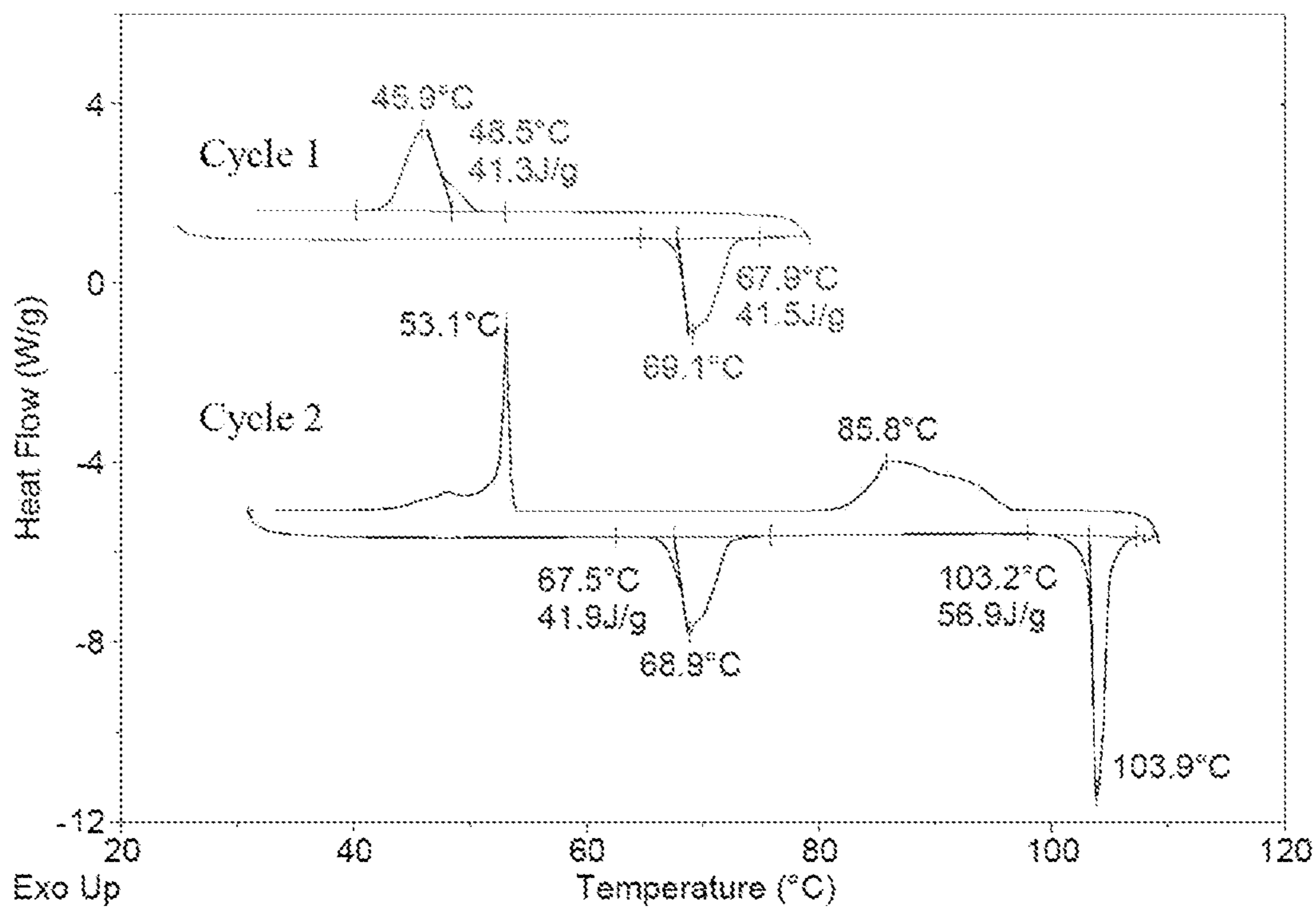


Figure 4

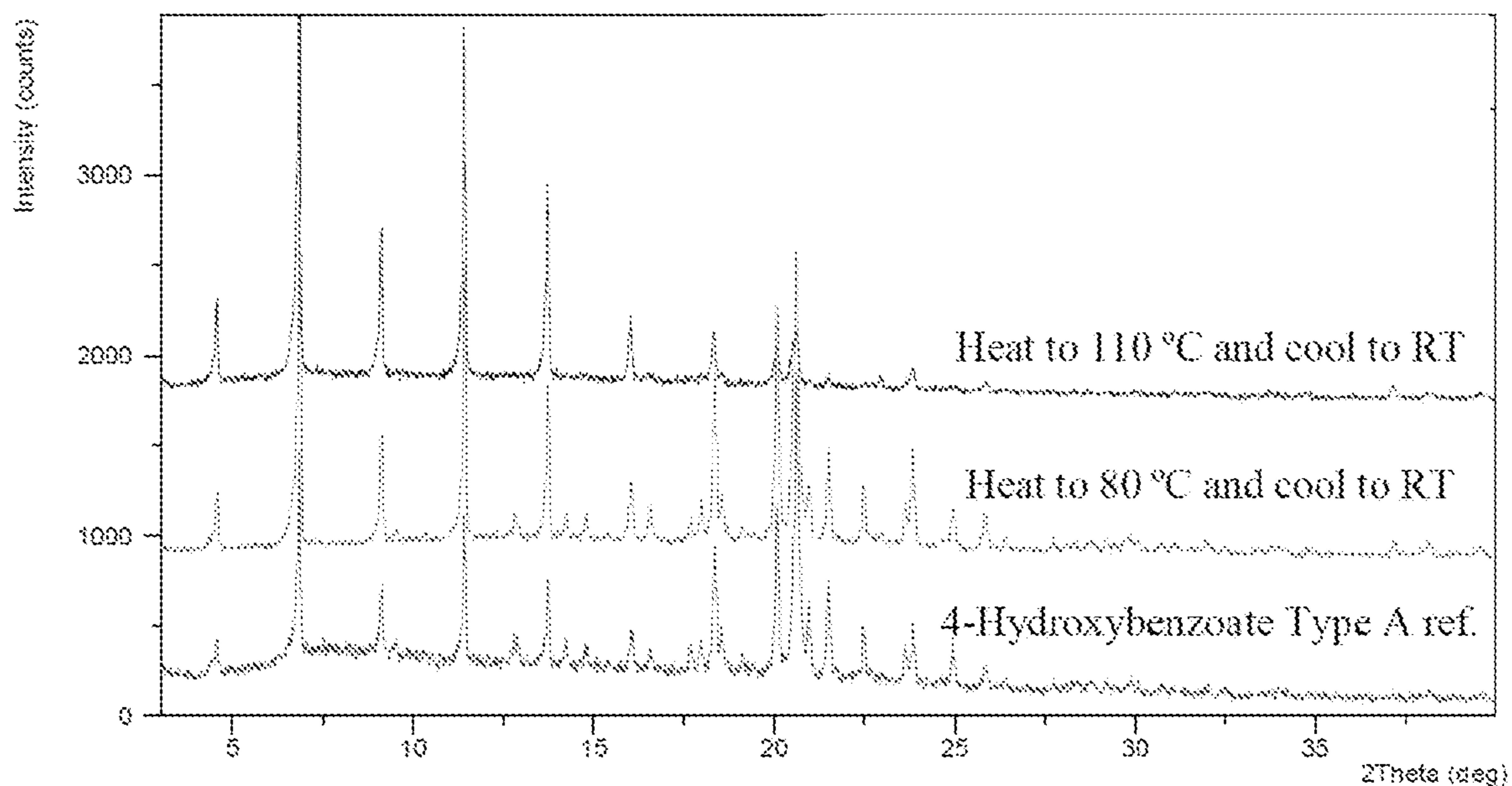


Figure 5

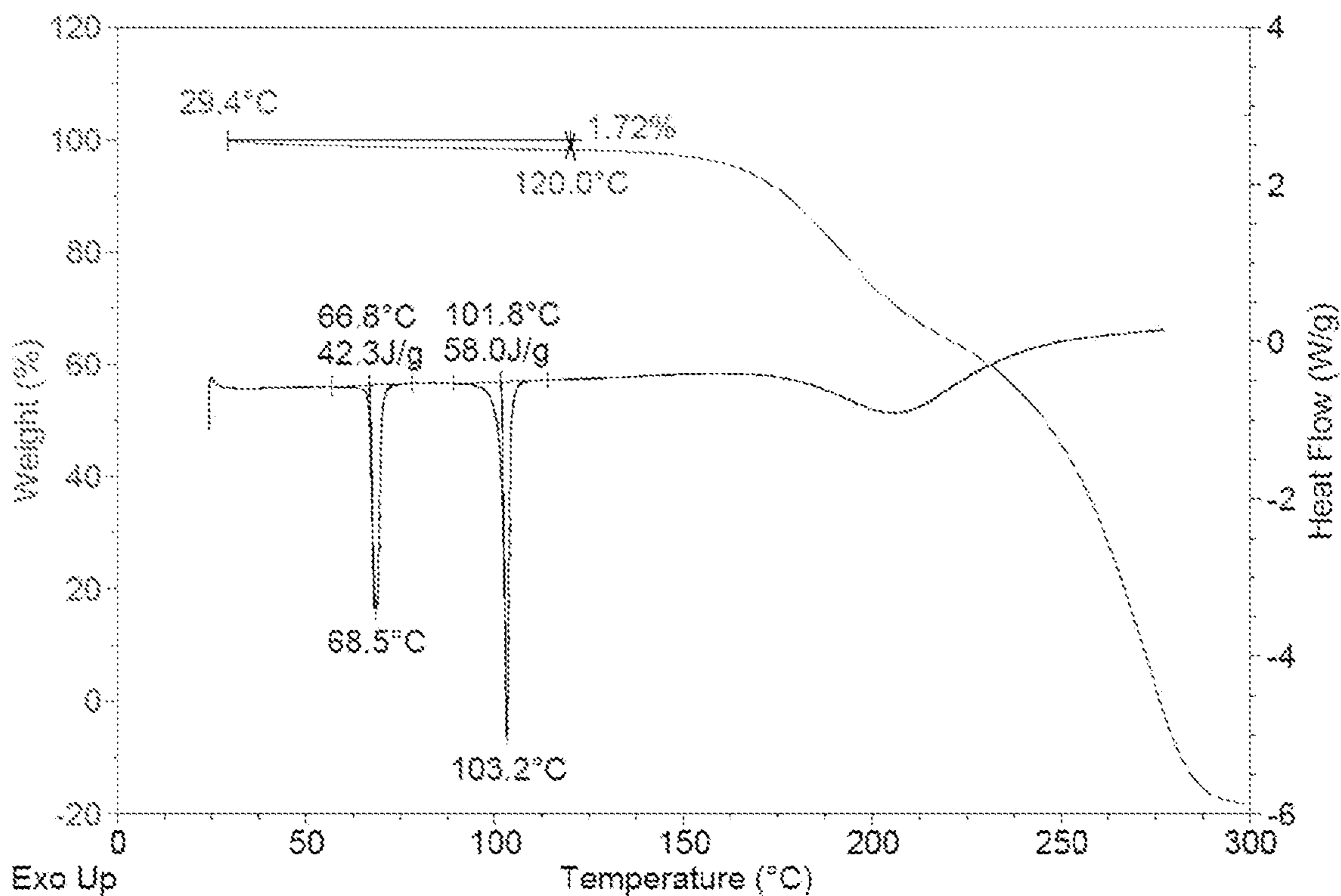


Figure 6

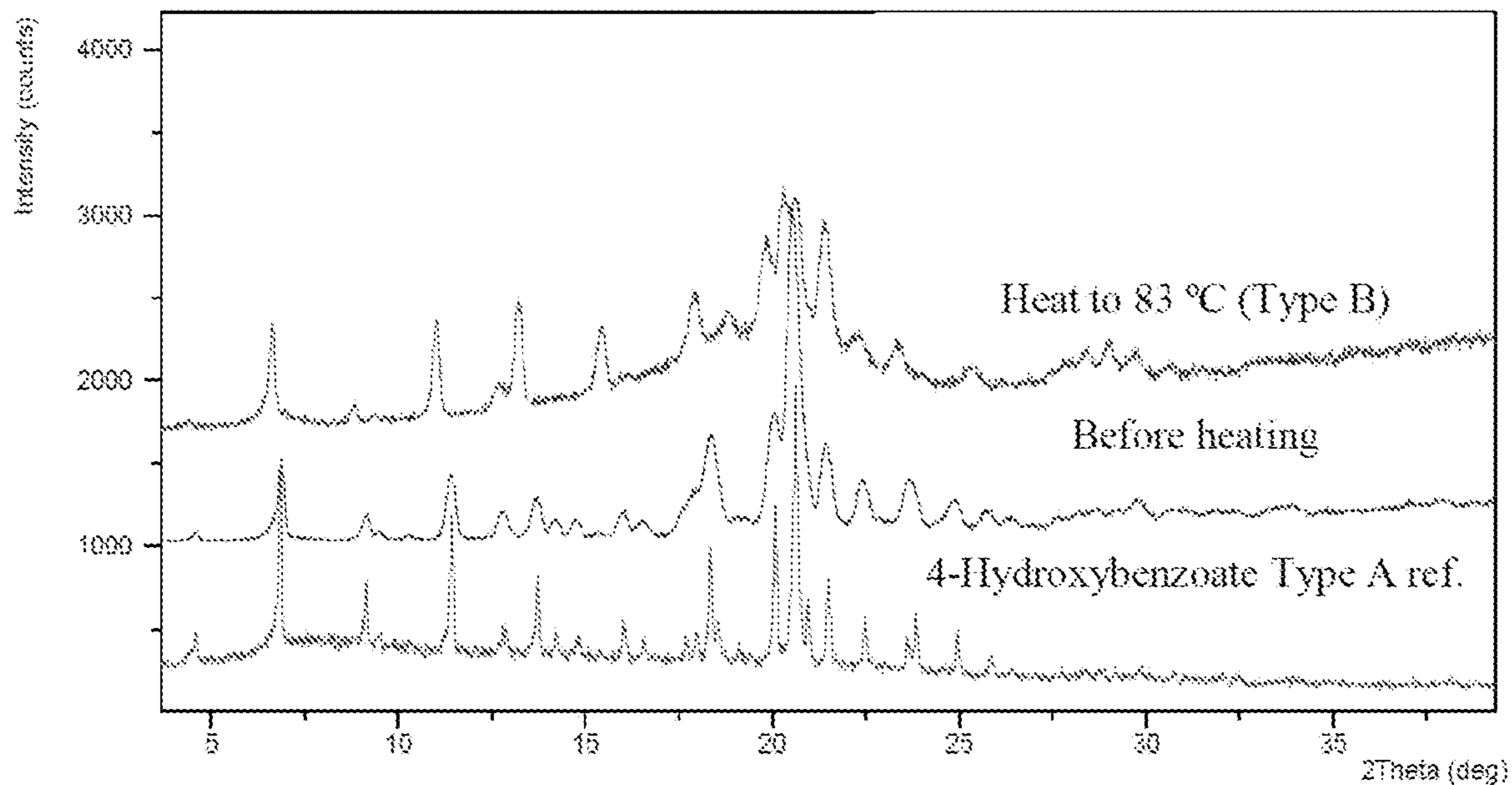


Figure 7

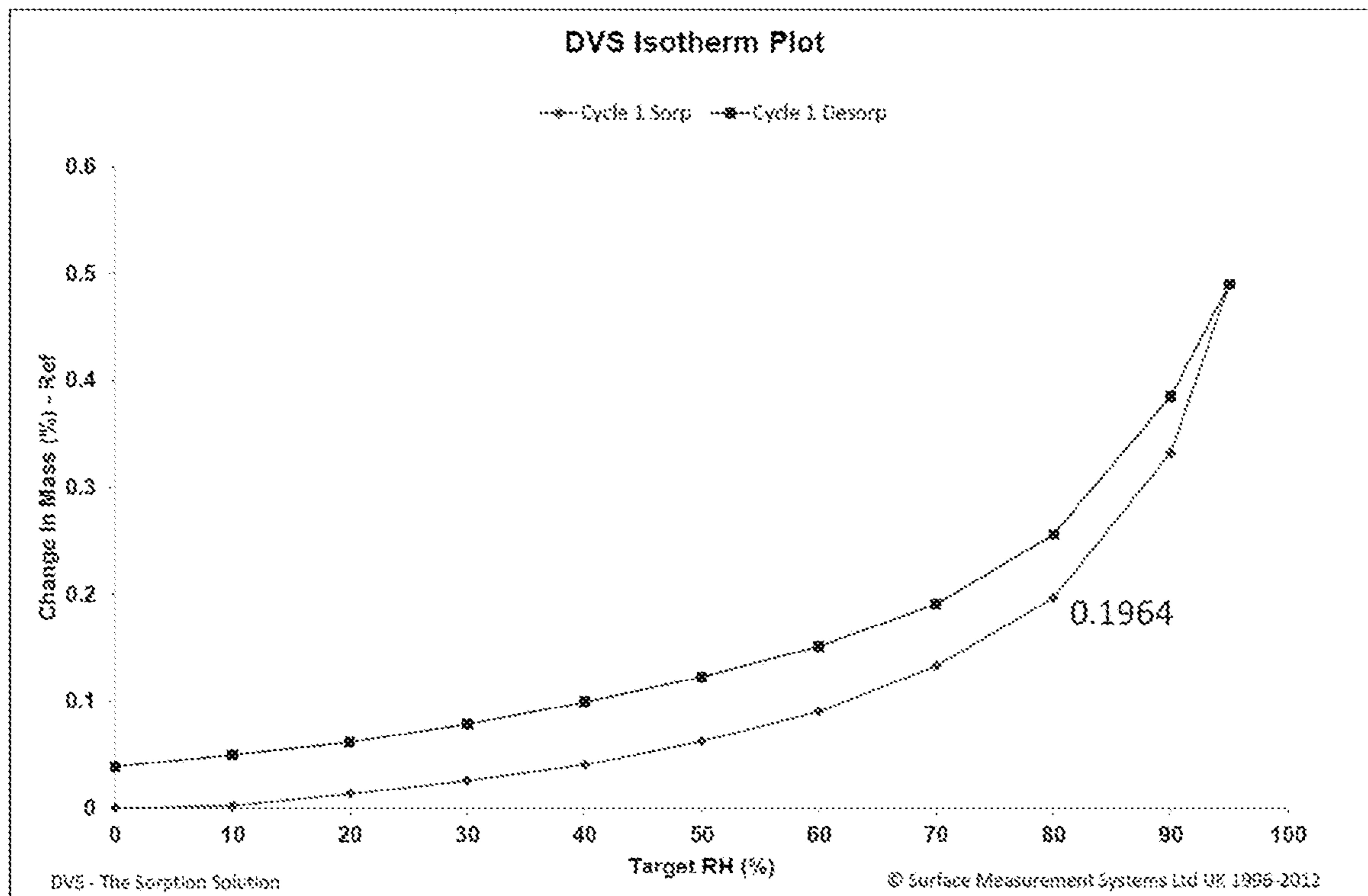


Figure 8

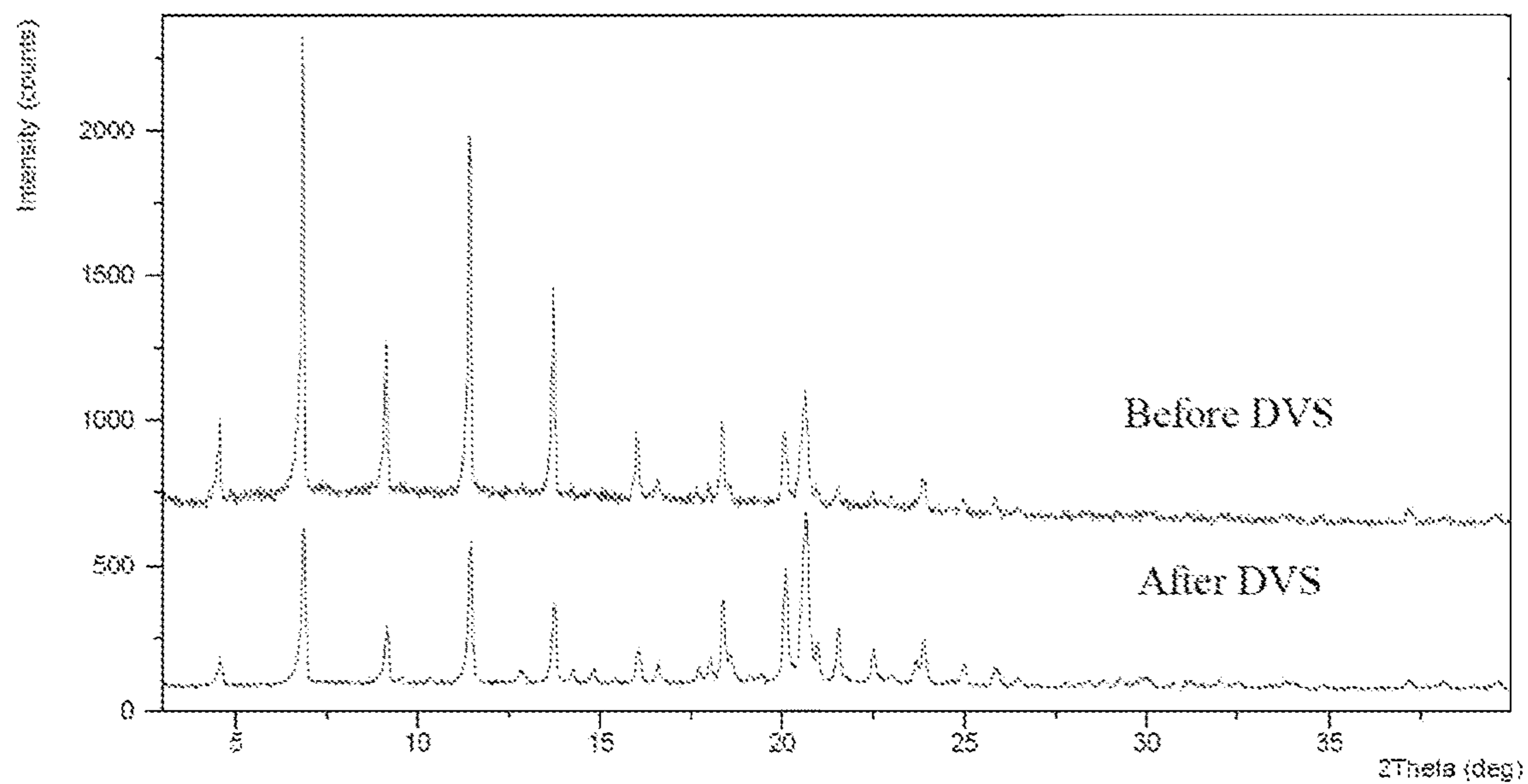


Figure 9

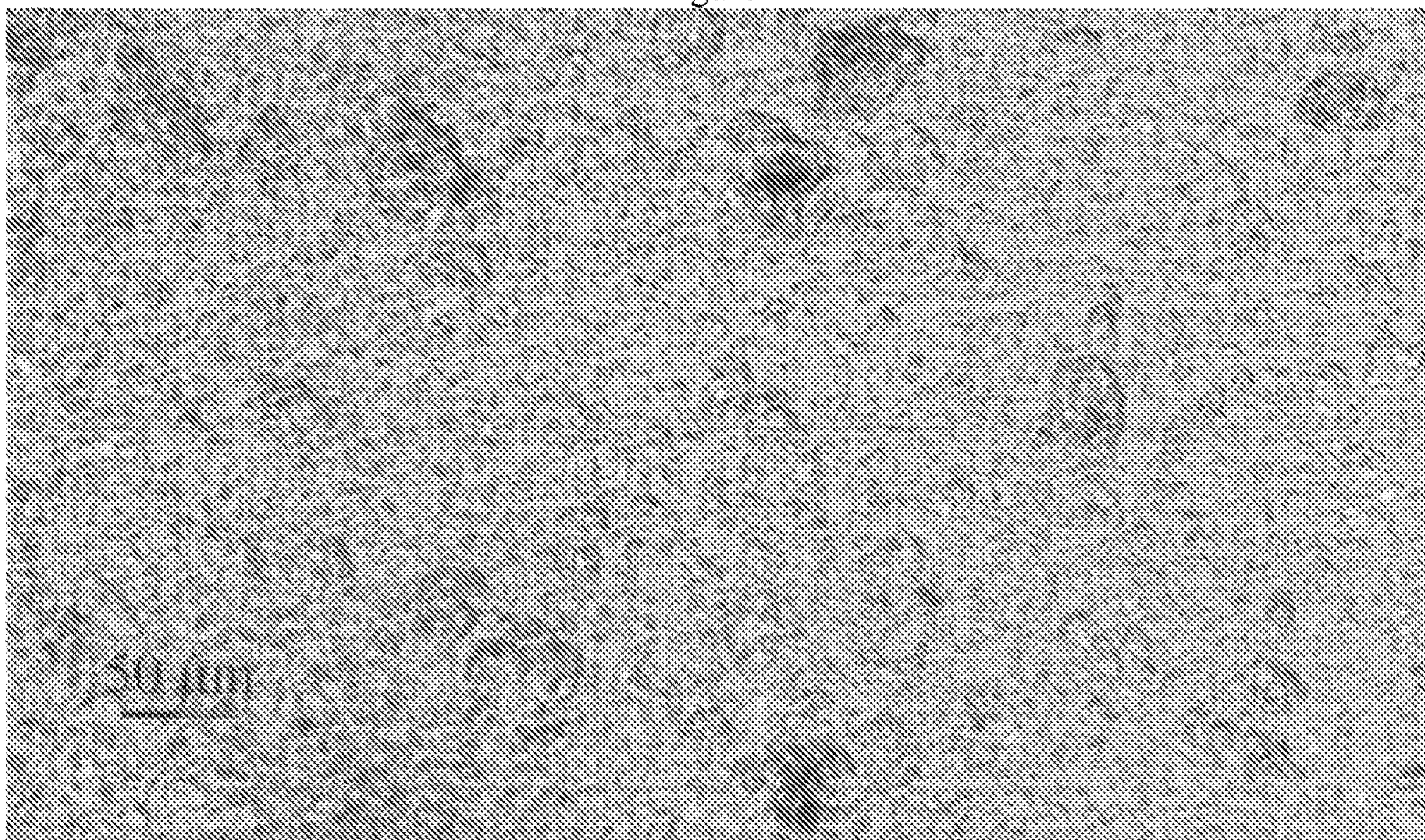


Figure 10

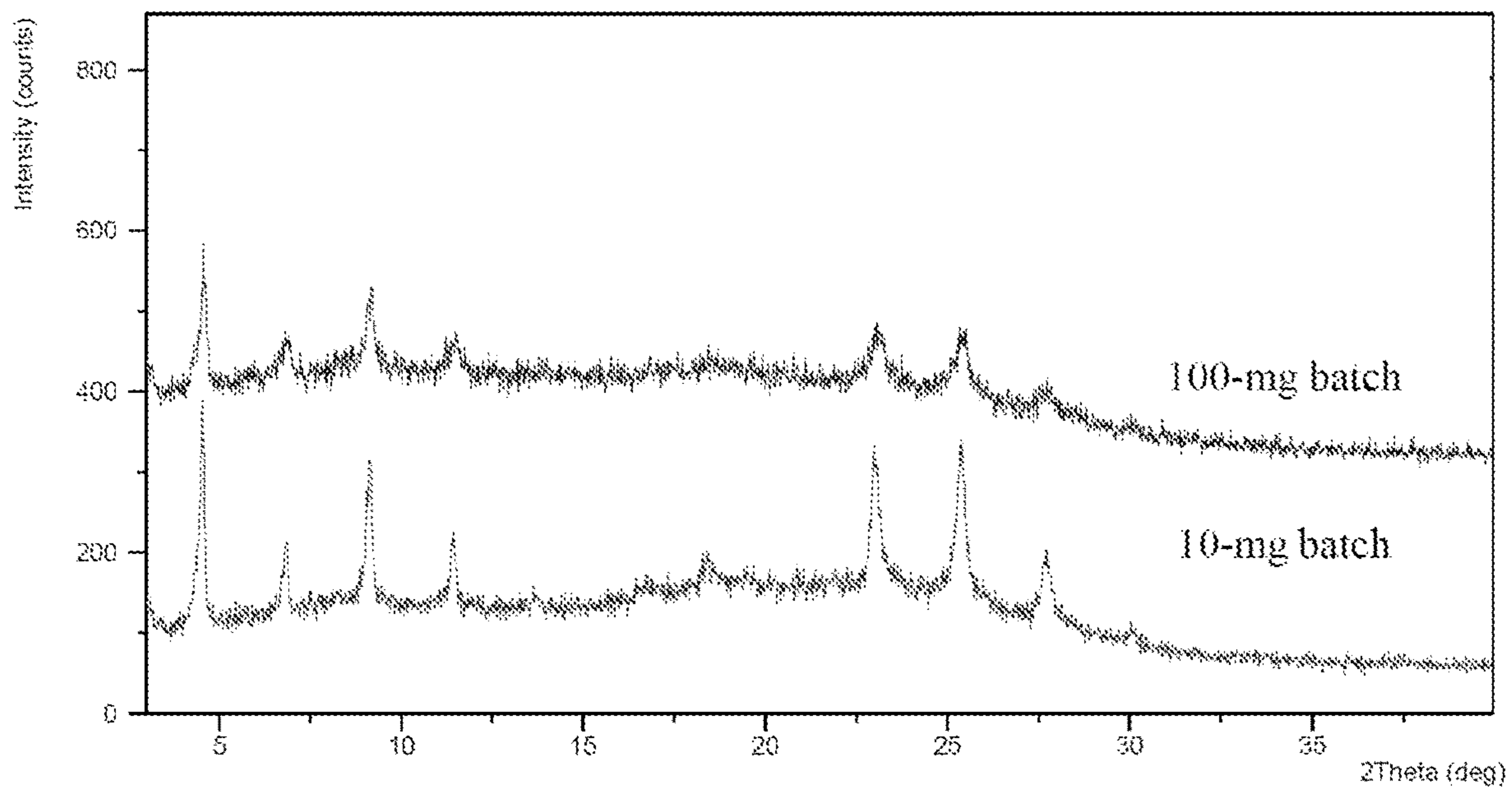


Figure 11

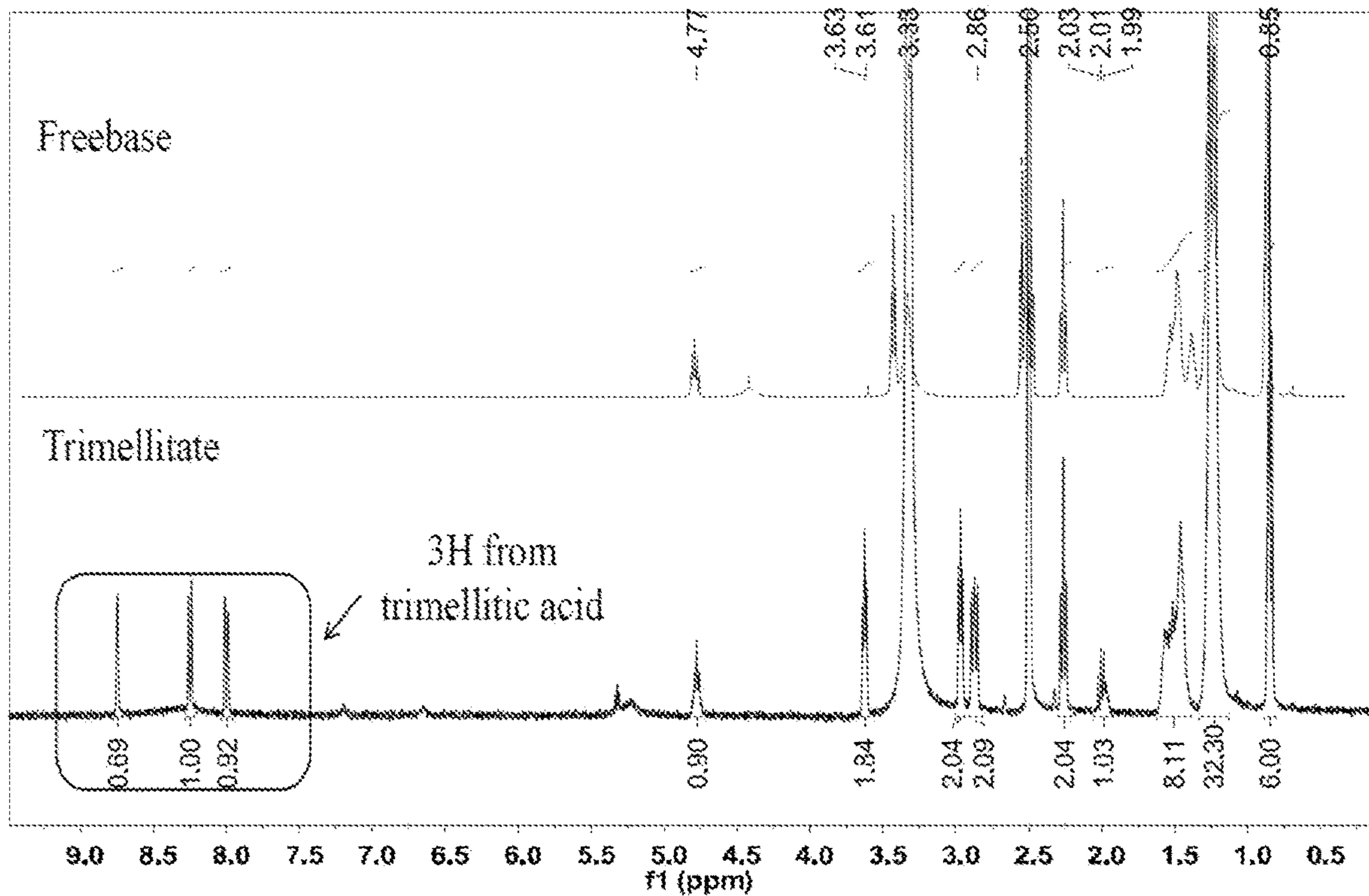


Figure 12

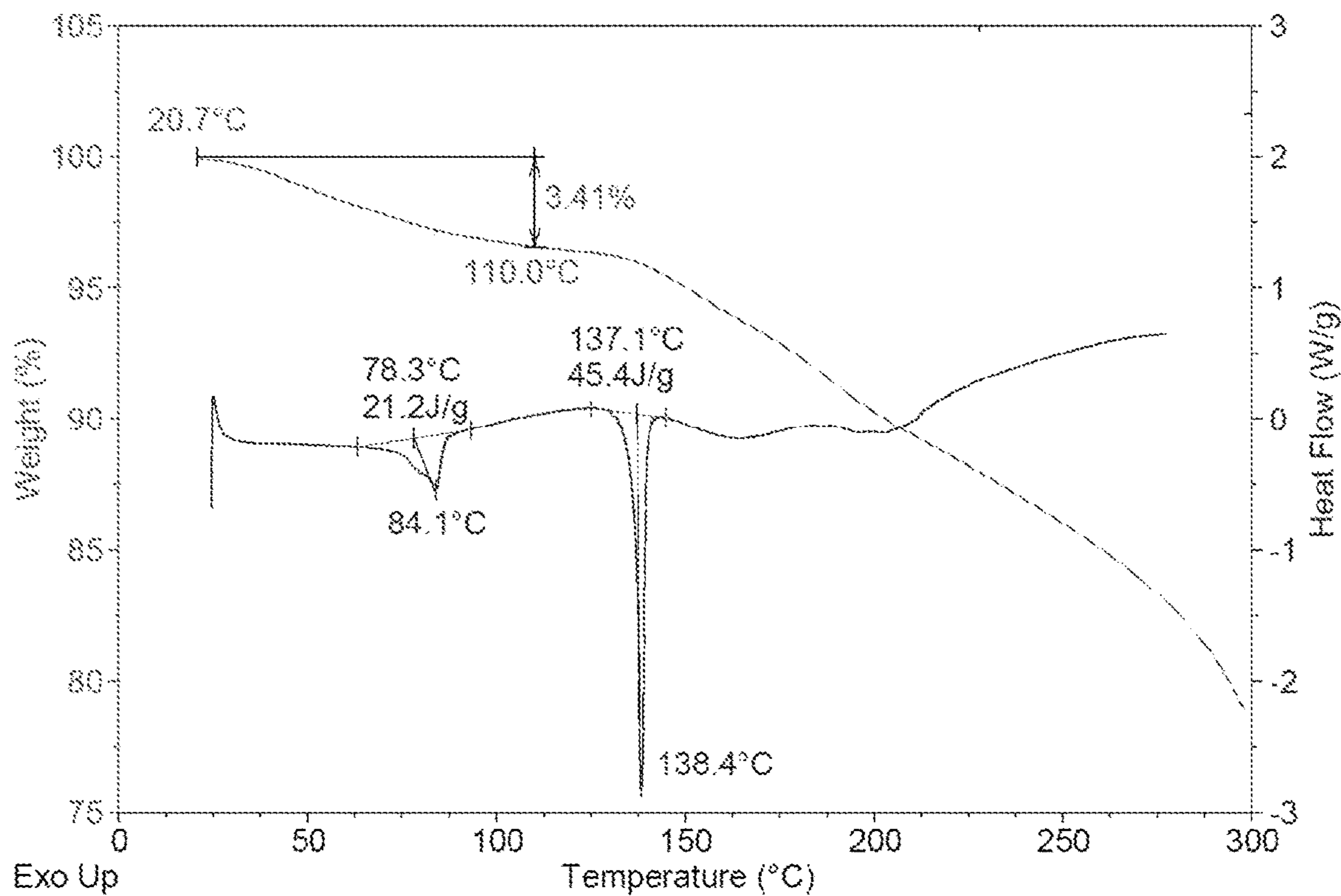


Figure 13

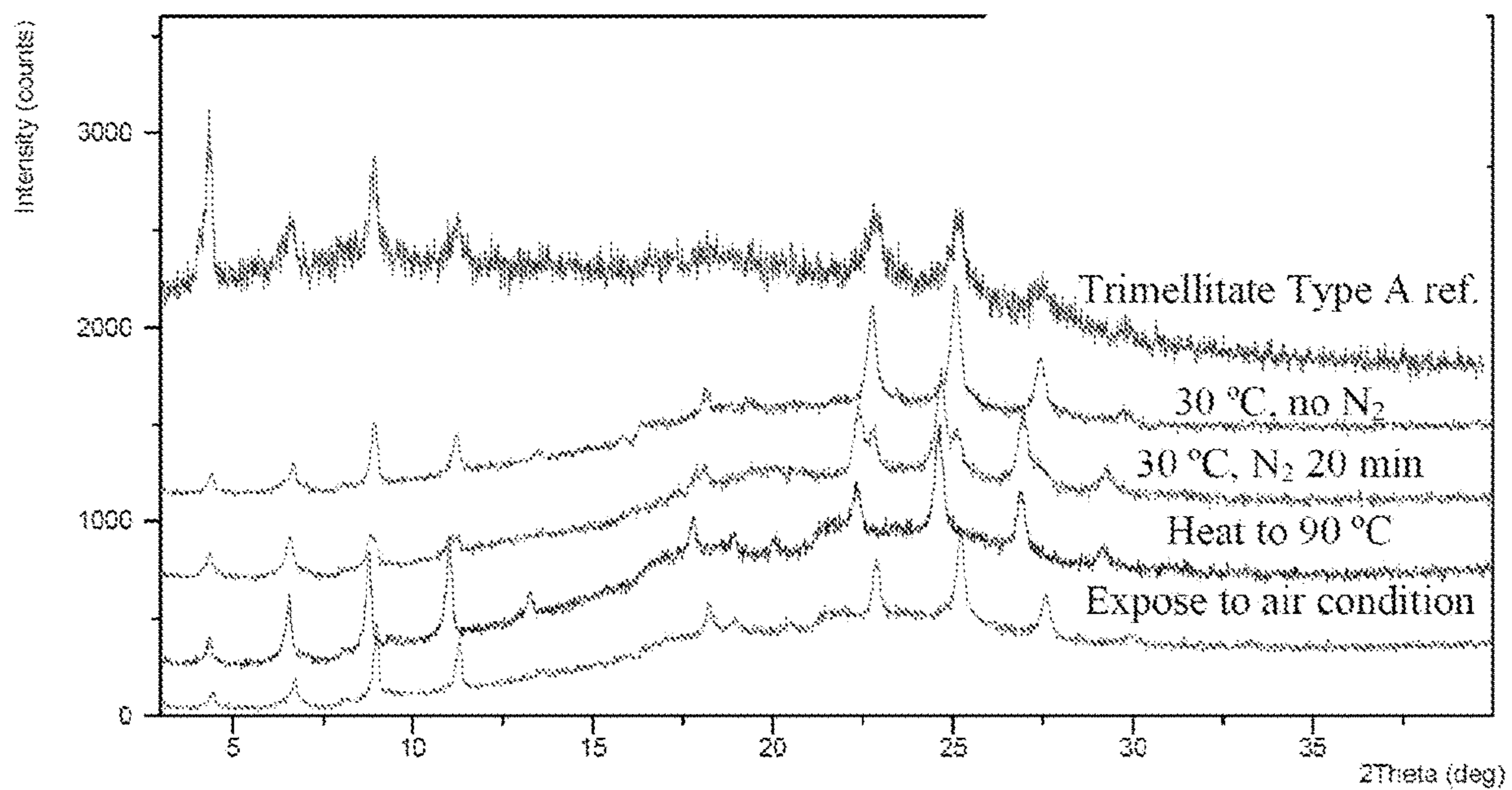


Figure 14

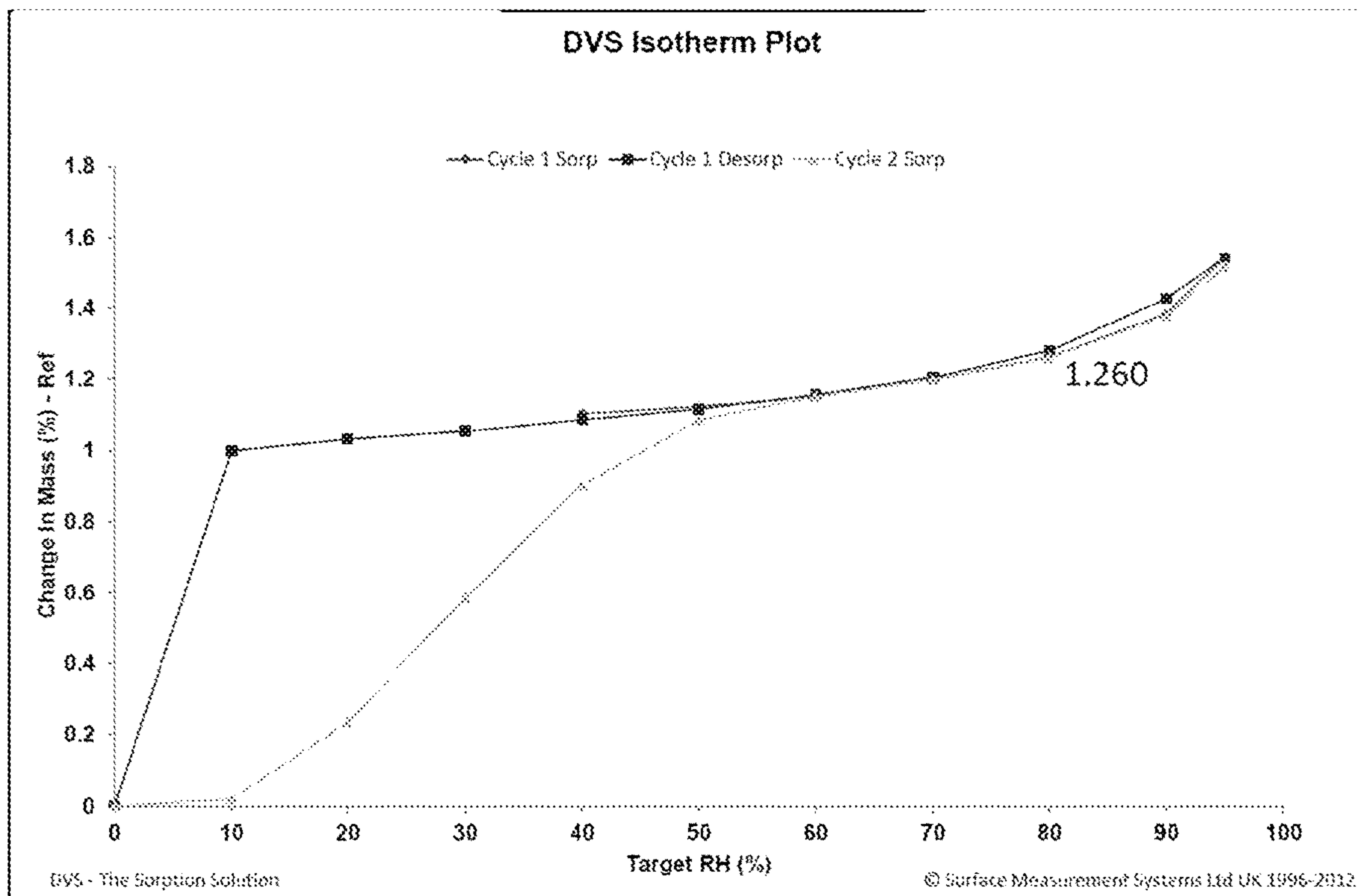


Figure 15

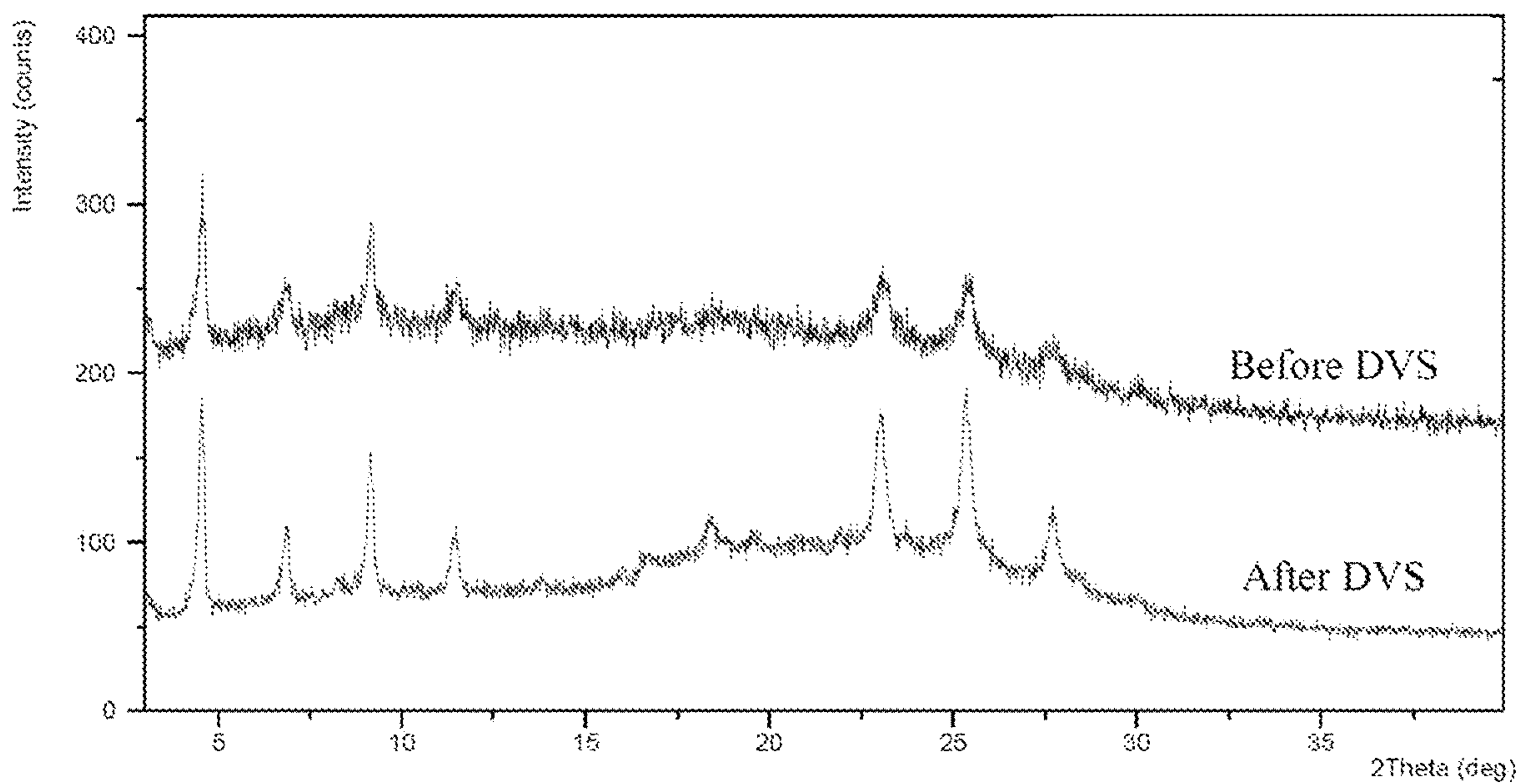


Figure 16

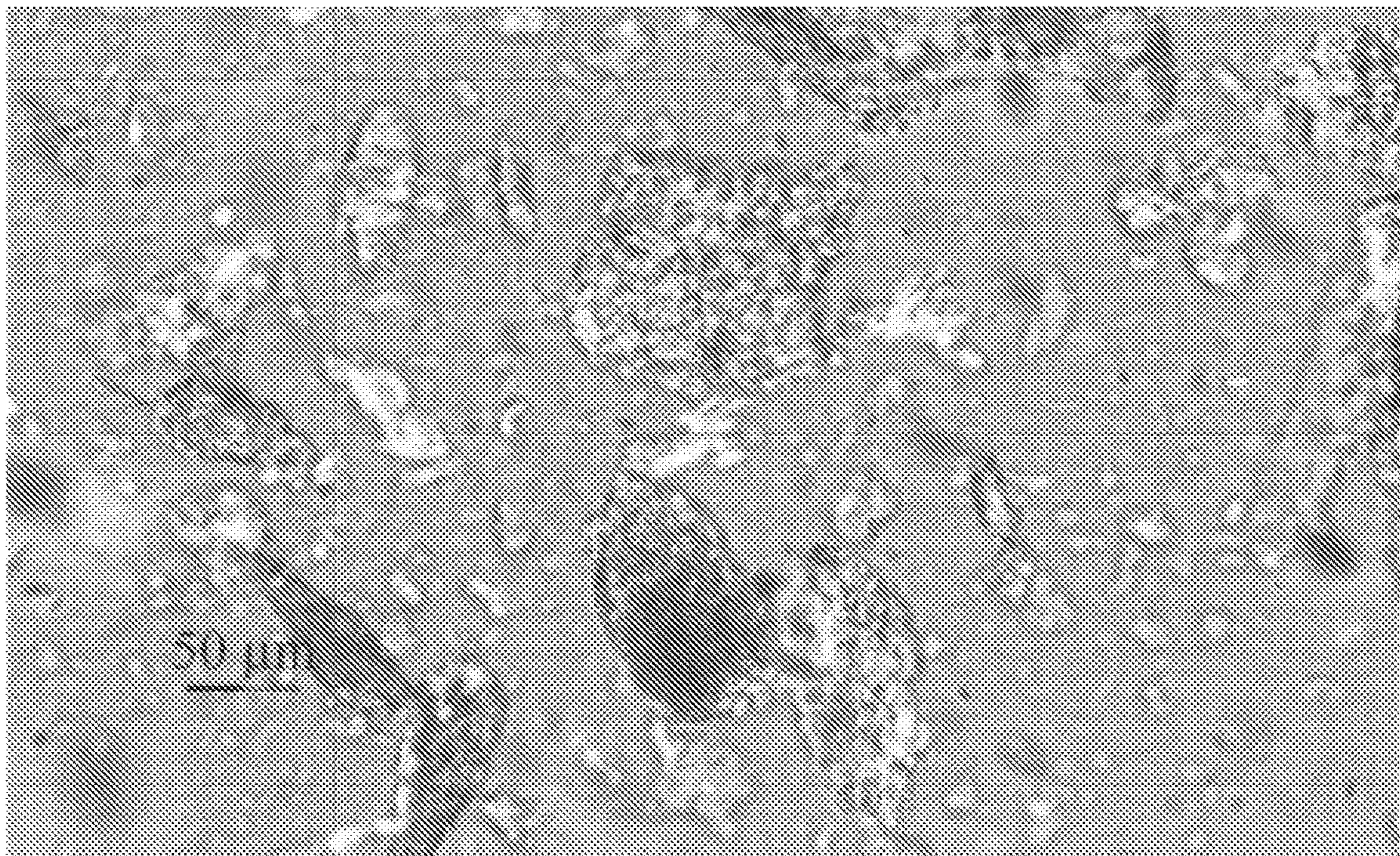


Figure 17

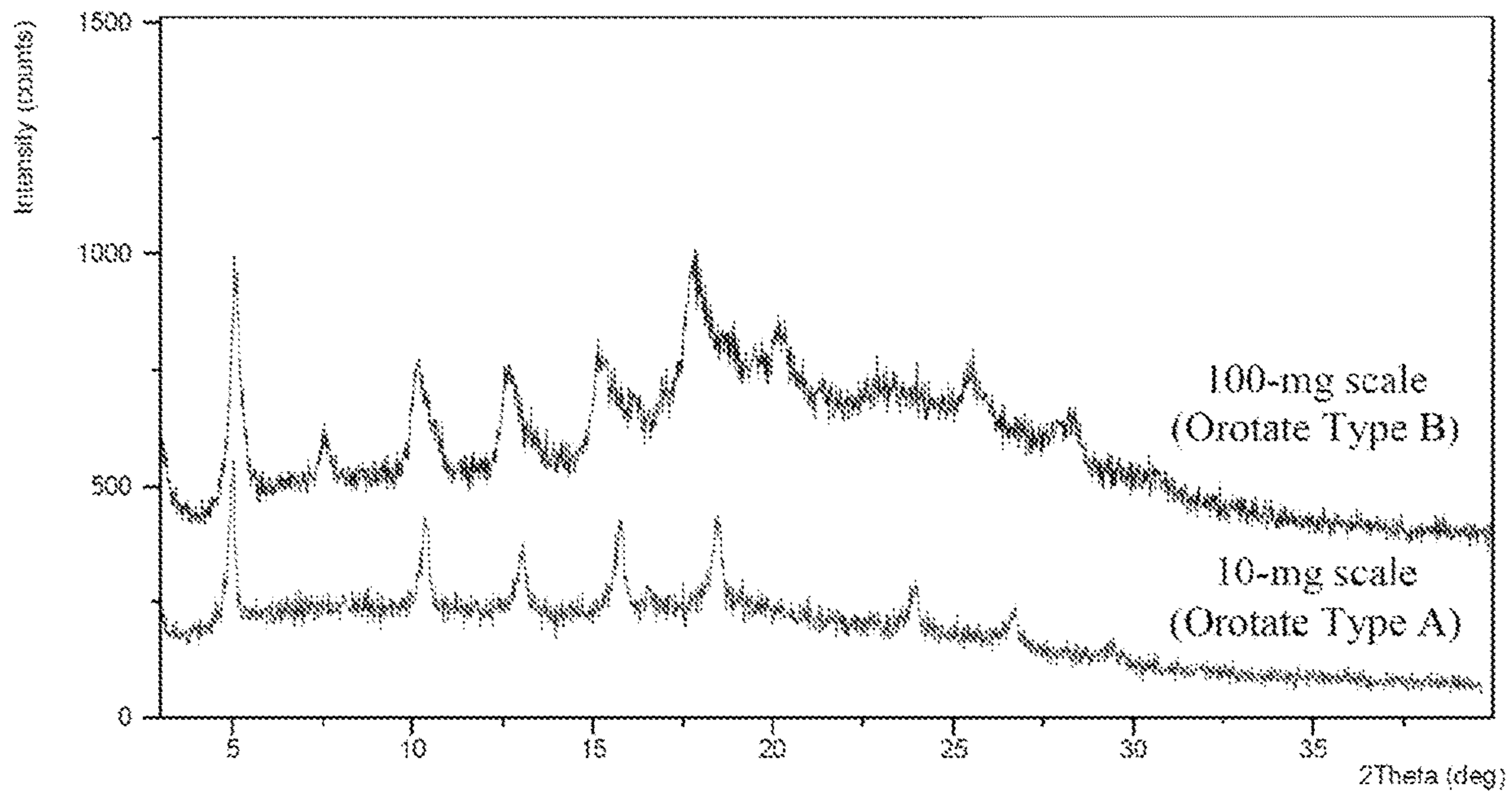


Figure 18

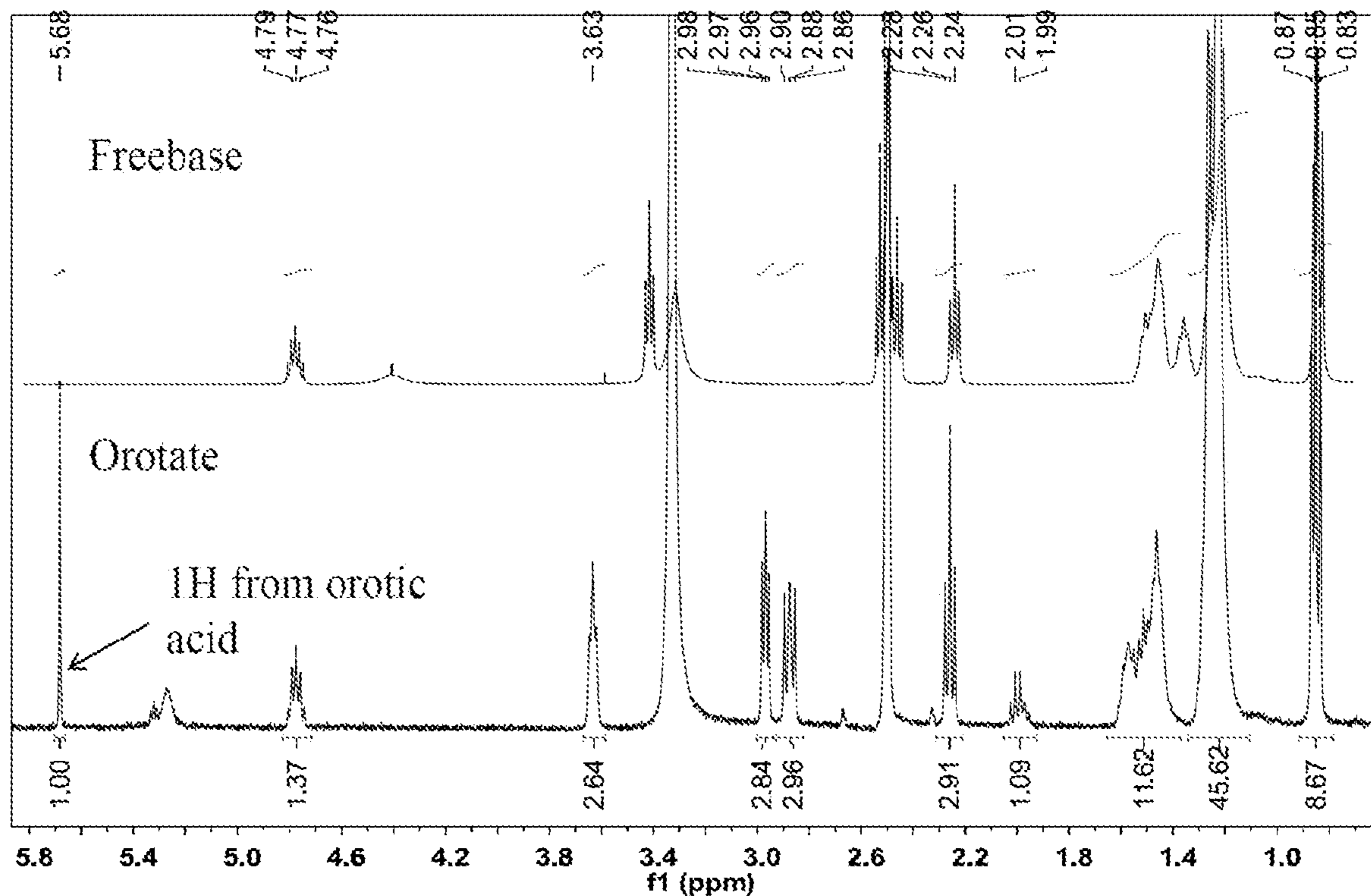


Figure 19

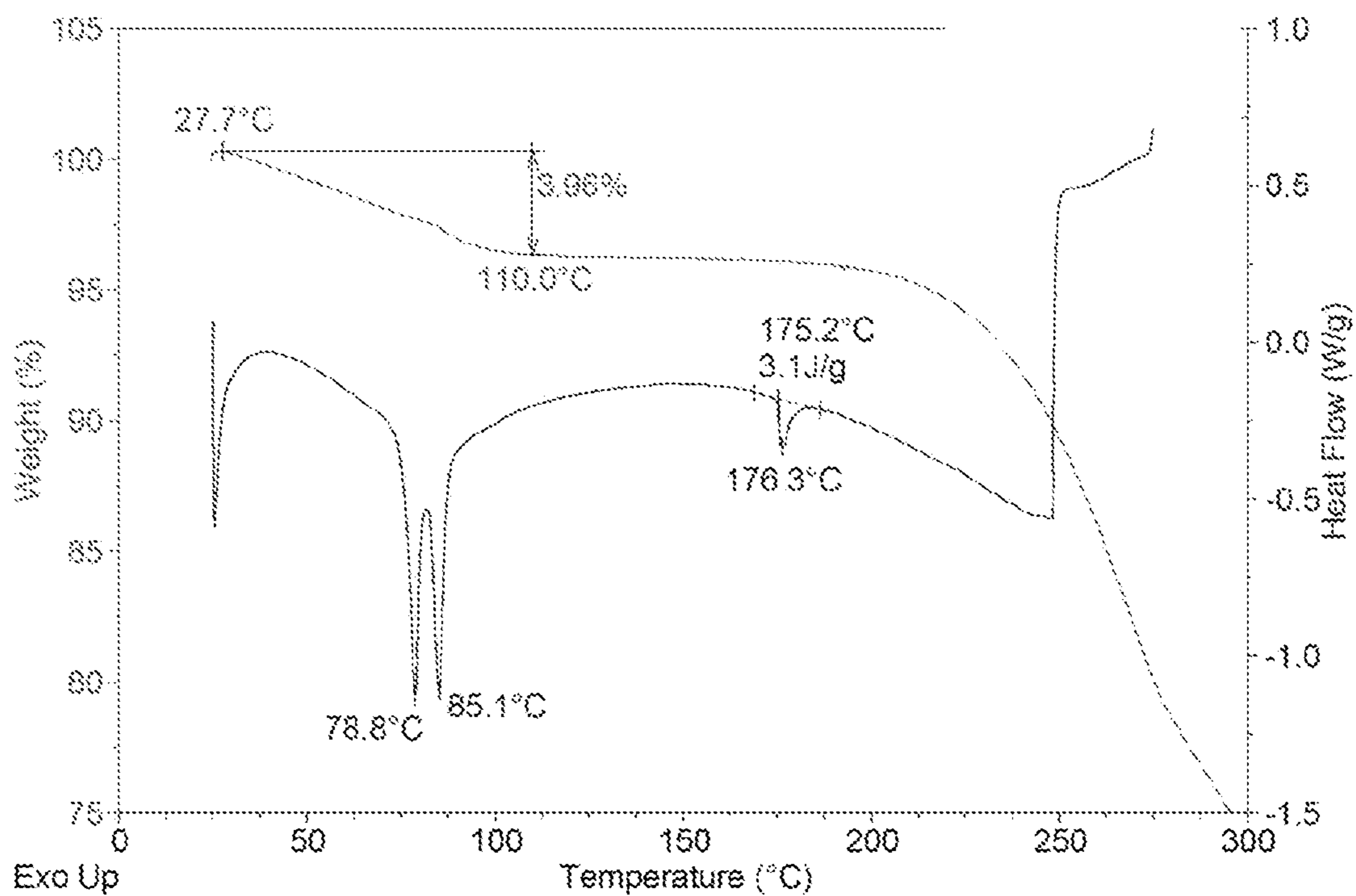


Figure 20

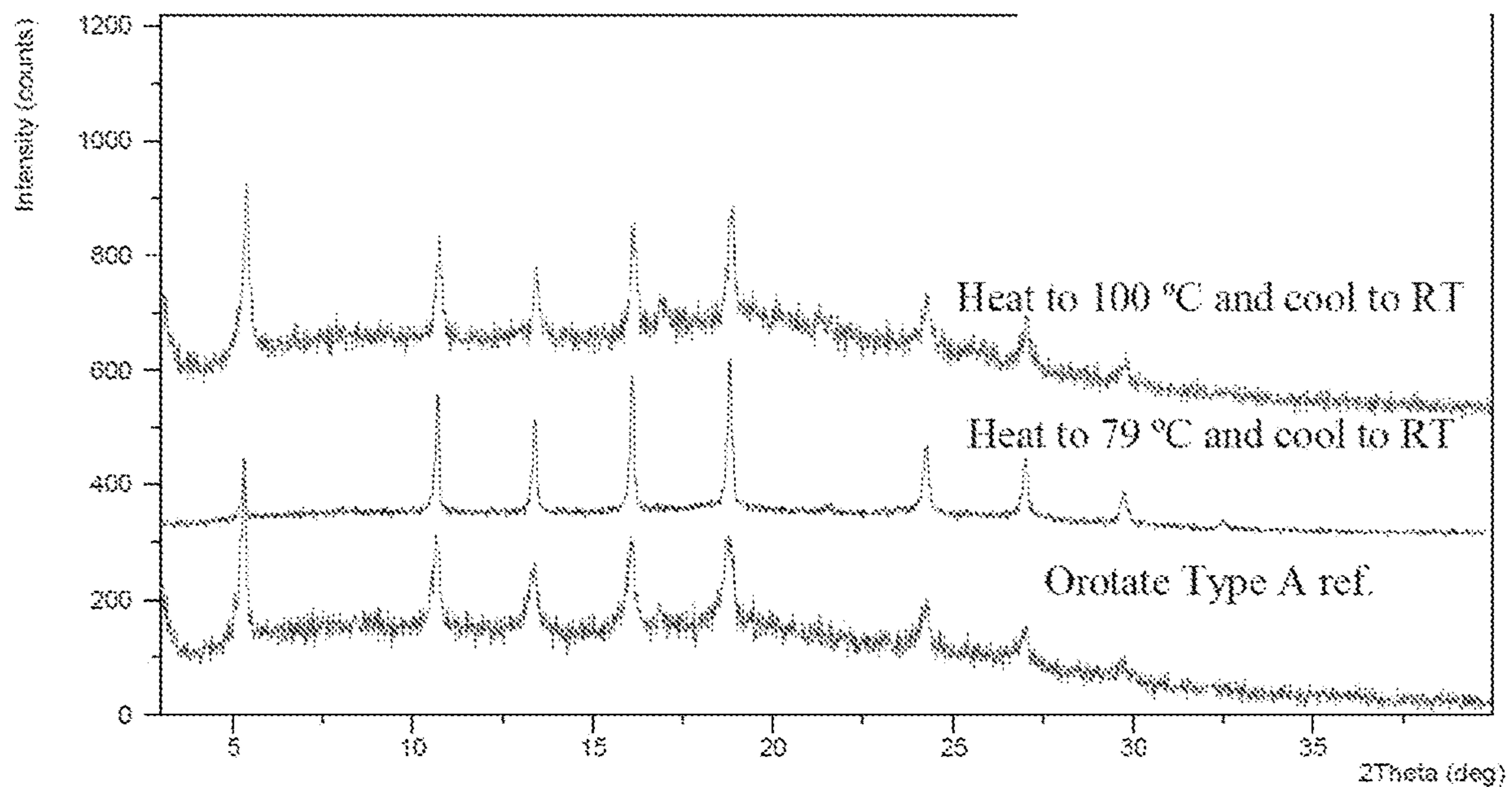


Figure 21

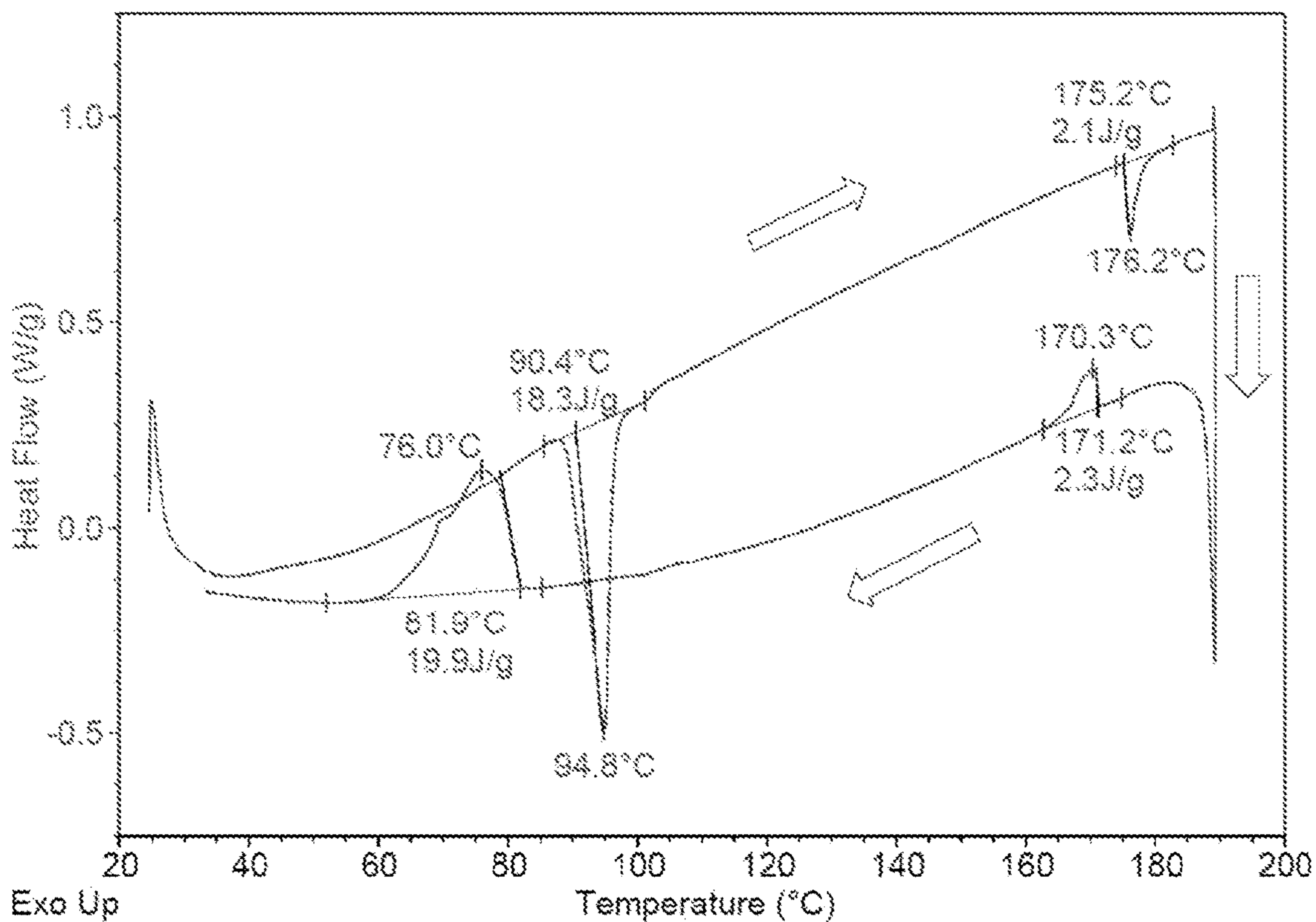


Figure 22

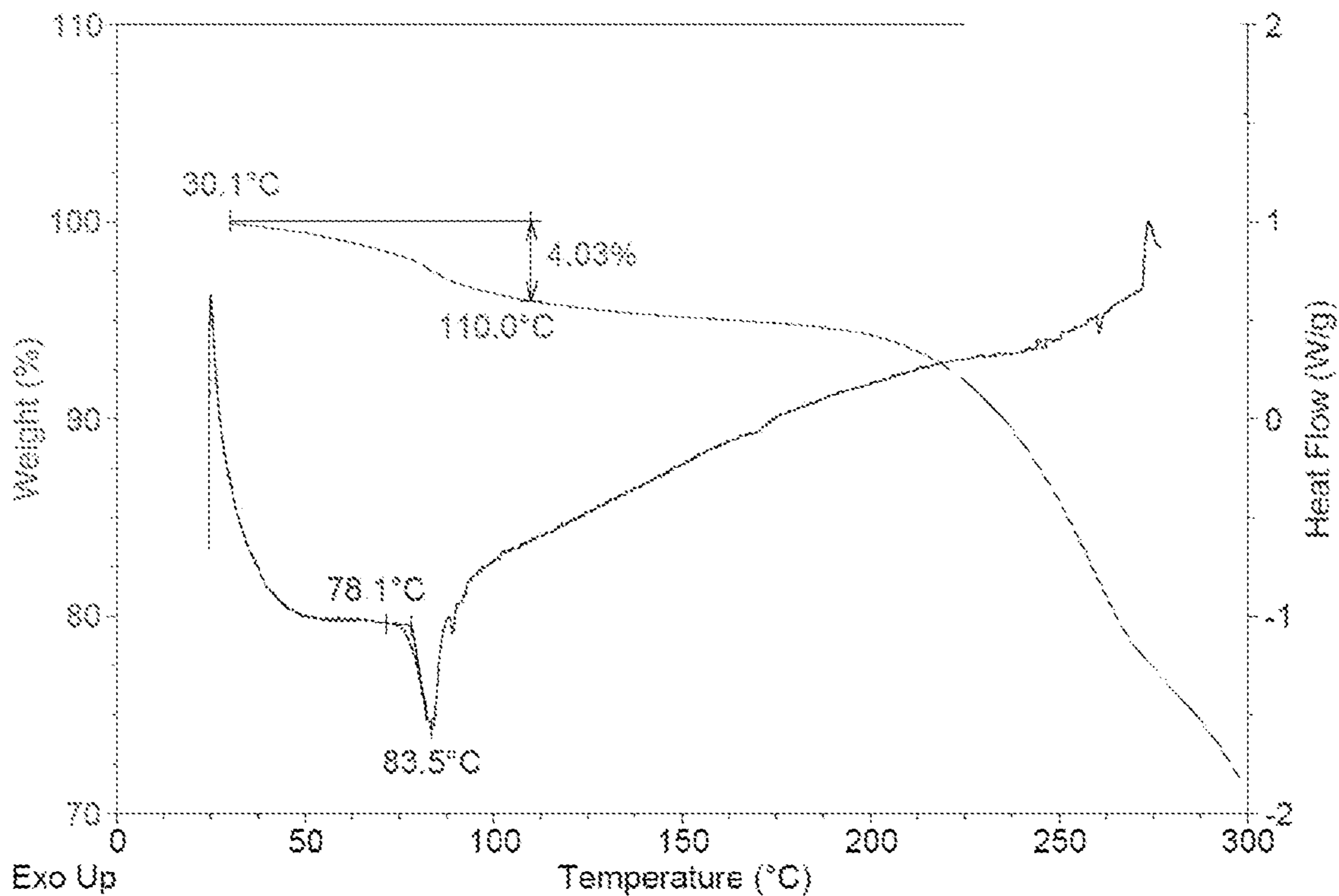


Figure 23

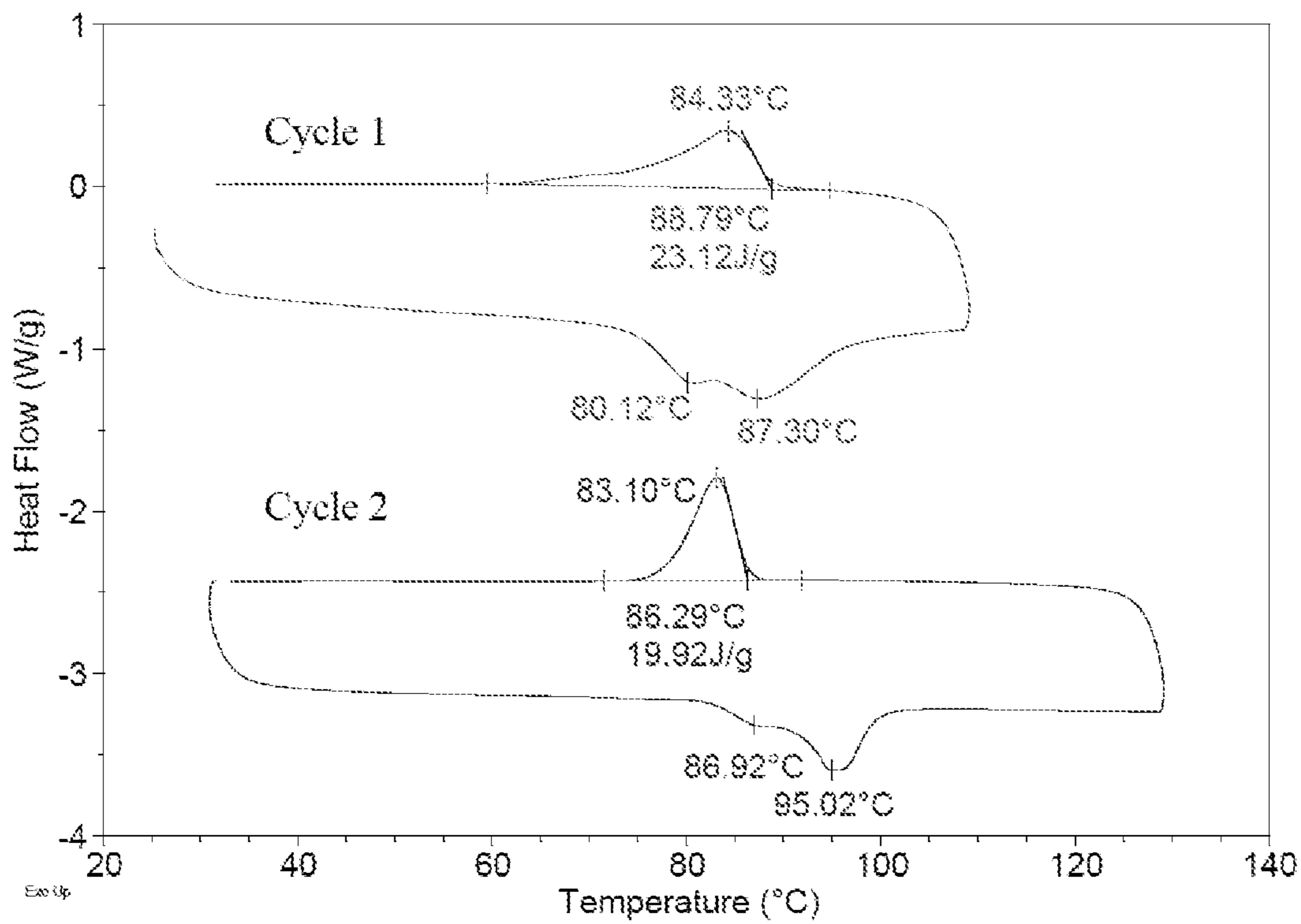


Figure 24

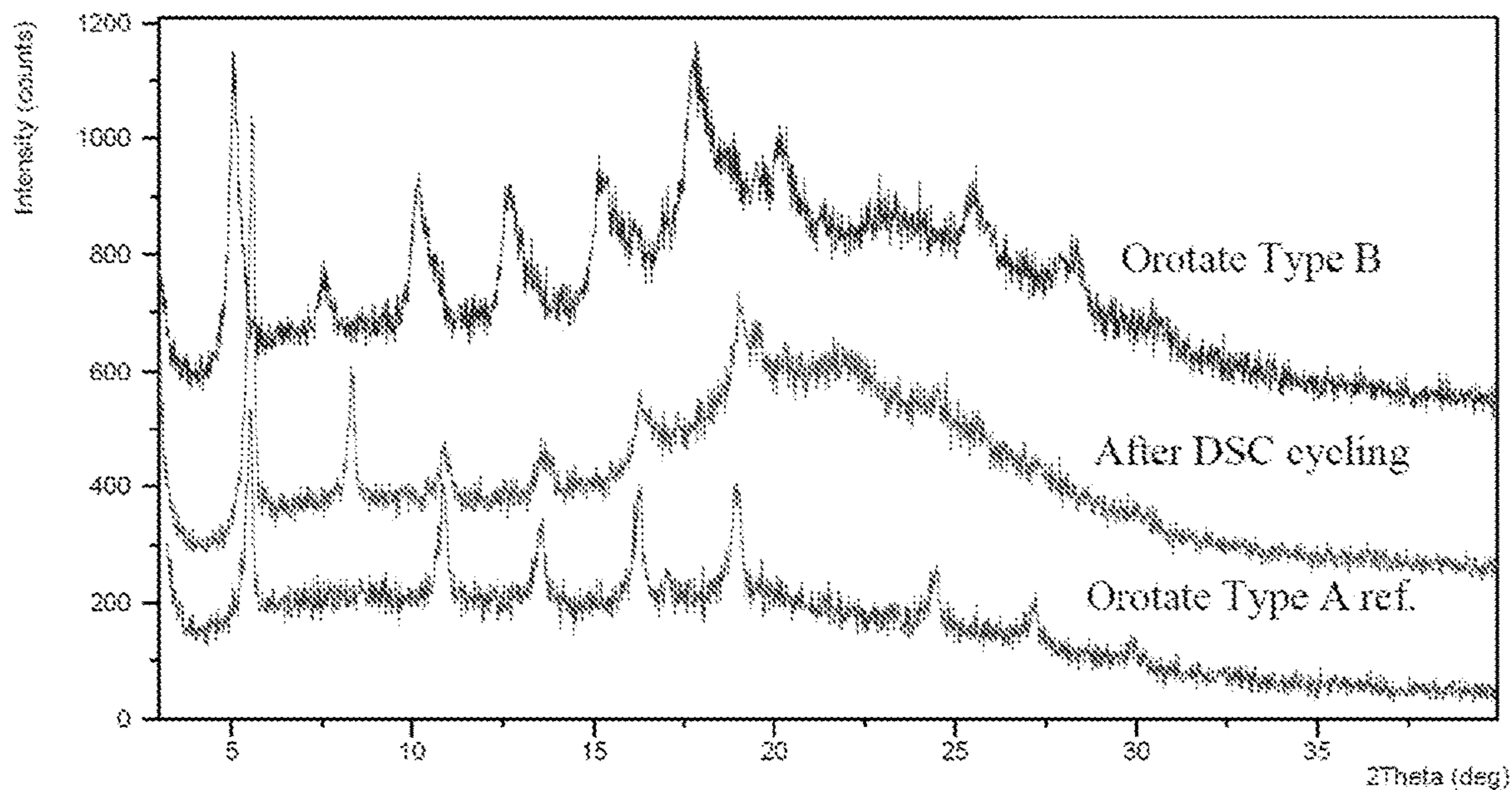


Figure 25

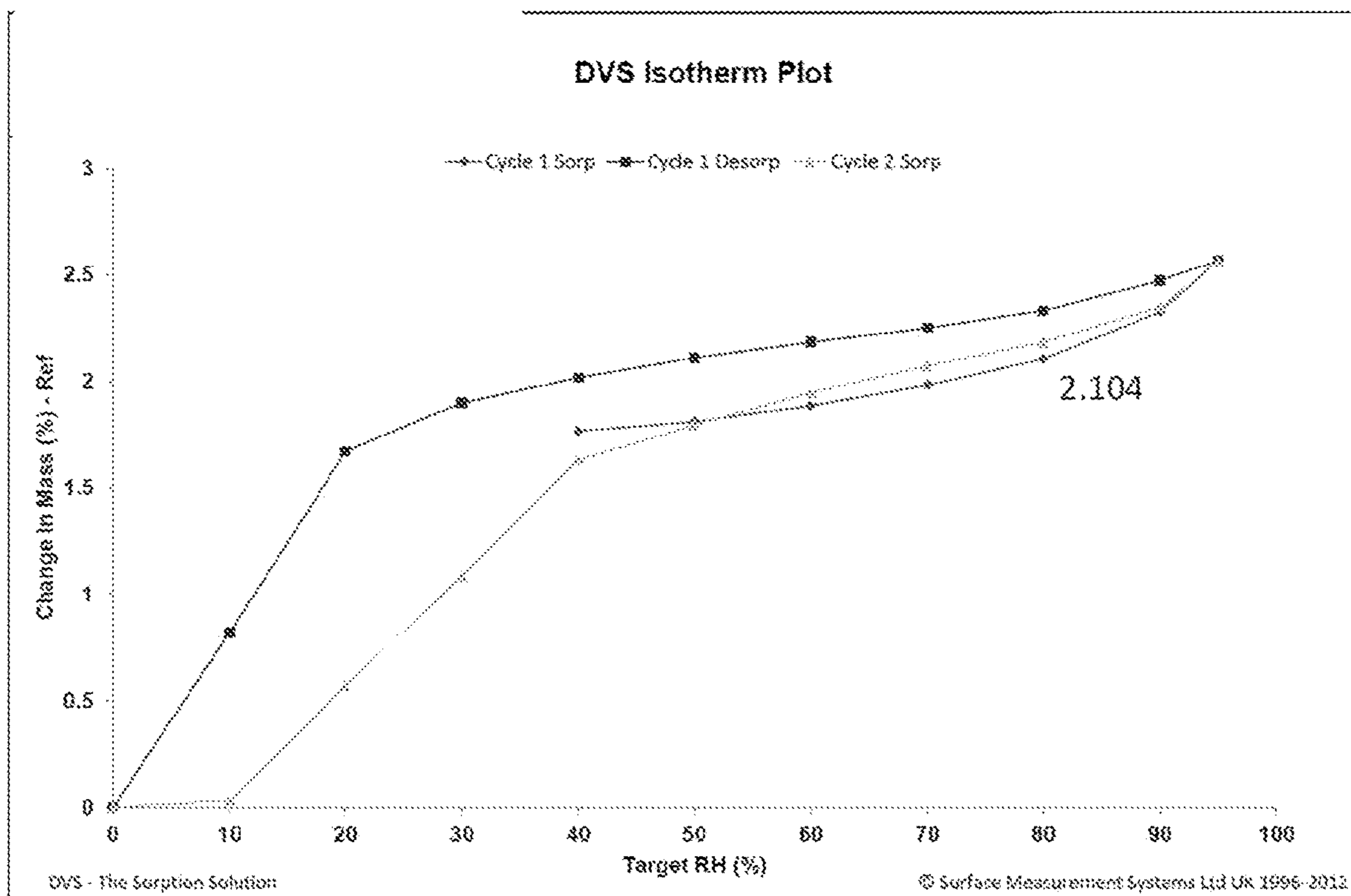


Figure 26

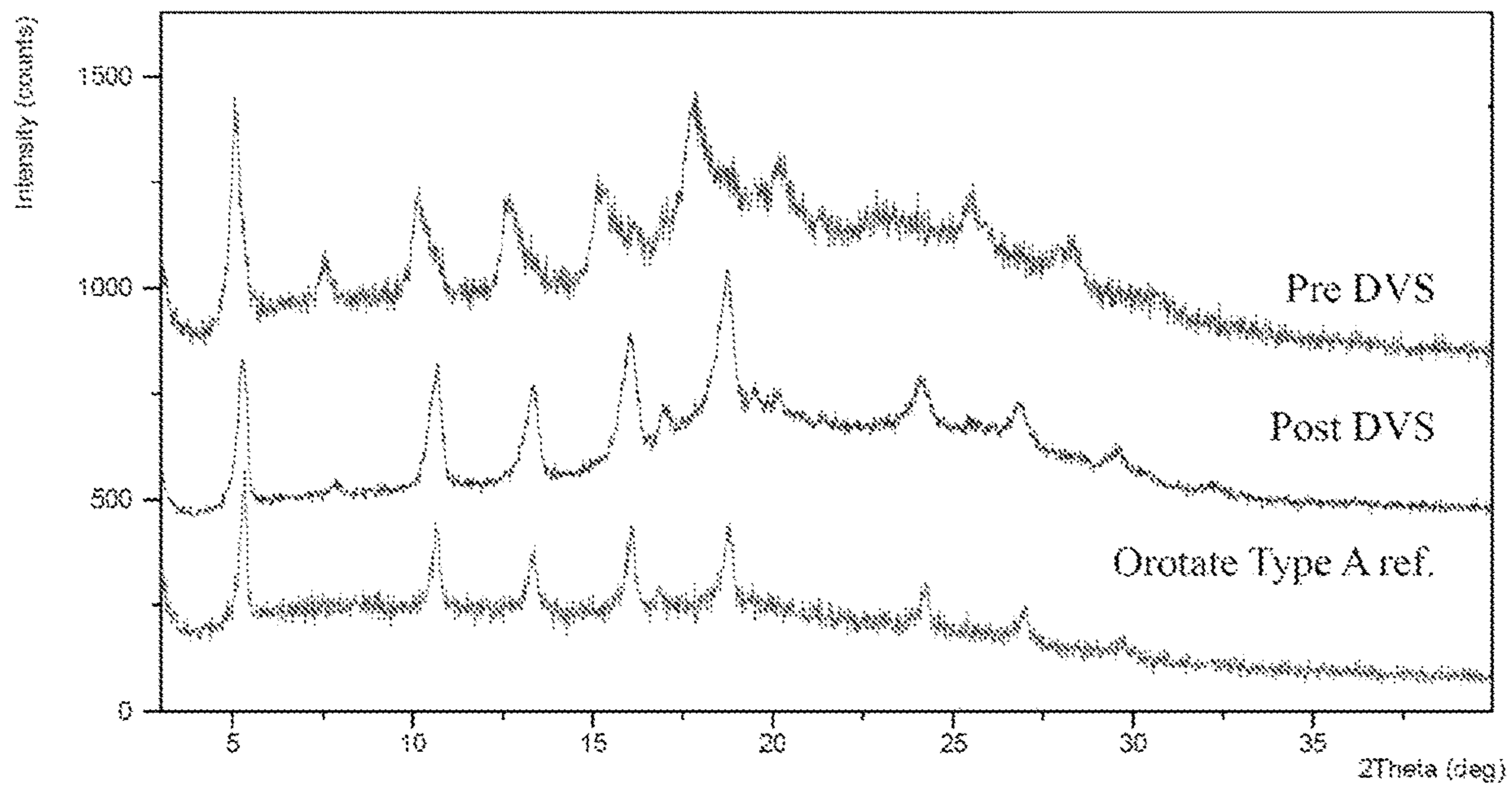


Figure 27

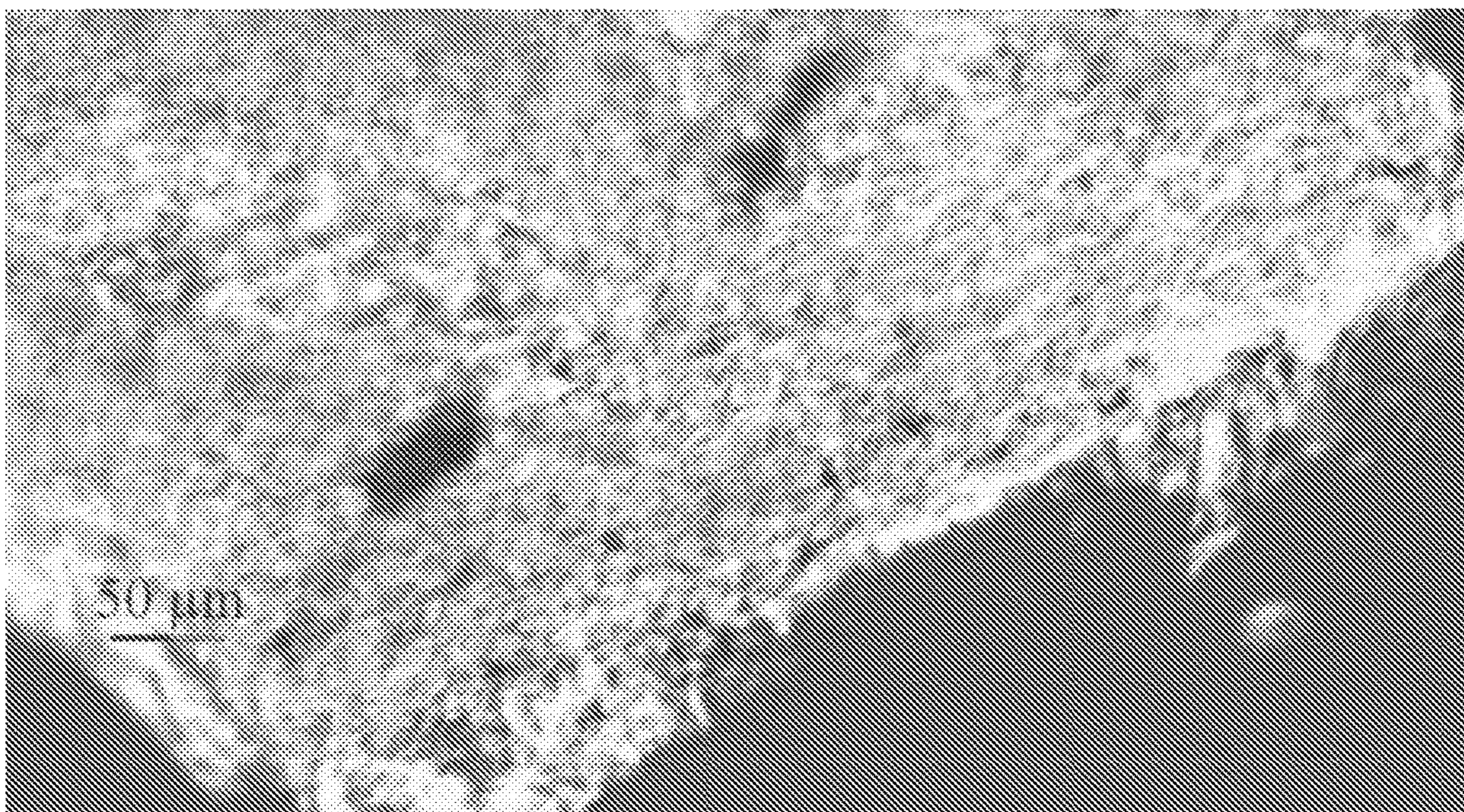


Figure 28

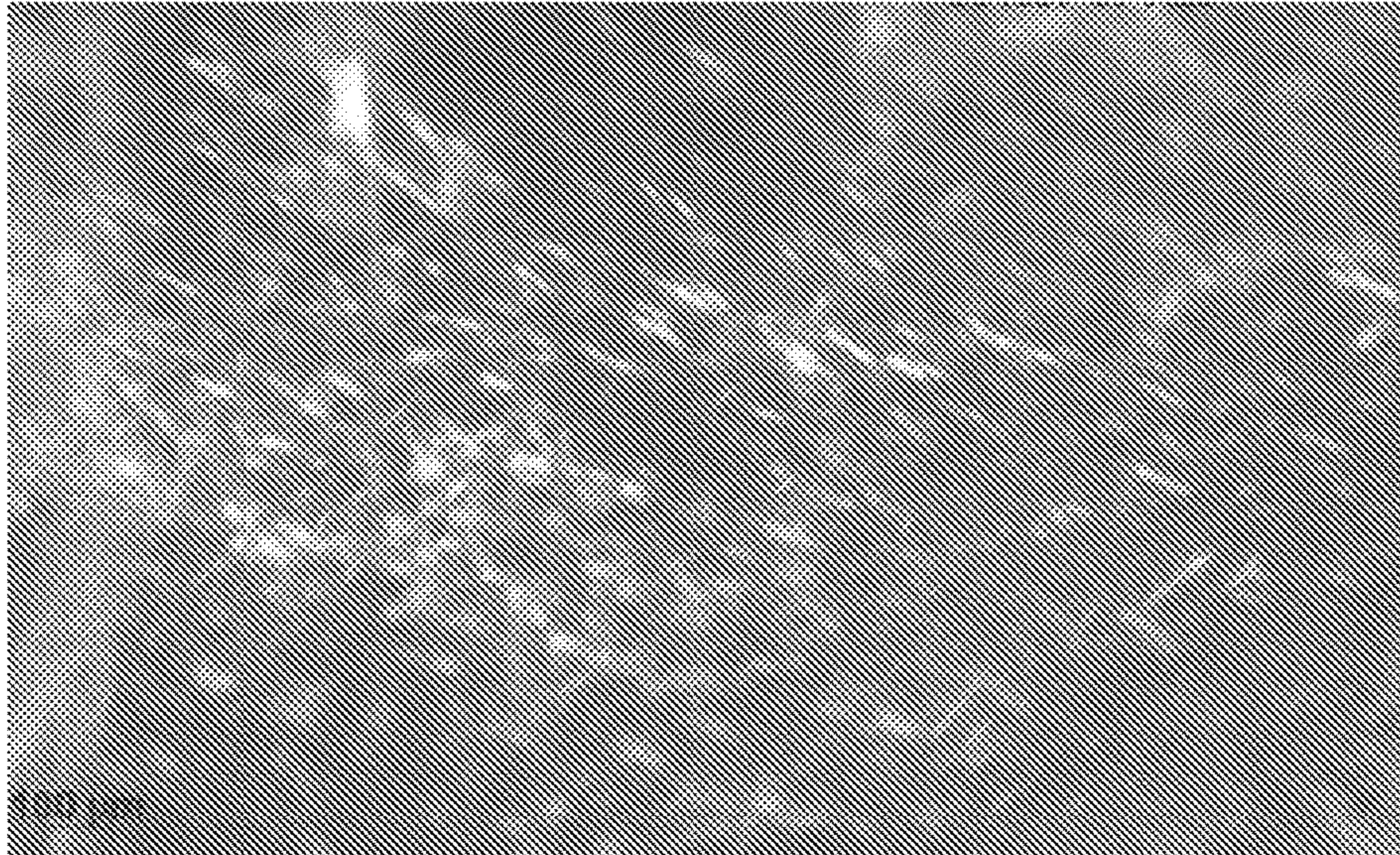


Figure 29

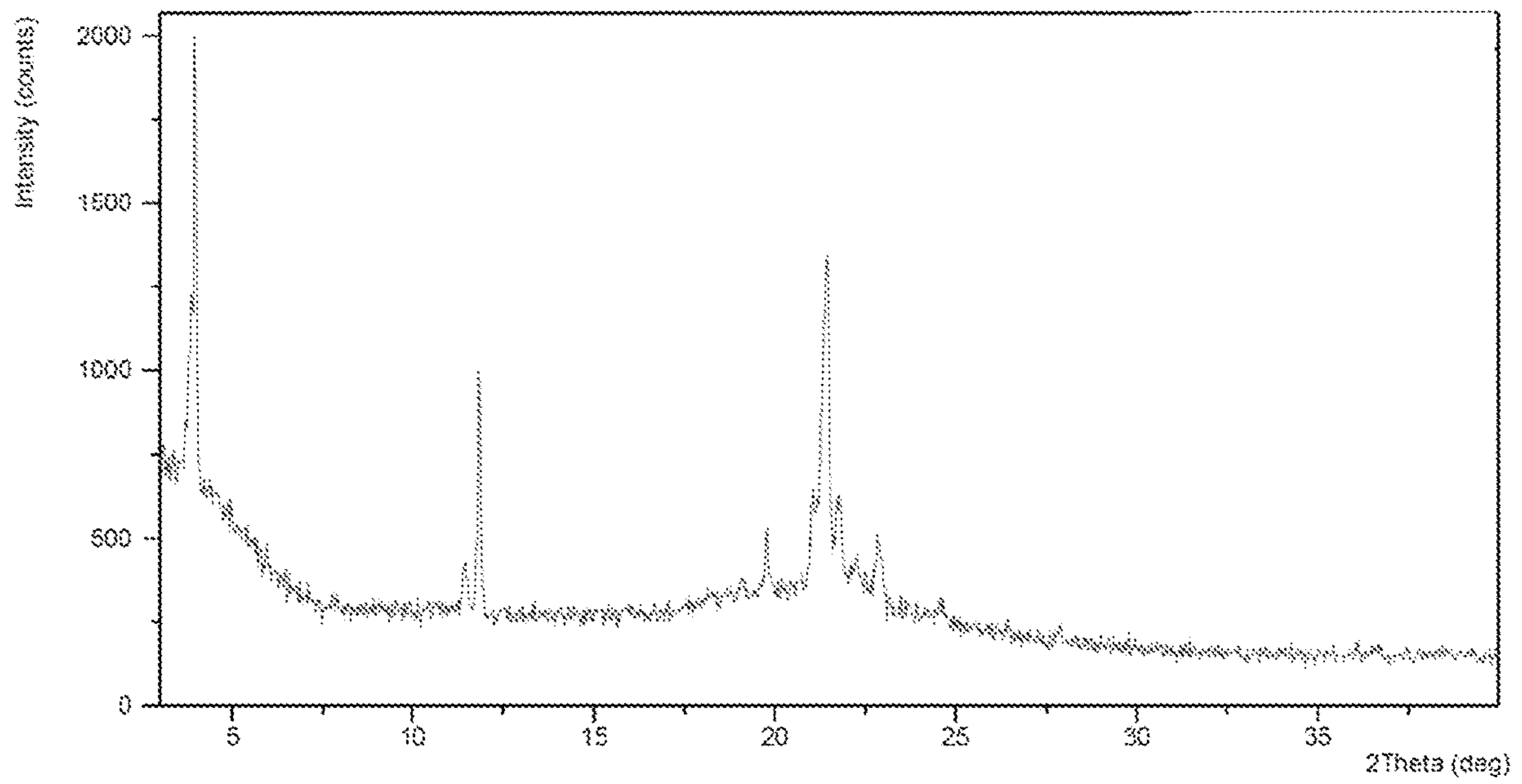


Figure 30

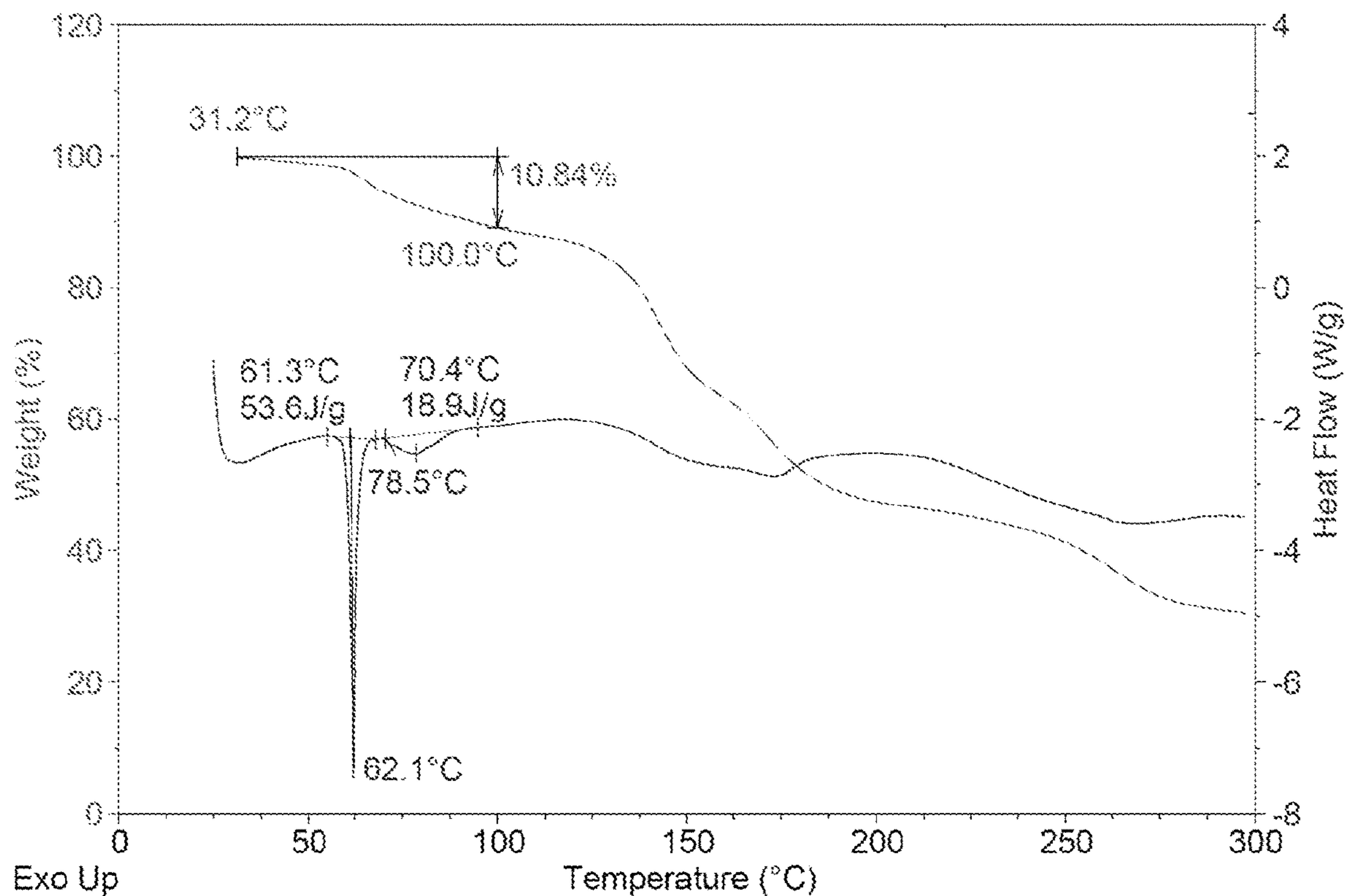


Figure 31

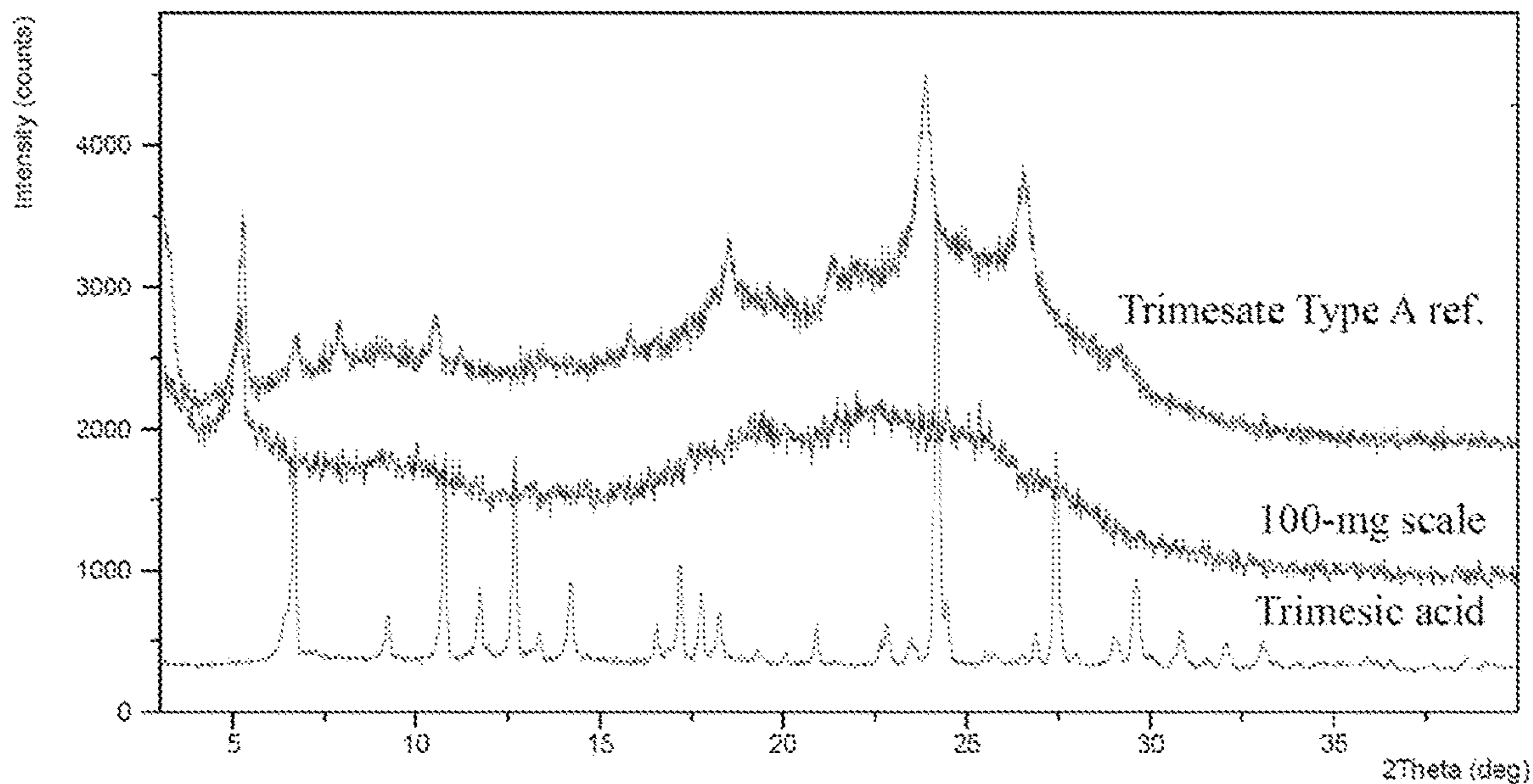


Figure 32

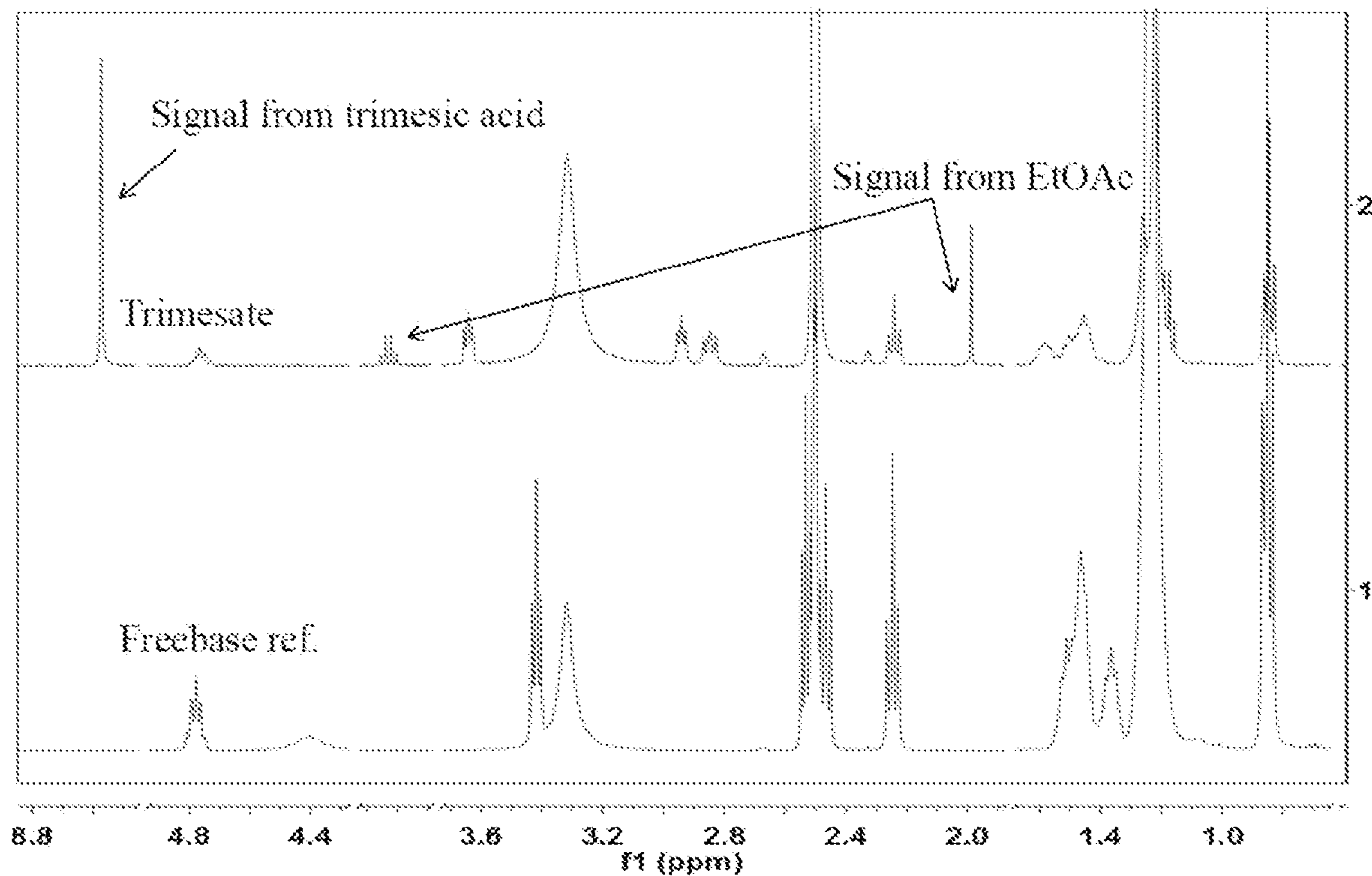


Figure 33

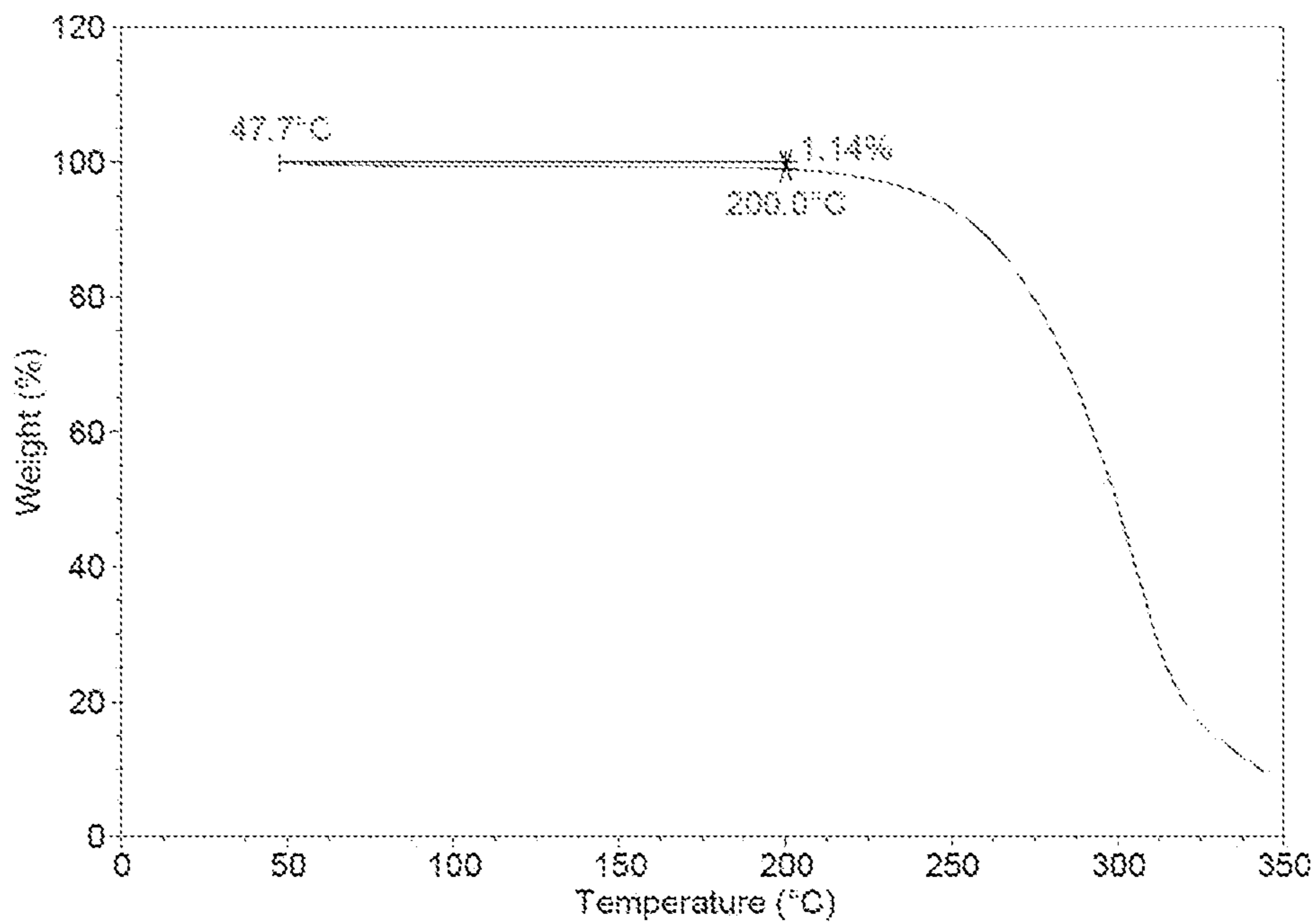


Figure 34

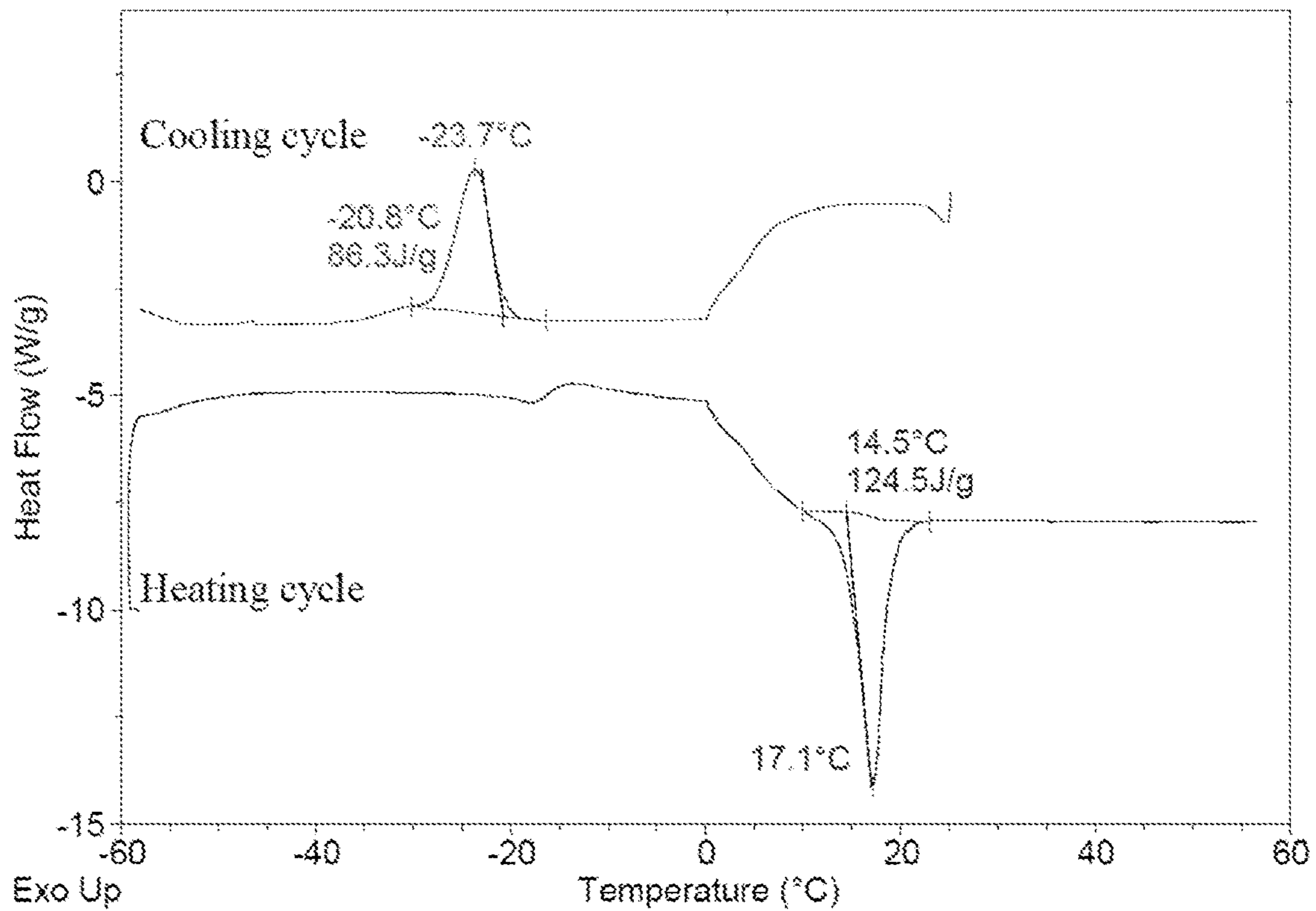


Figure 35

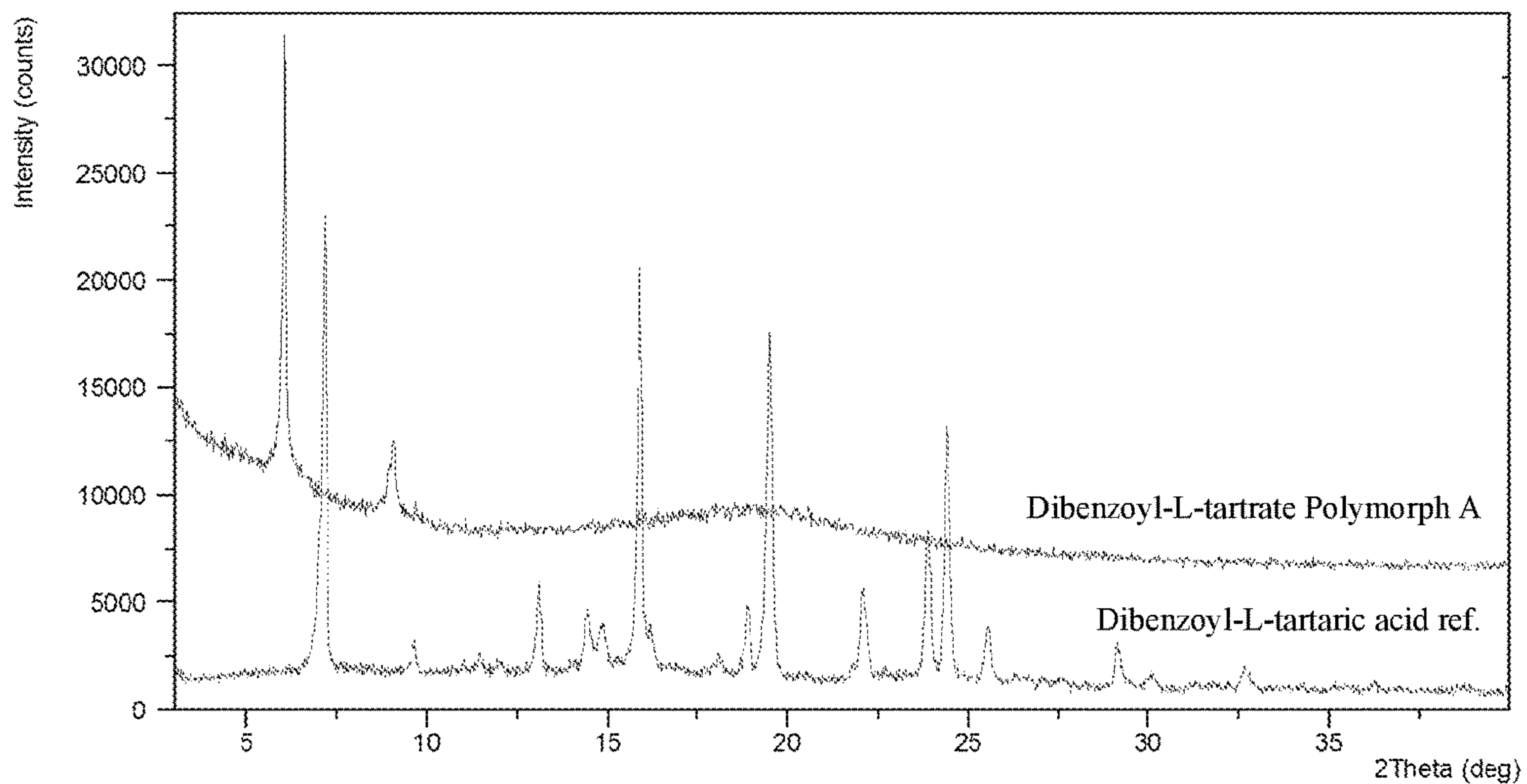


Figure 36

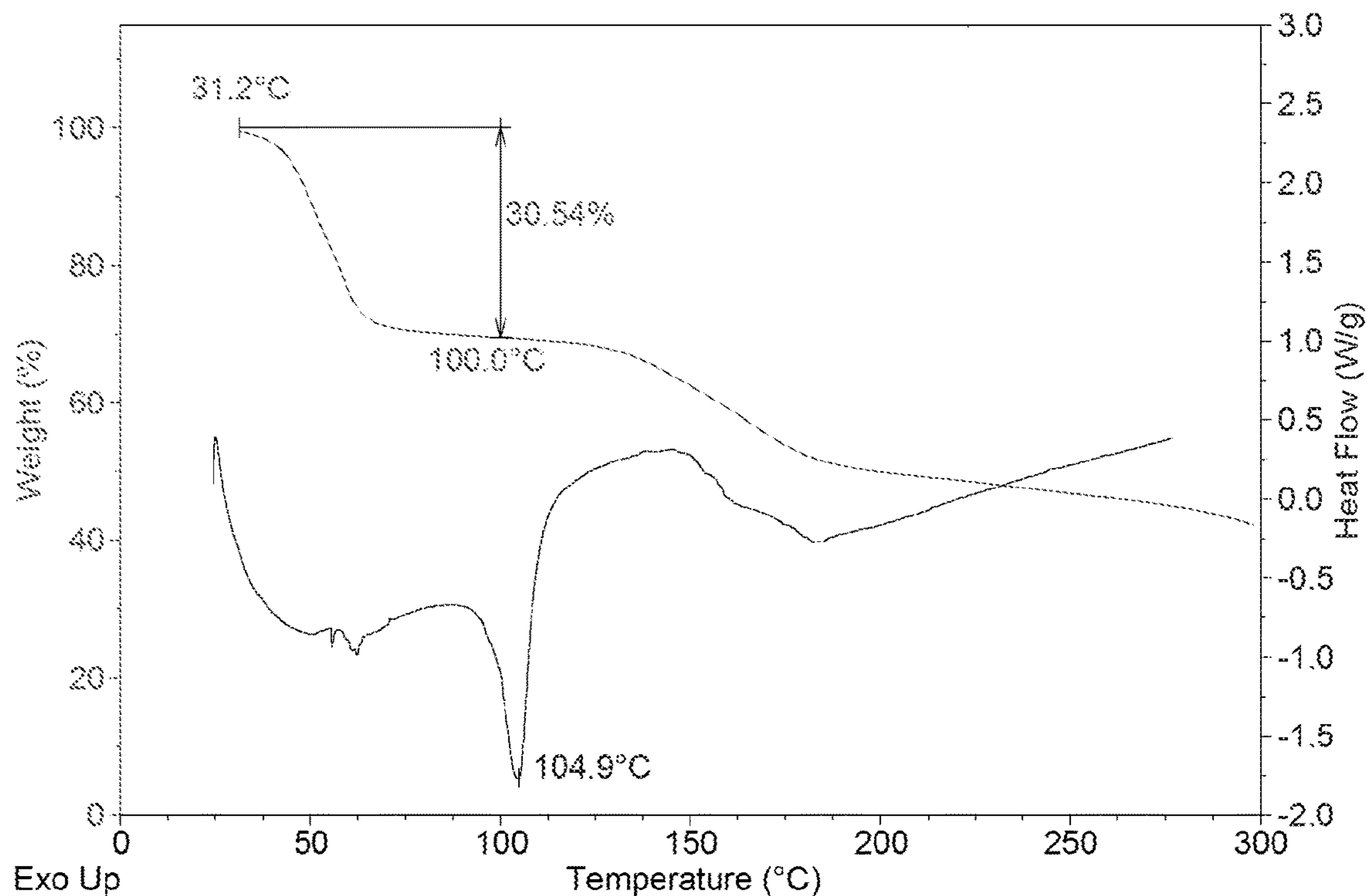


Figure 37

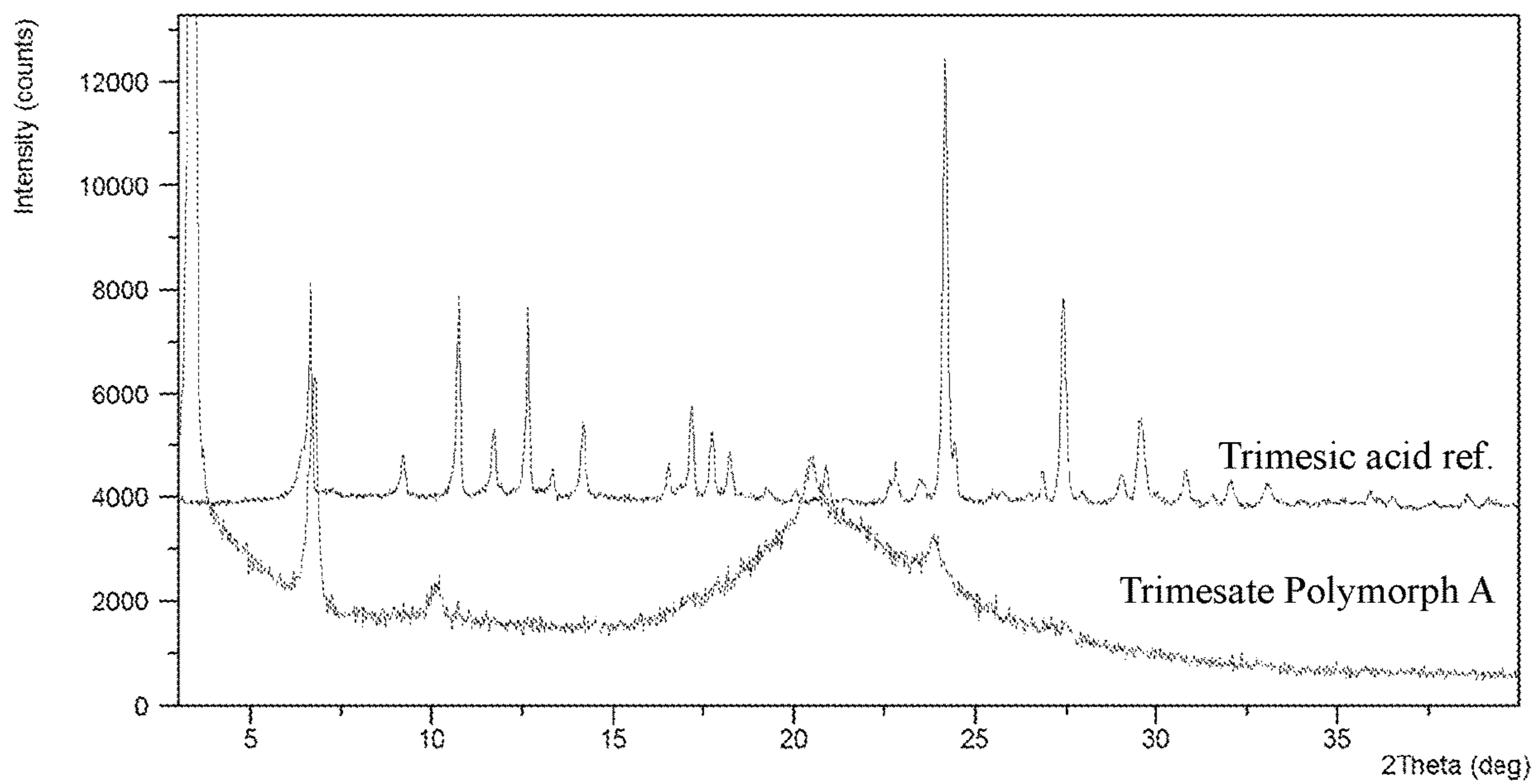


Figure 38

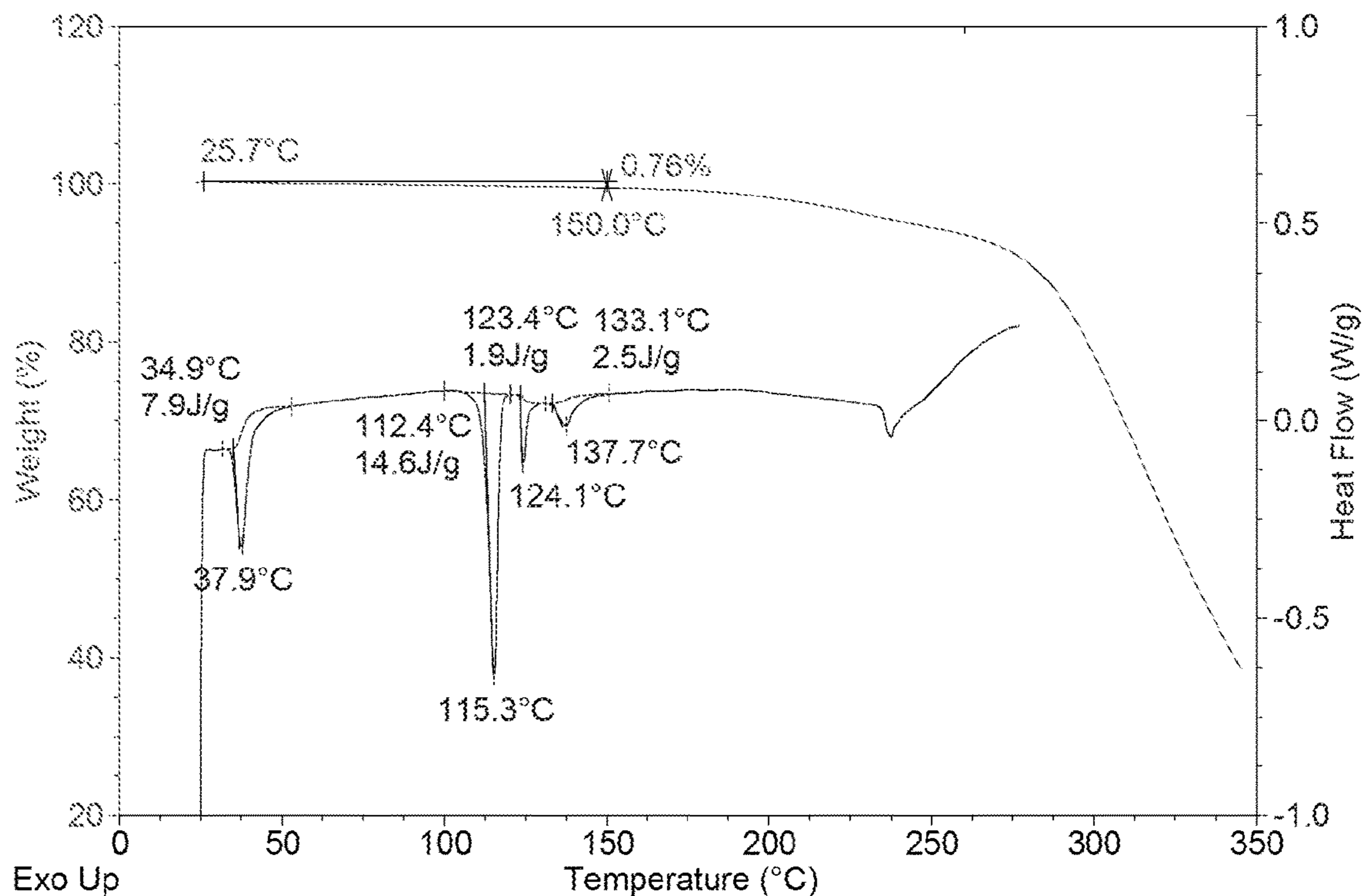


Figure 39

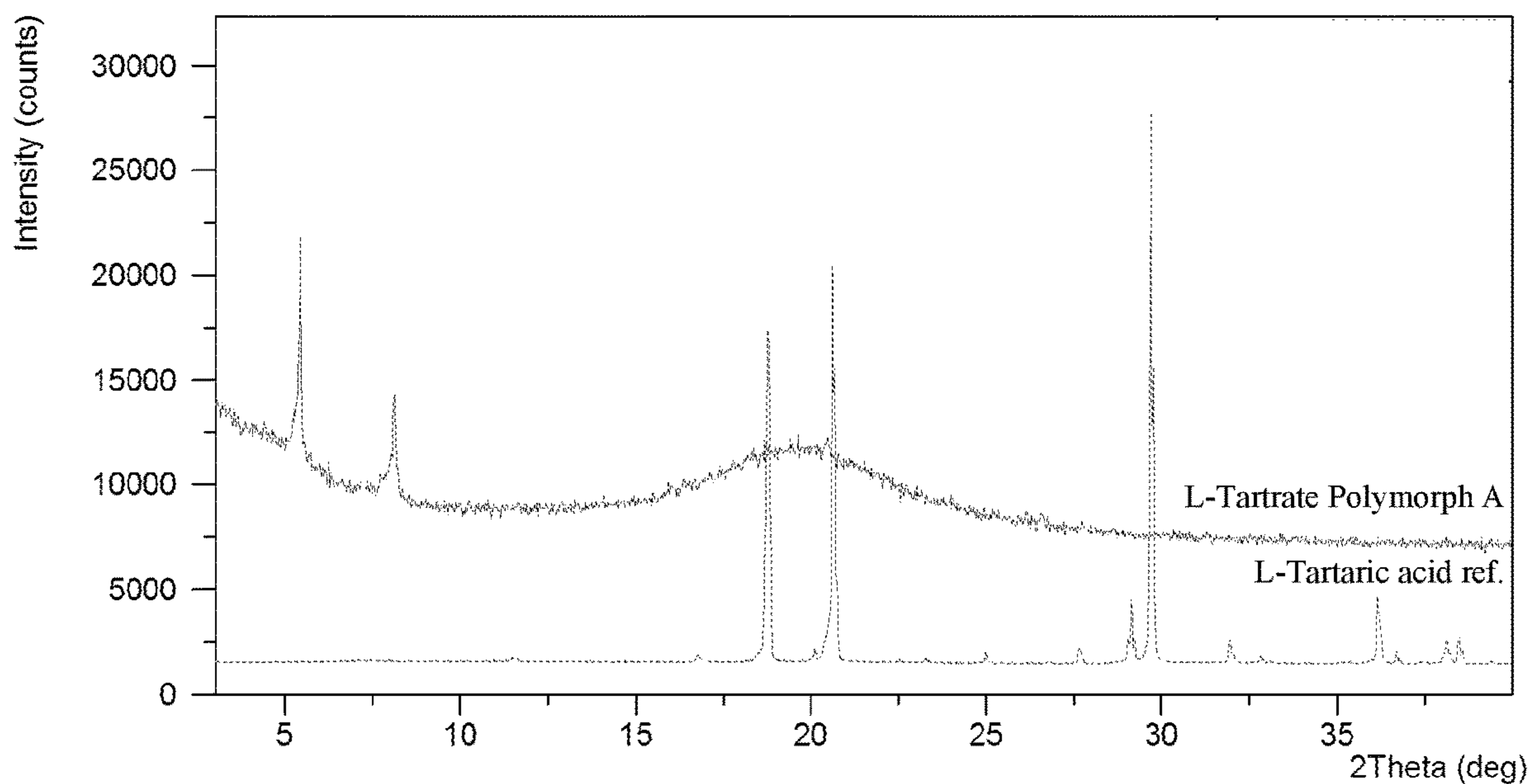


Figure 40

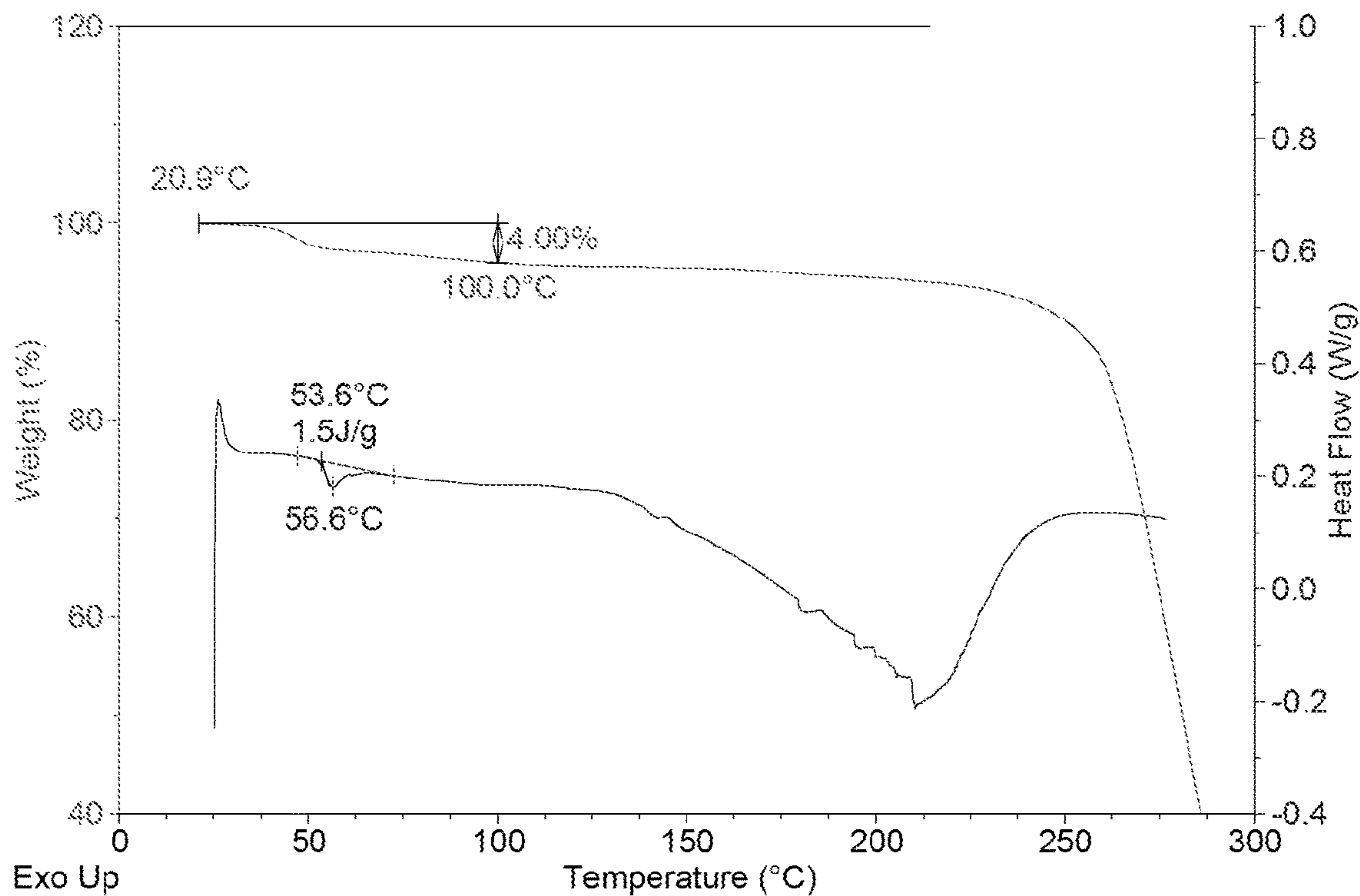


Figure 41

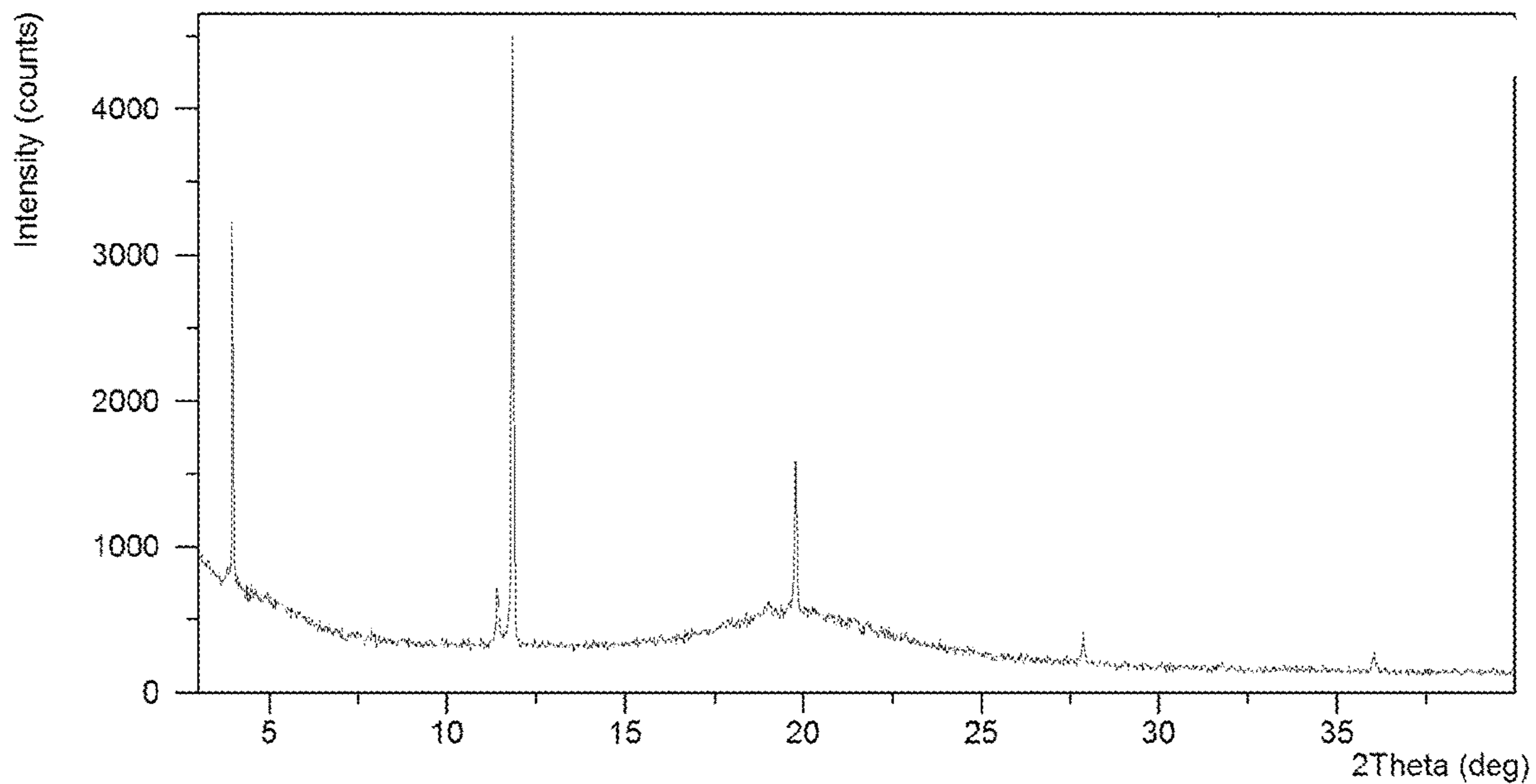


Figure 42

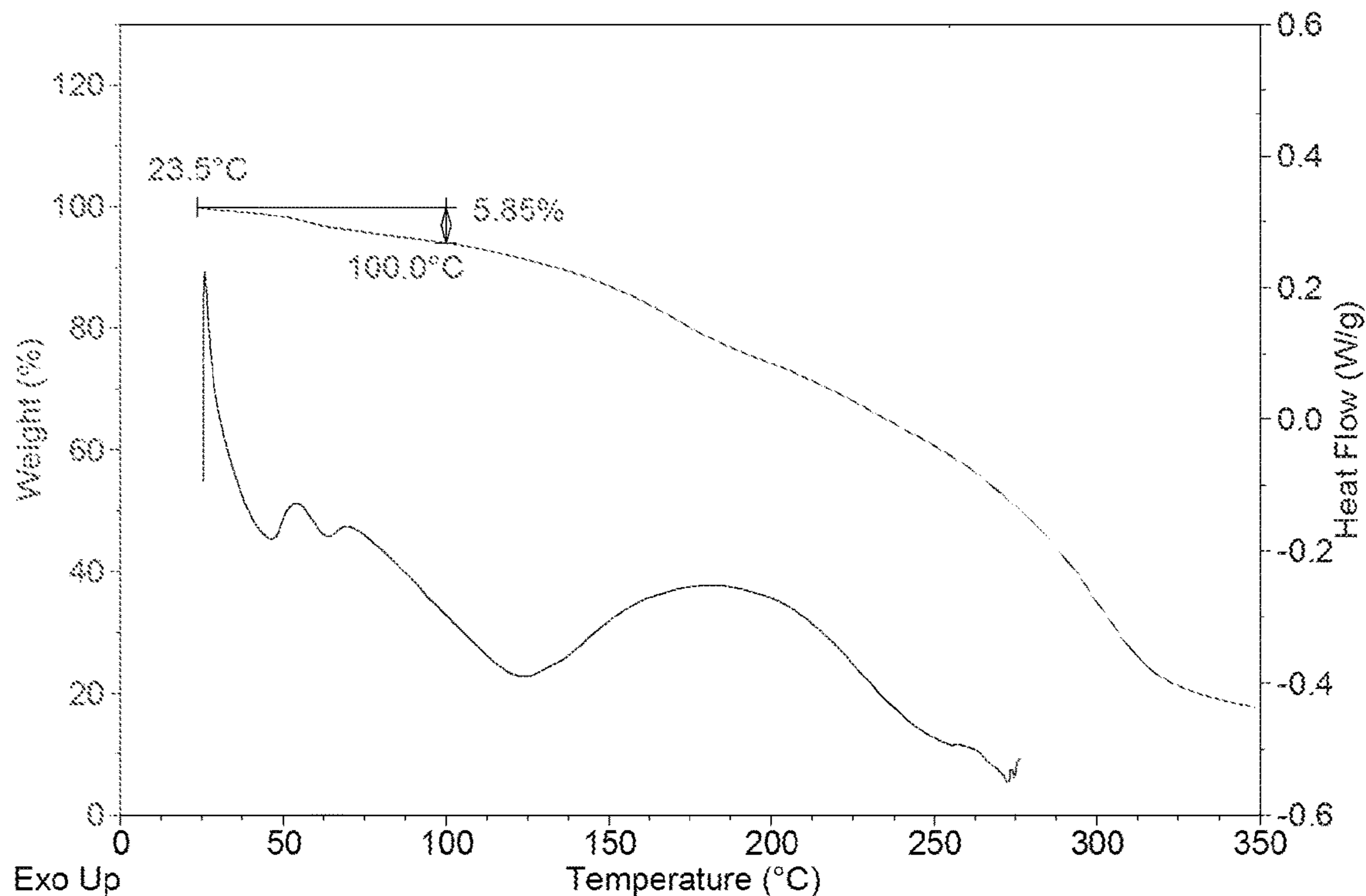


Figure 43

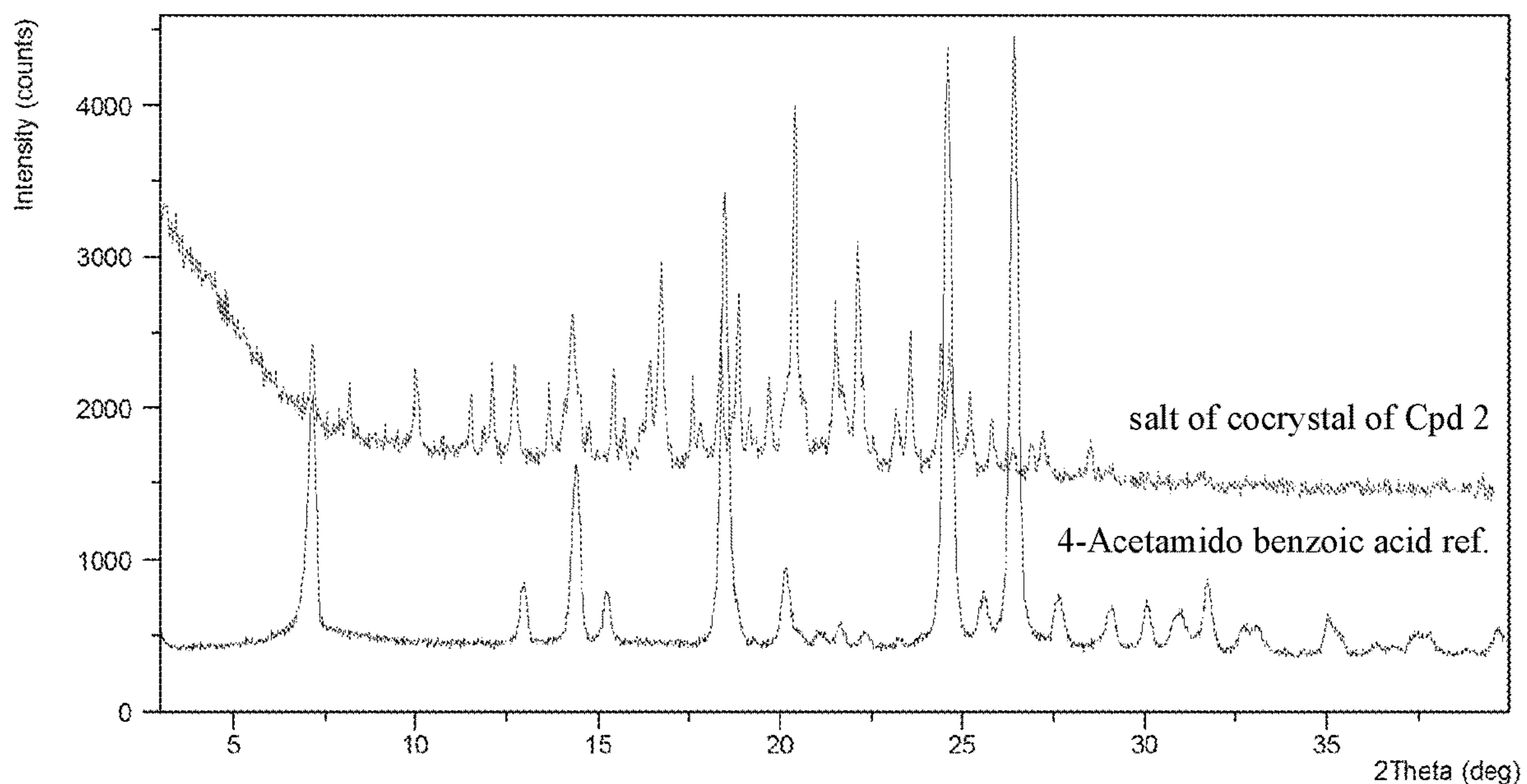


Figure 44

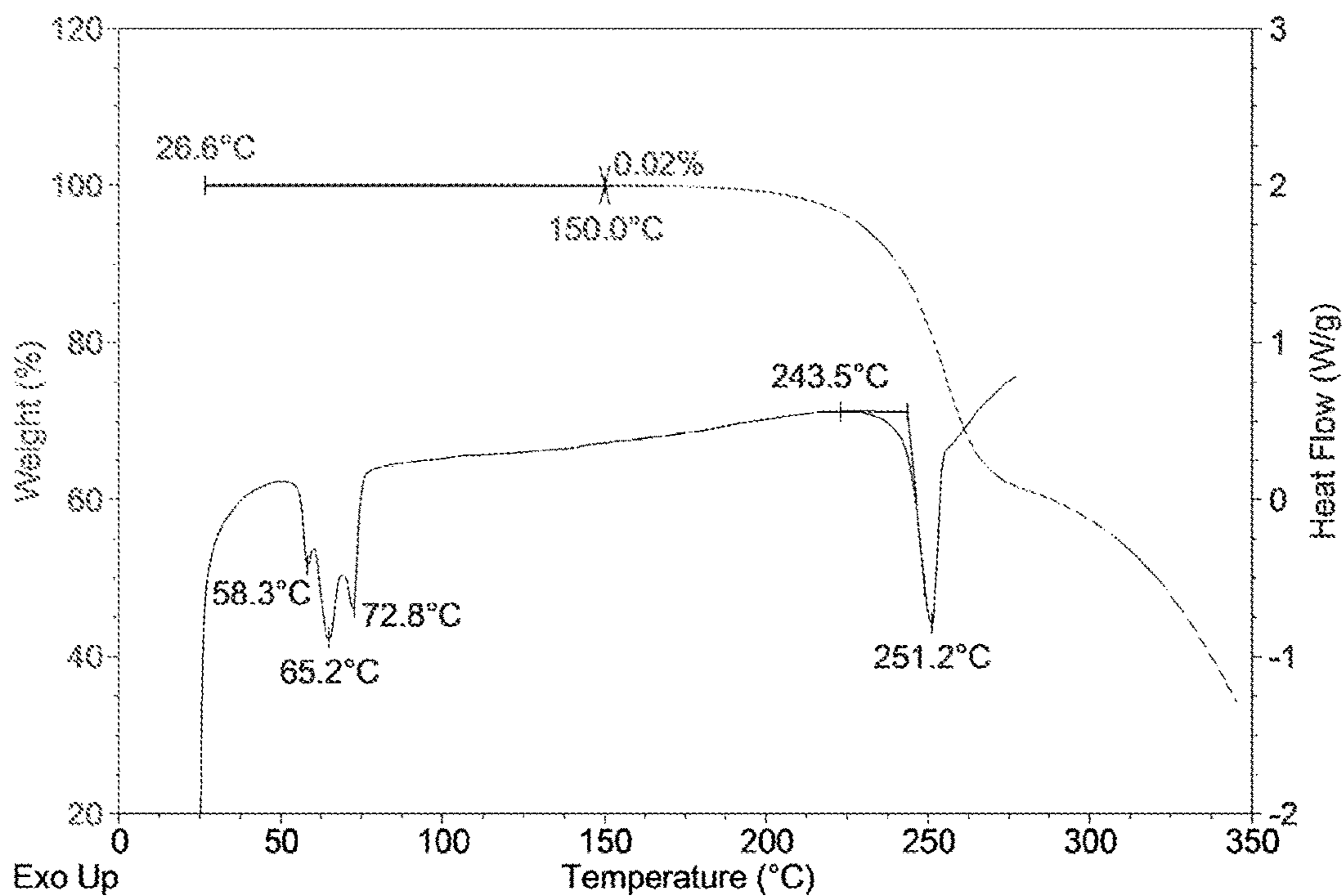


Figure 45

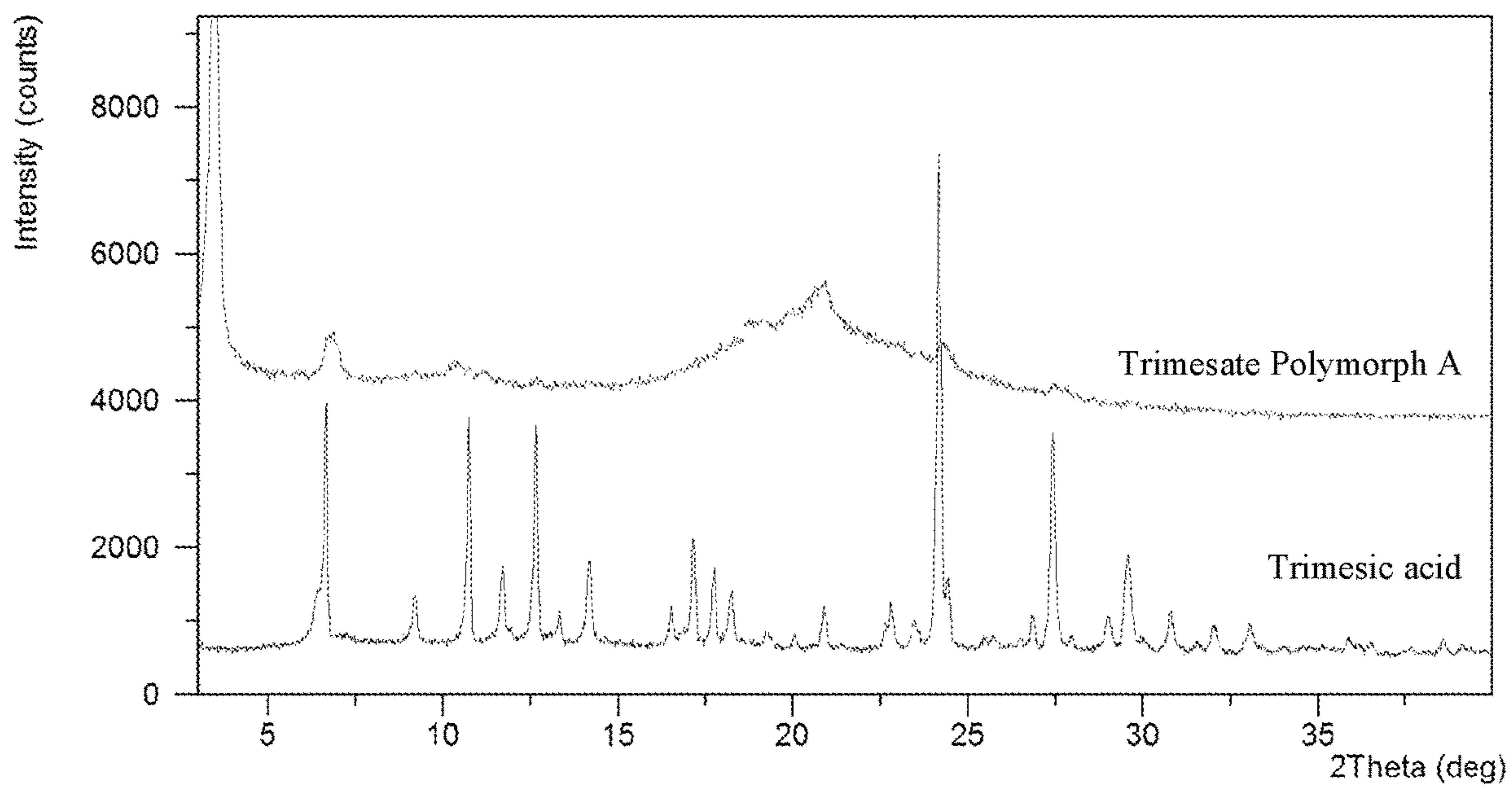


Figure 46

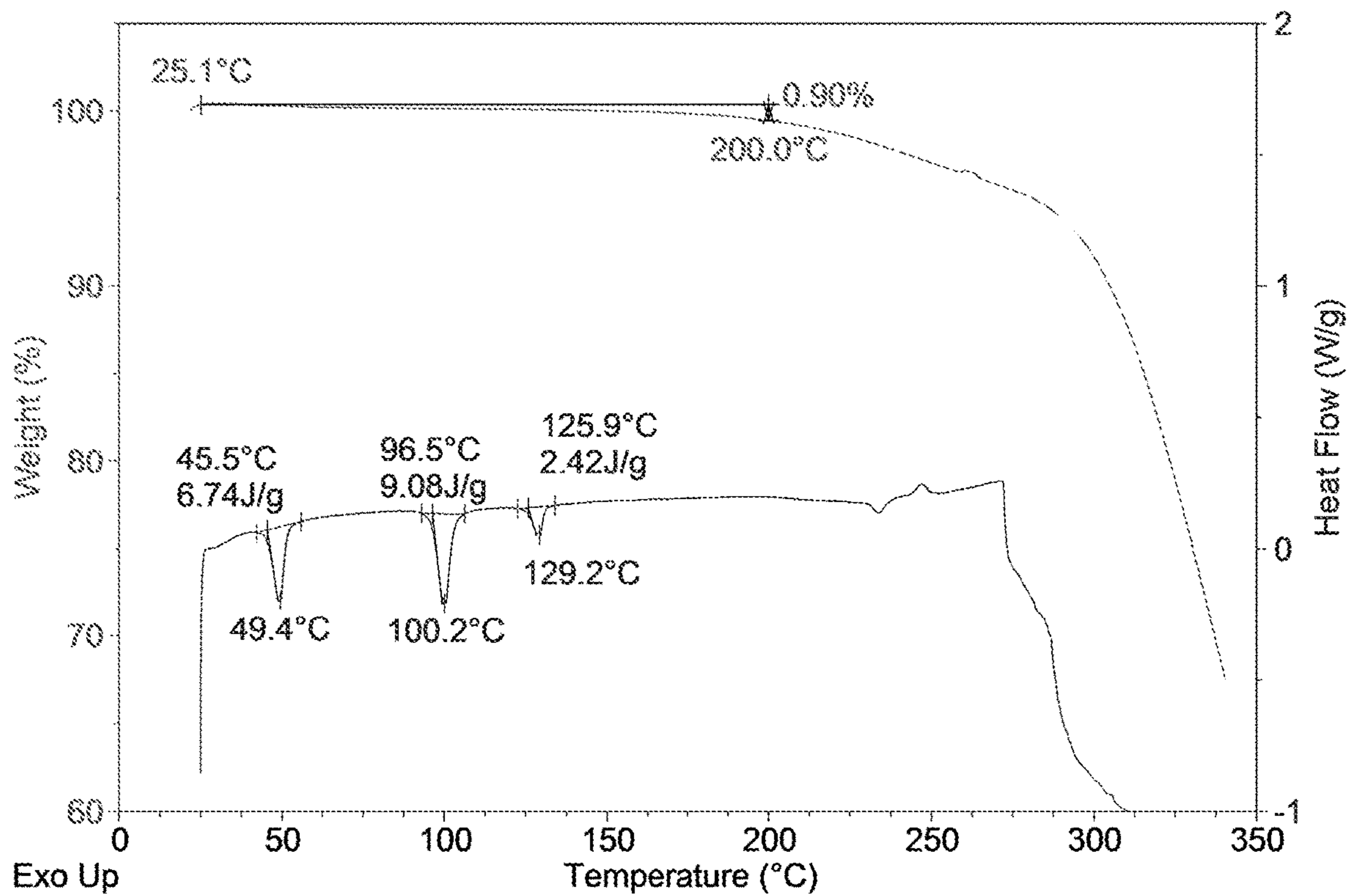


Figure 47

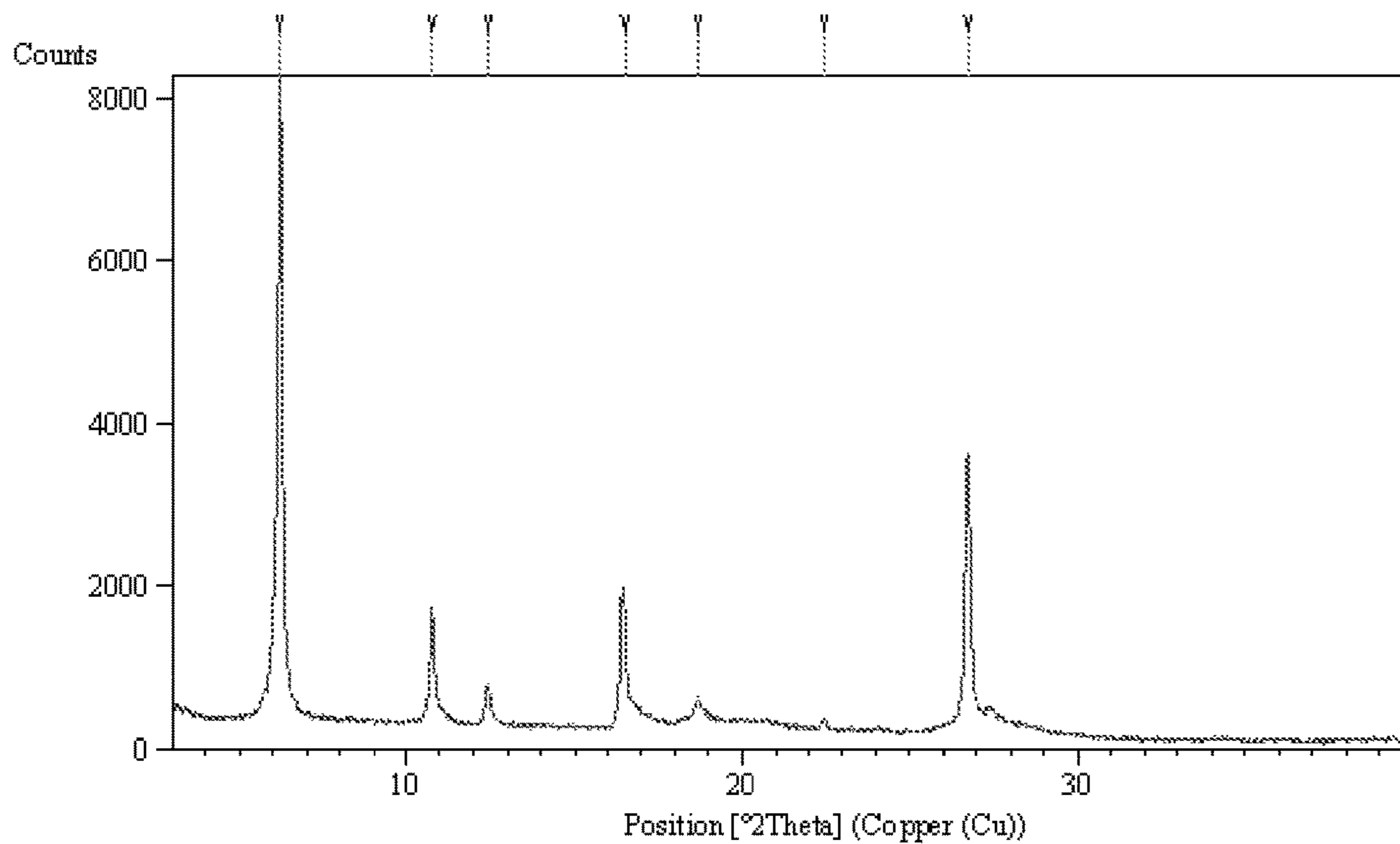


Figure 48

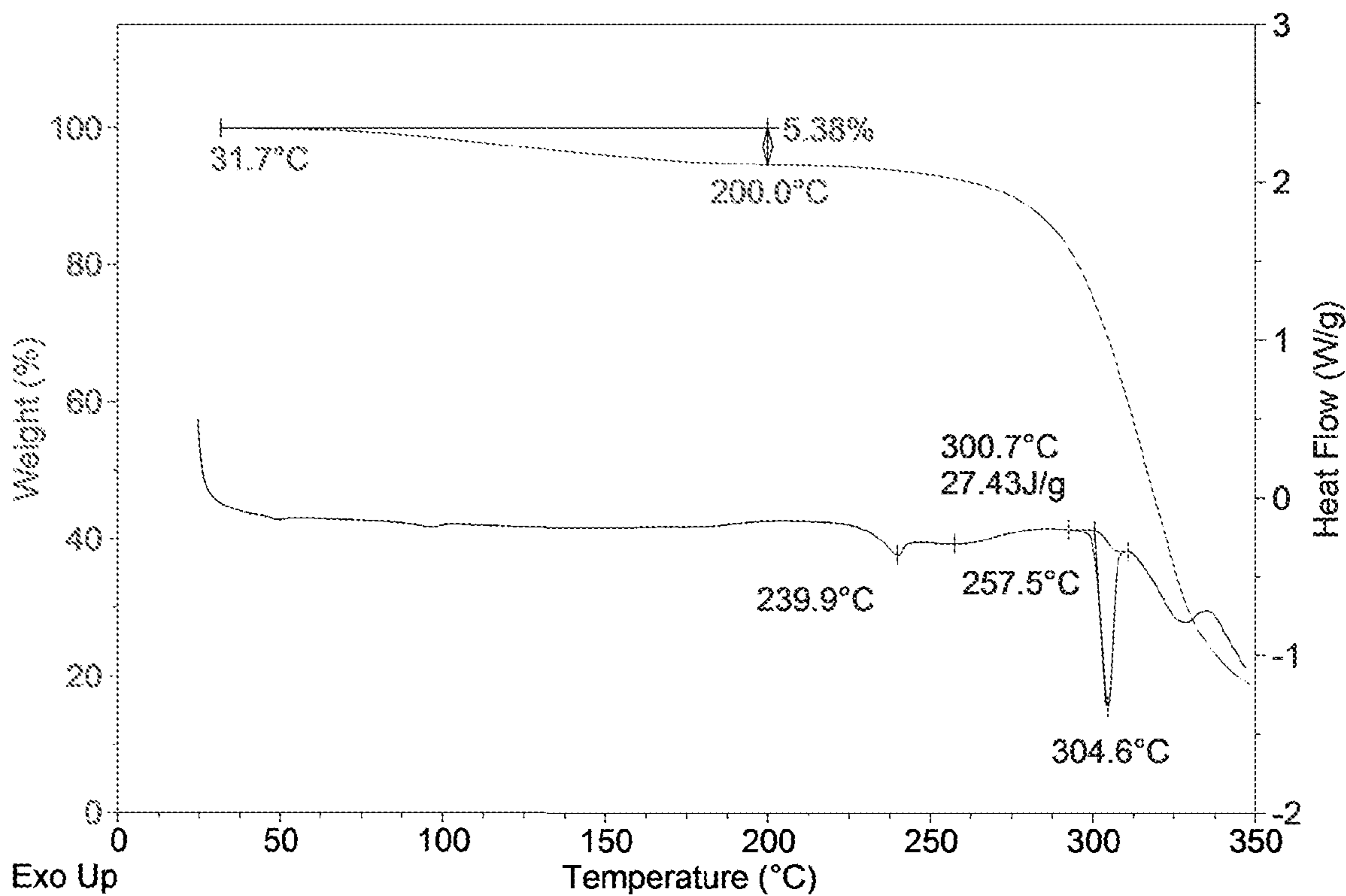


Figure 49

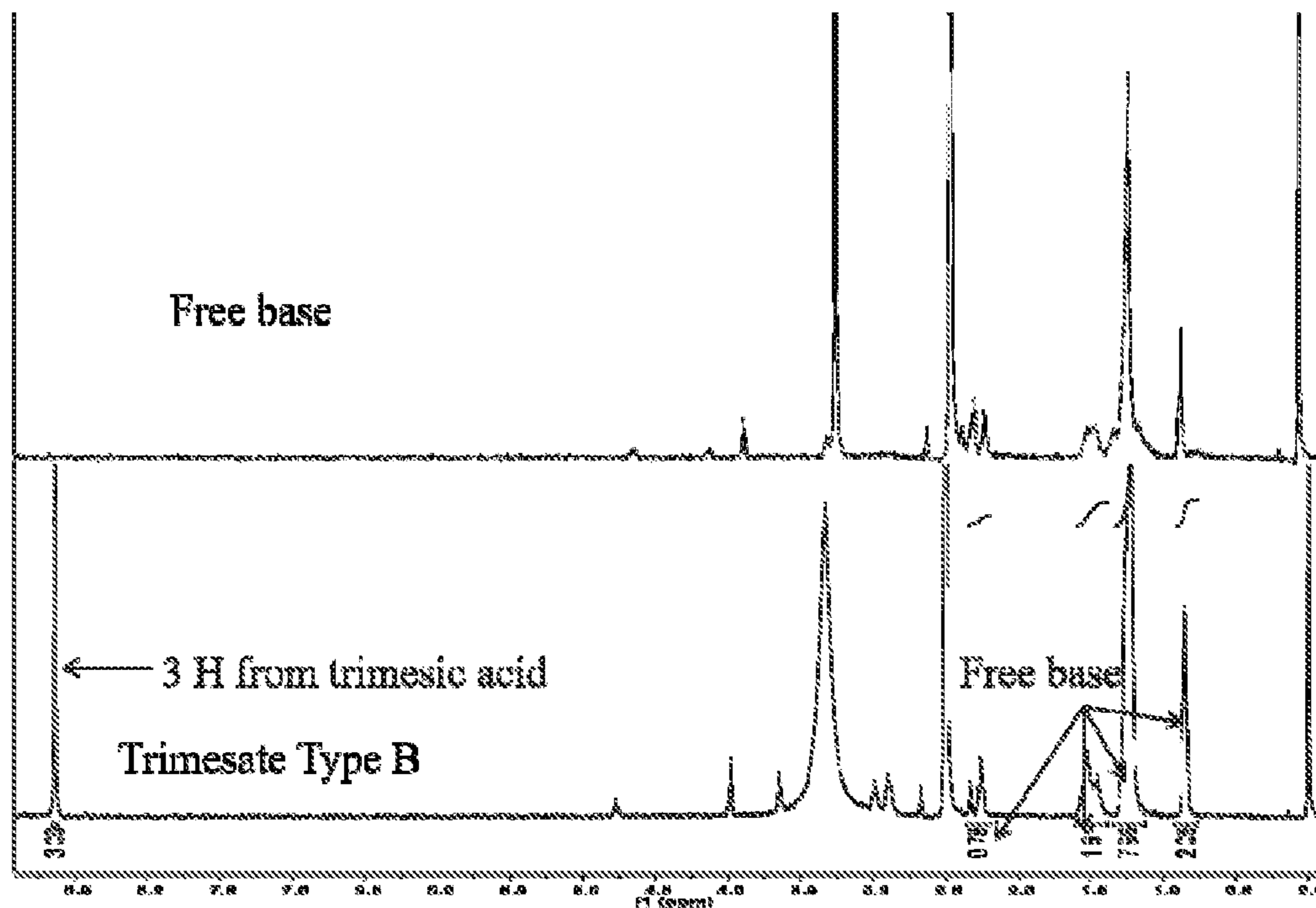


Figure 50

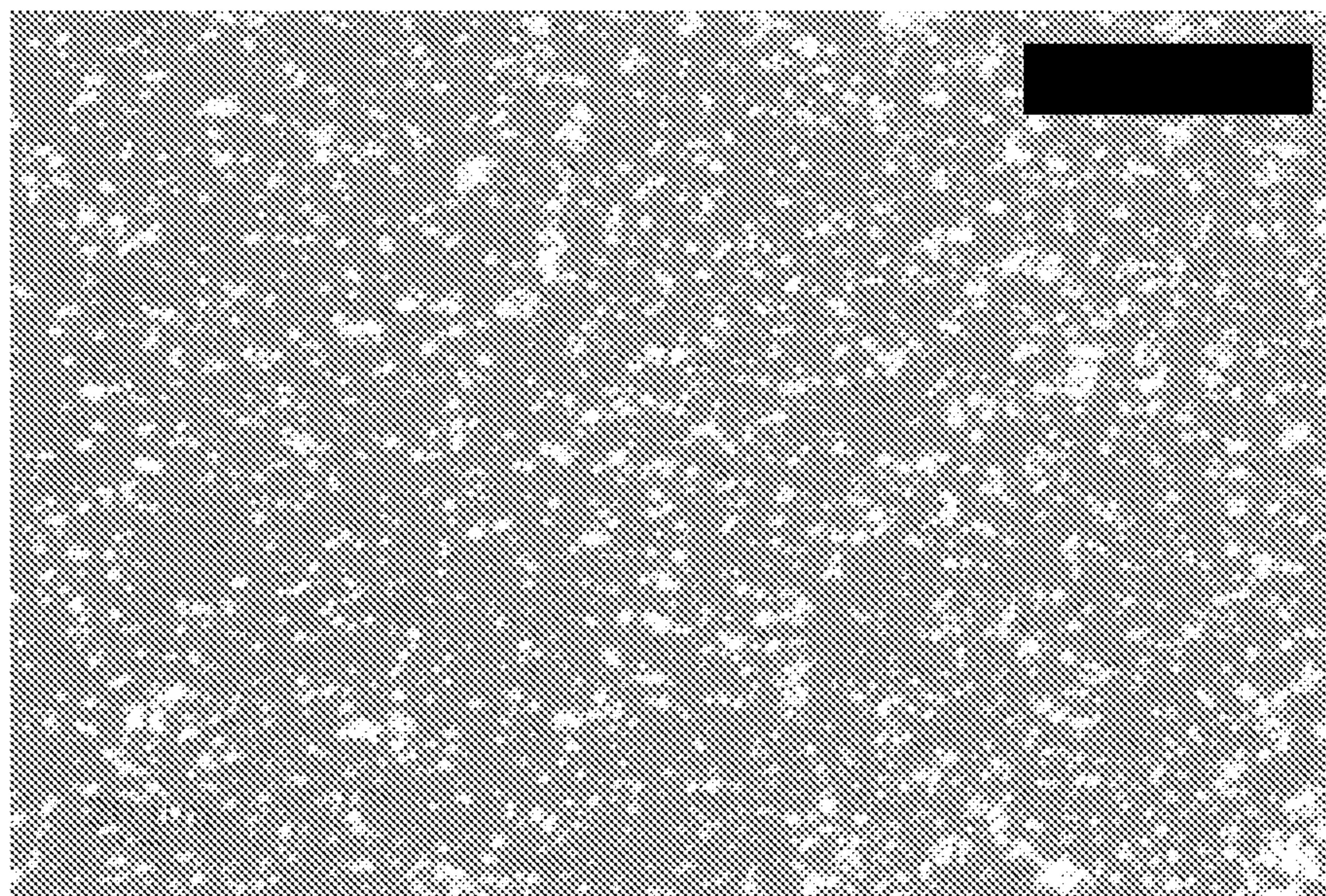


Figure 51

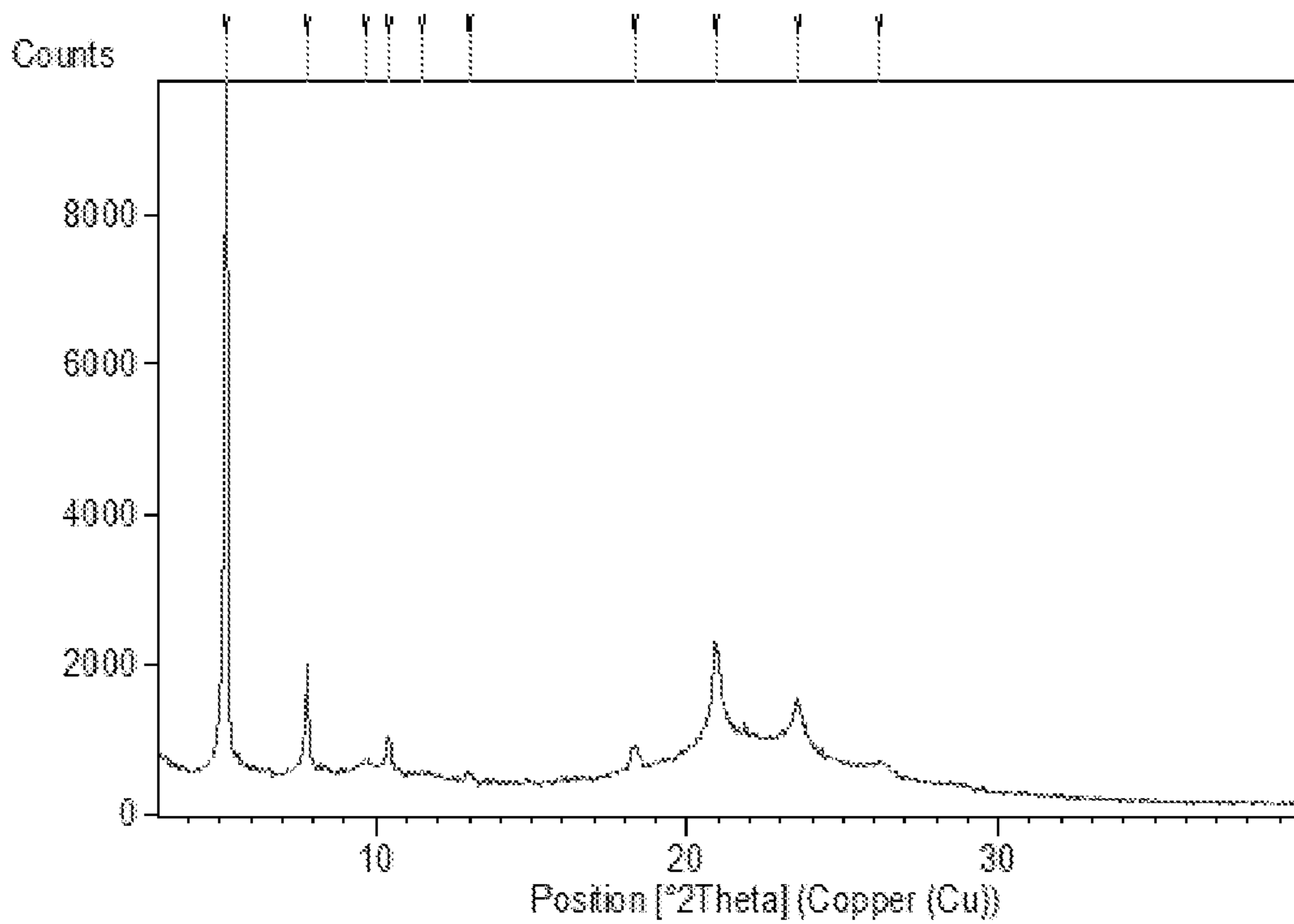


Figure 52

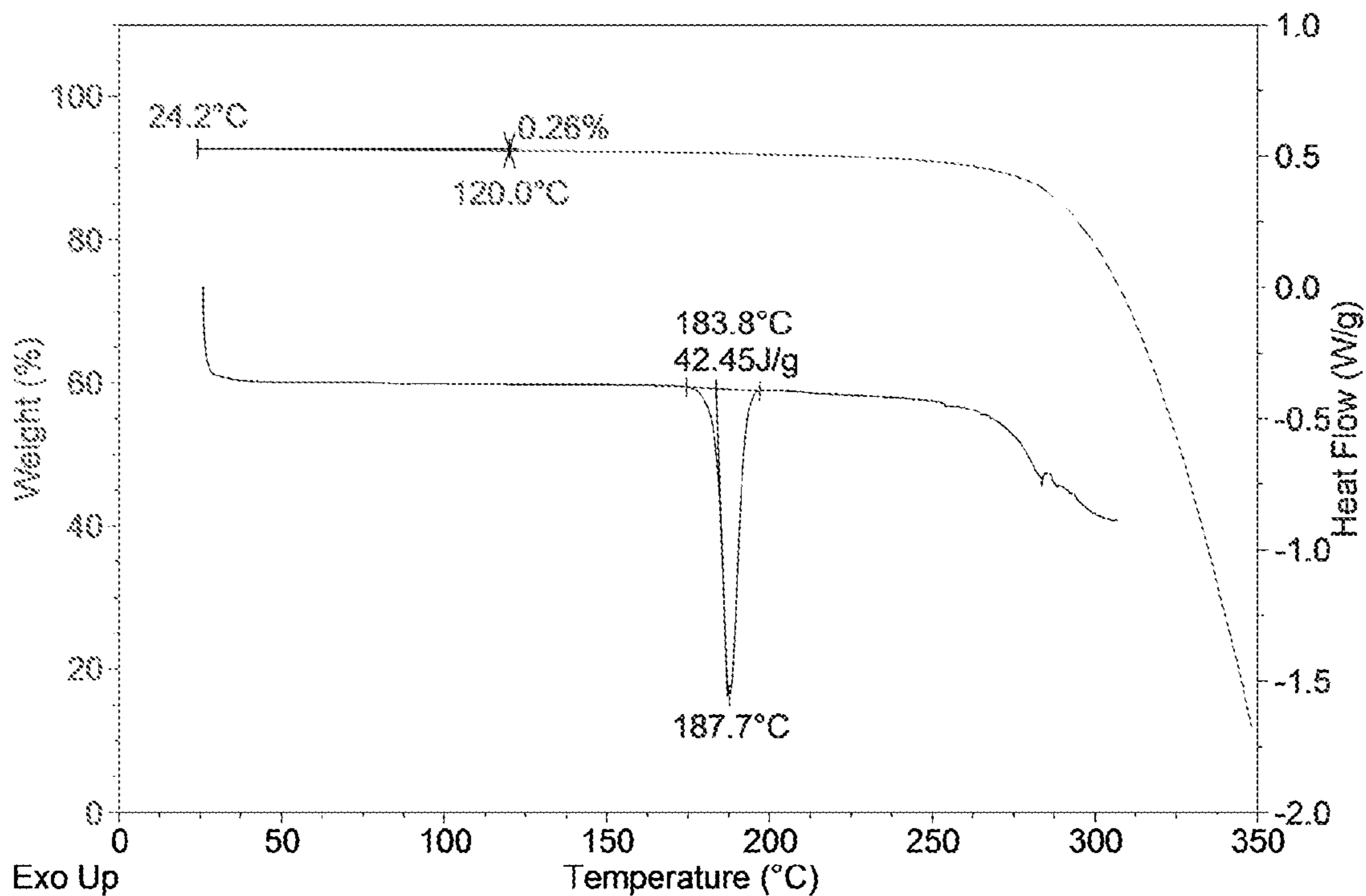


Figure 53

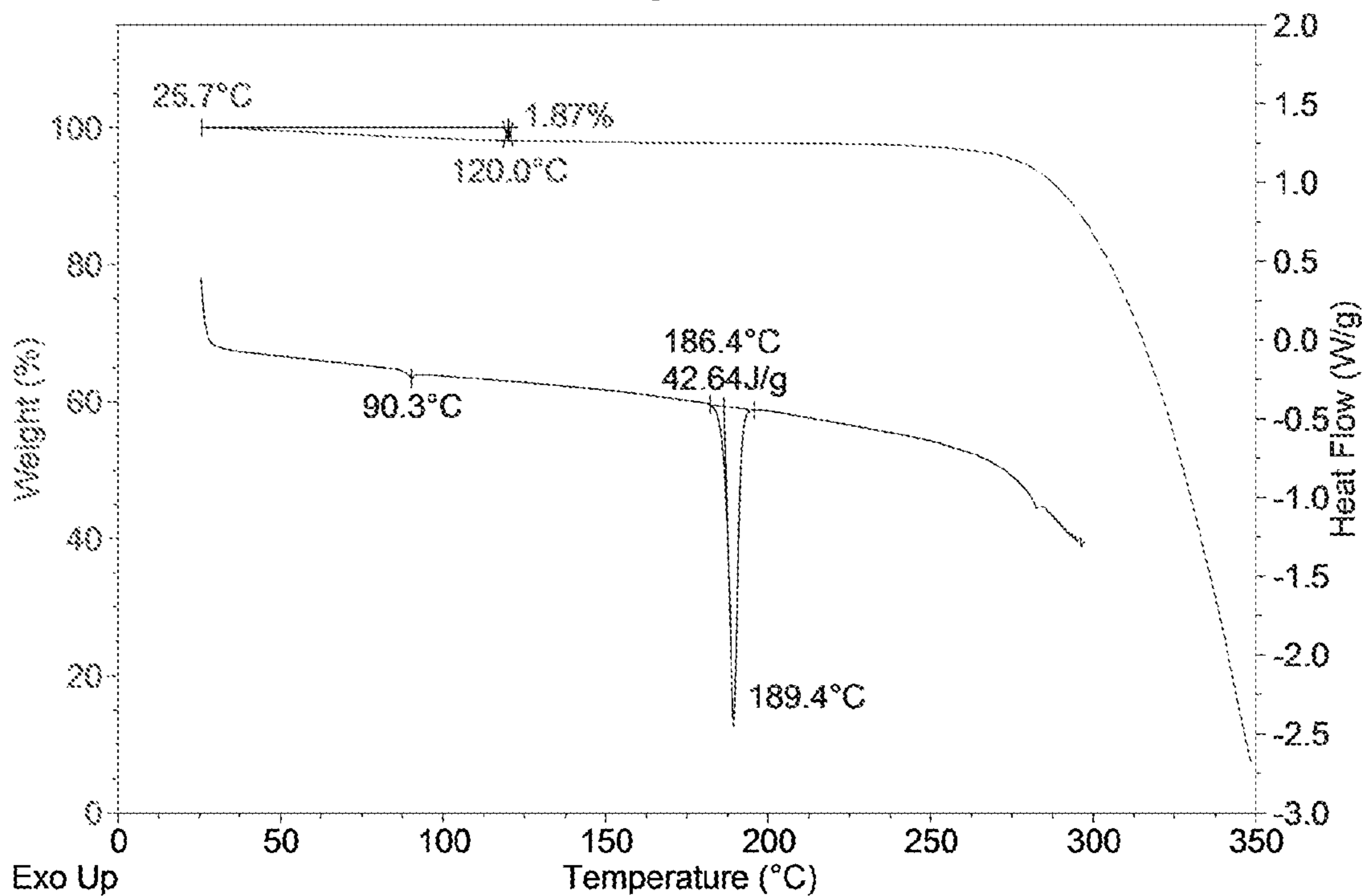


Figure 54

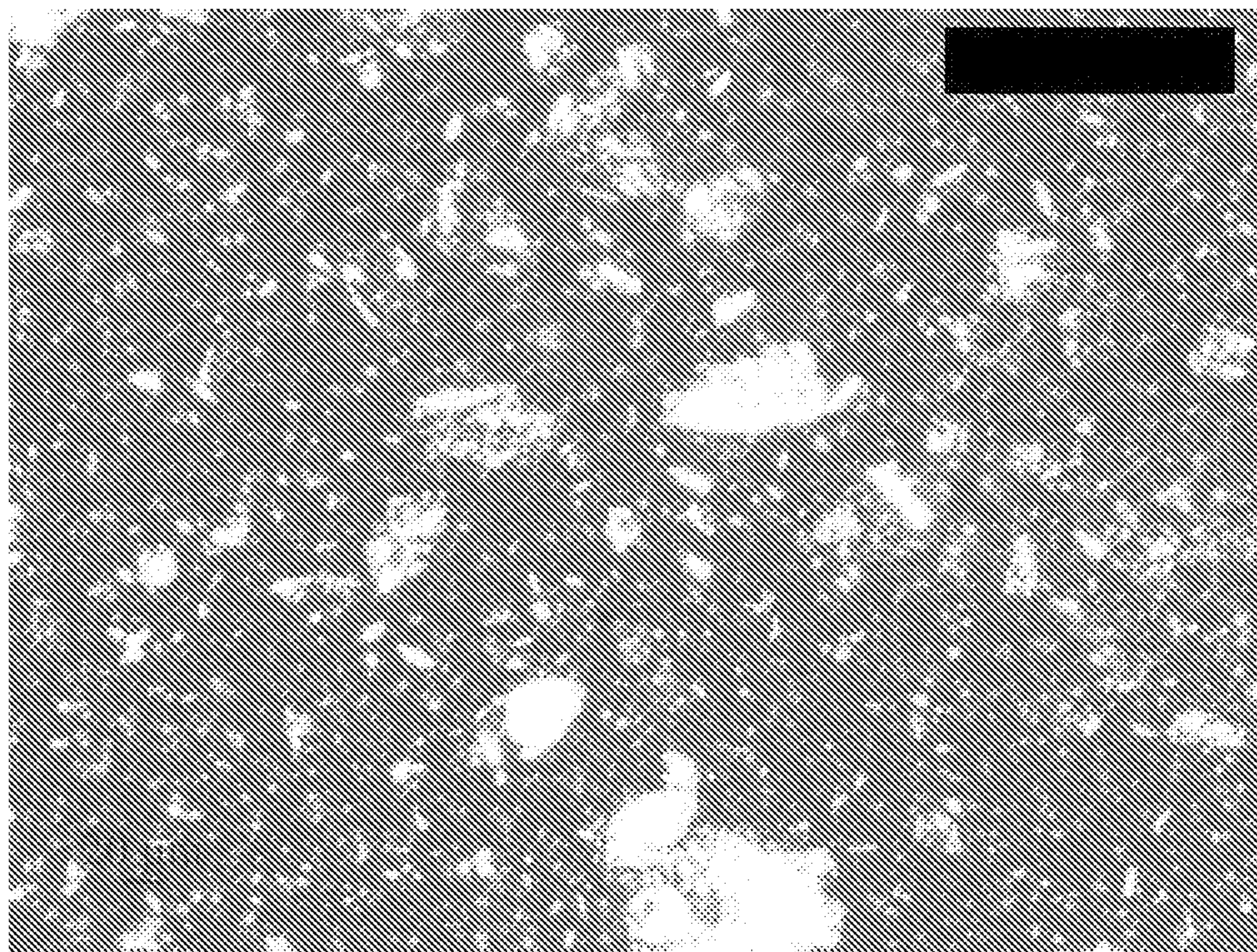


Figure 55

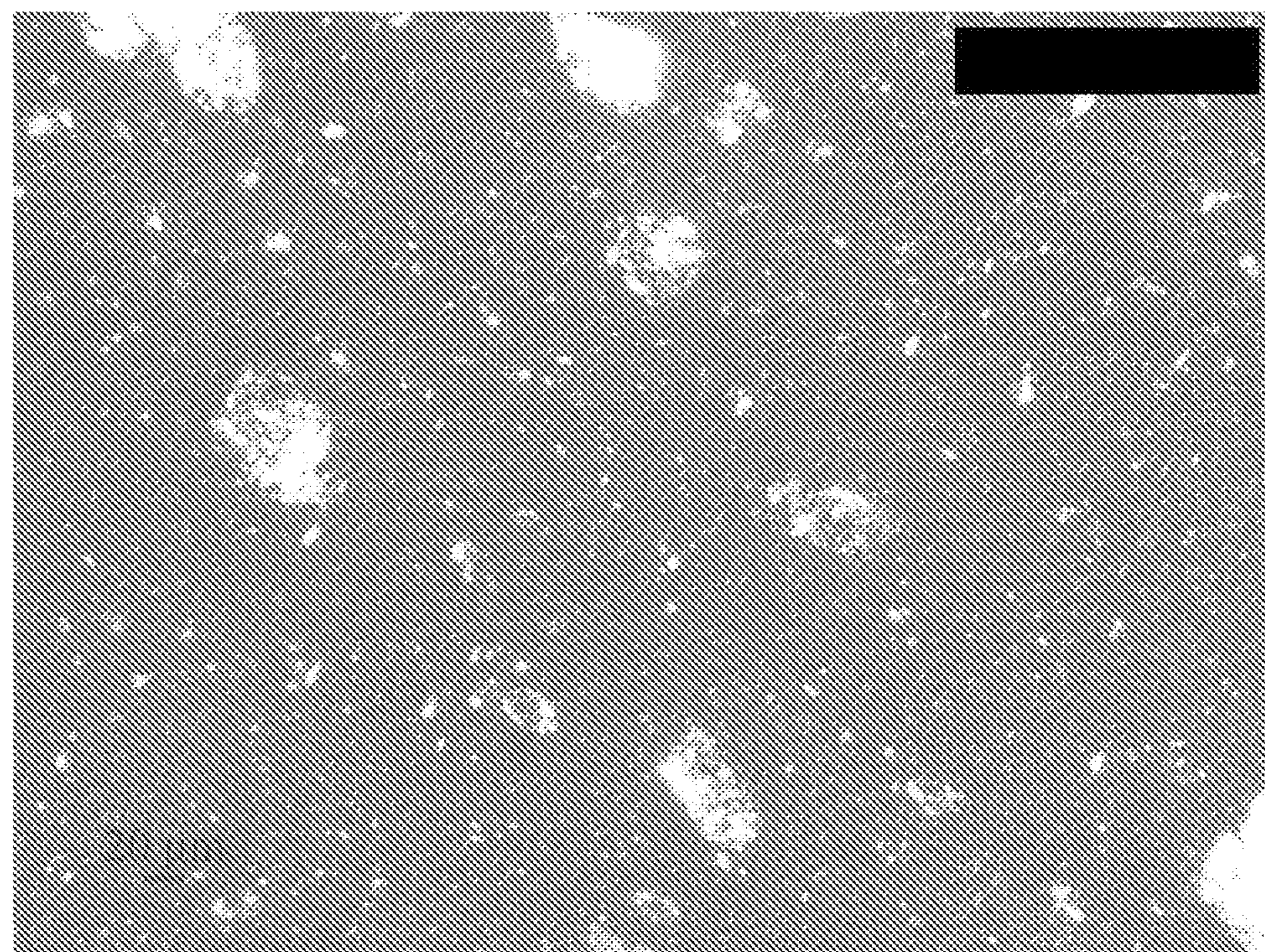


Figure 56

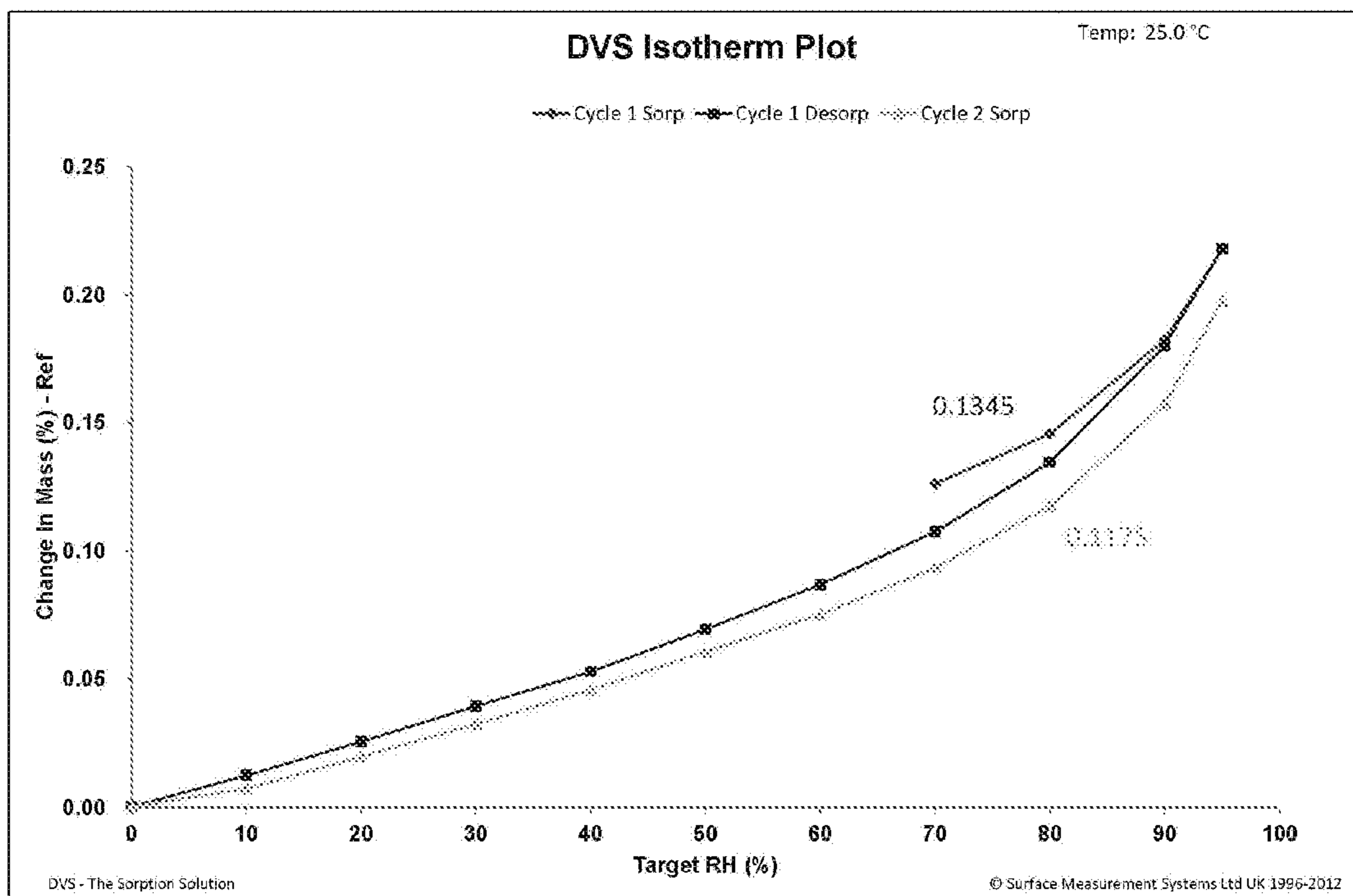


Figure 57

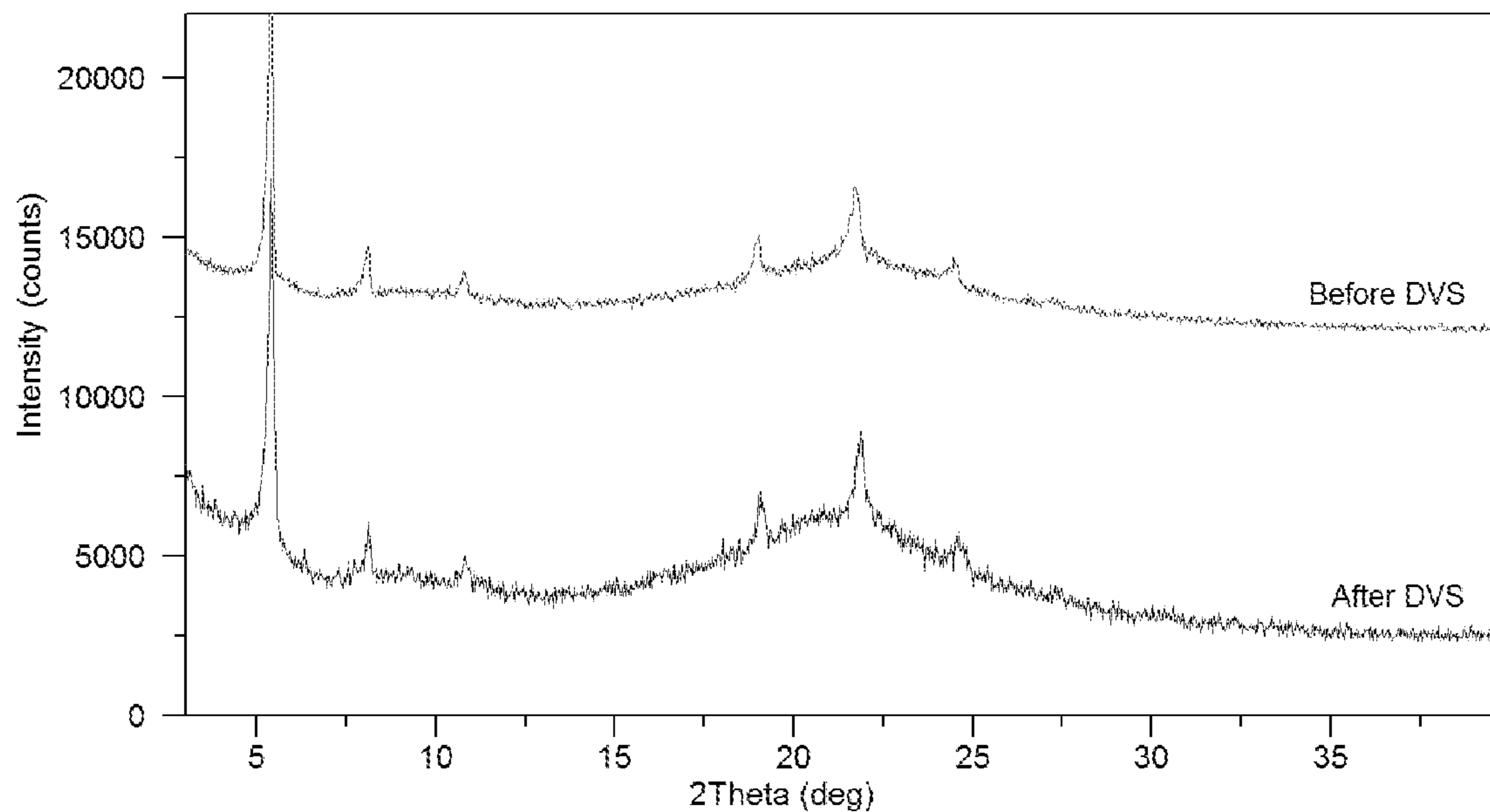


Figure 58

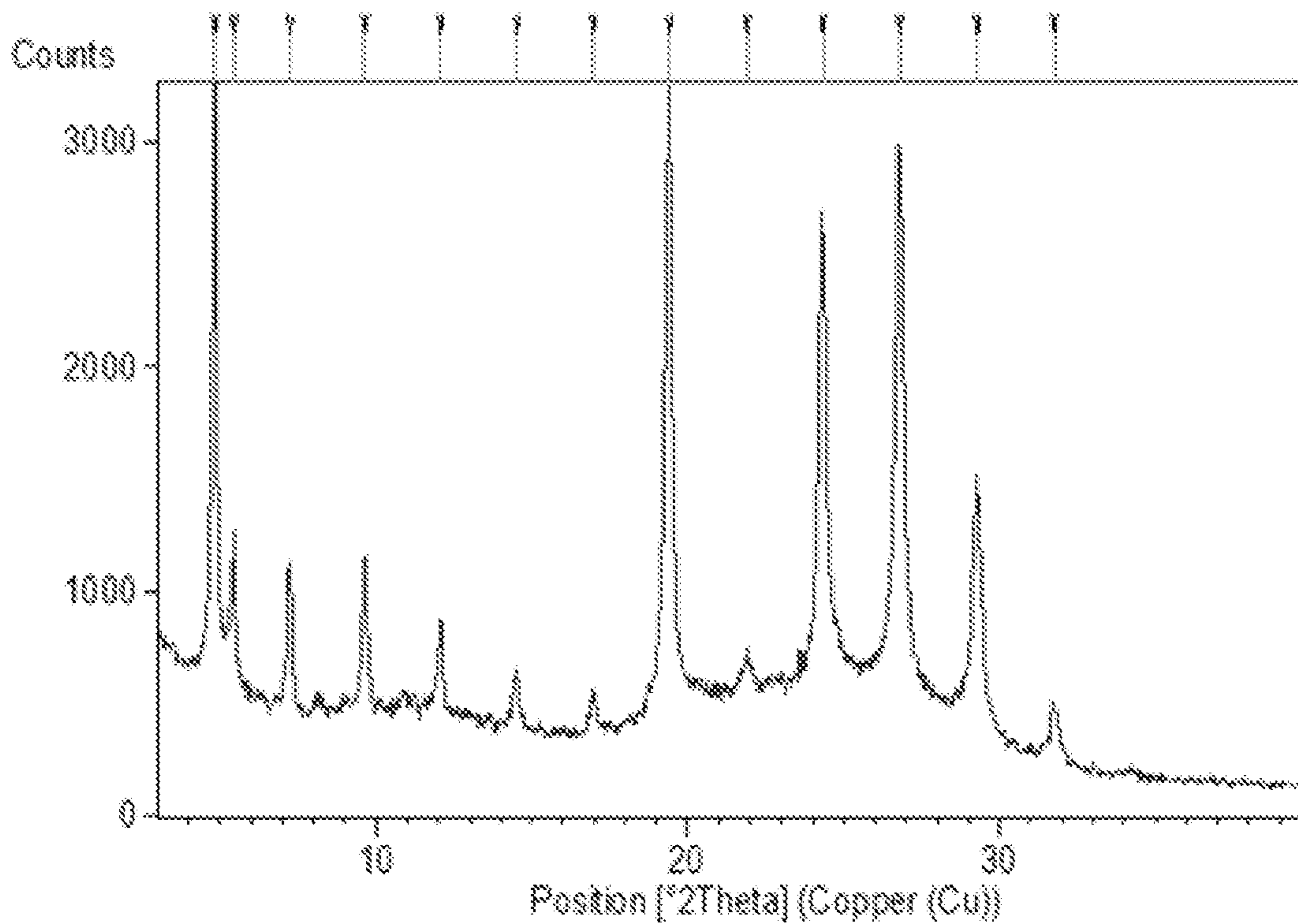


Figure 59

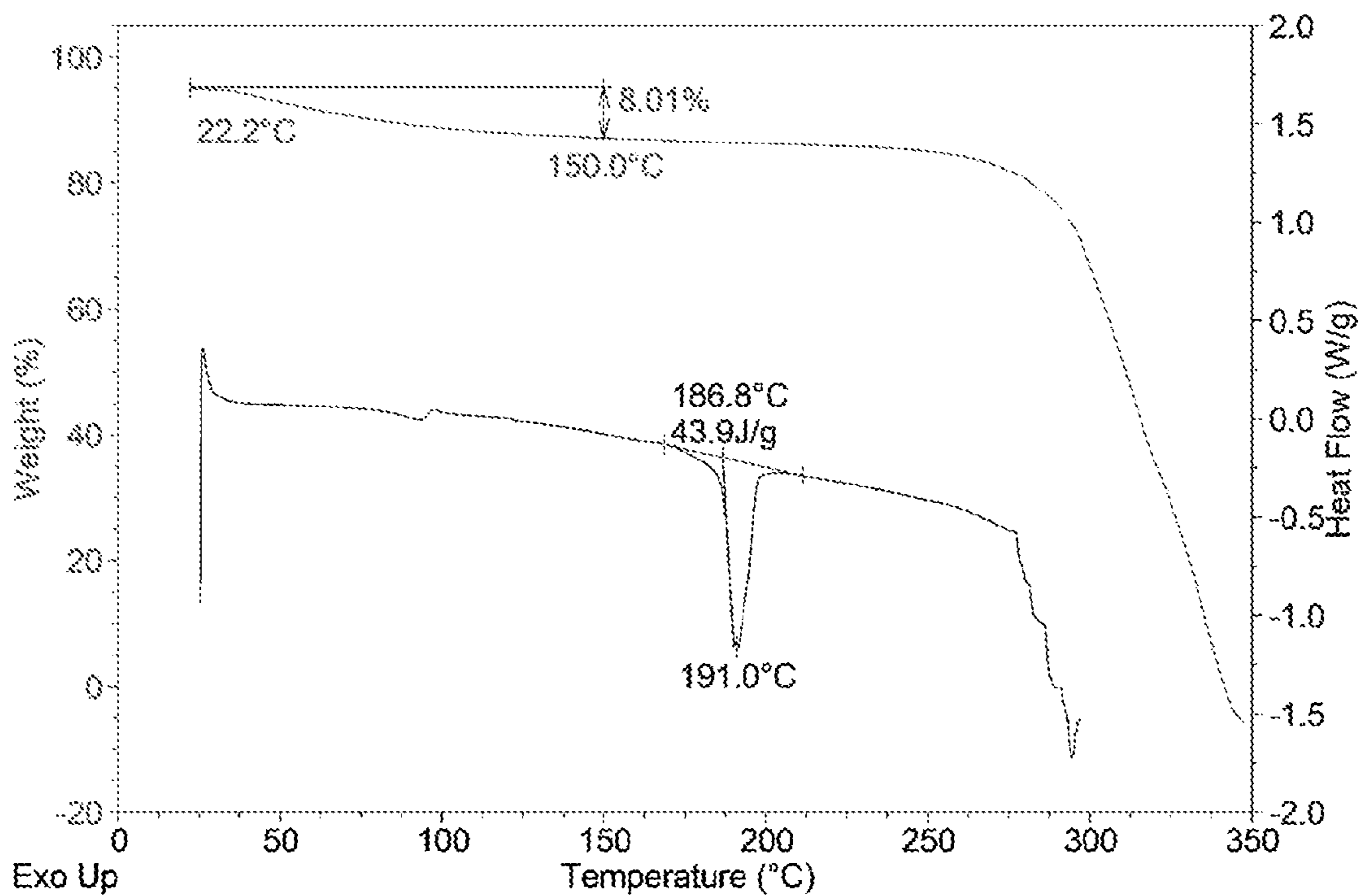


Figure 60

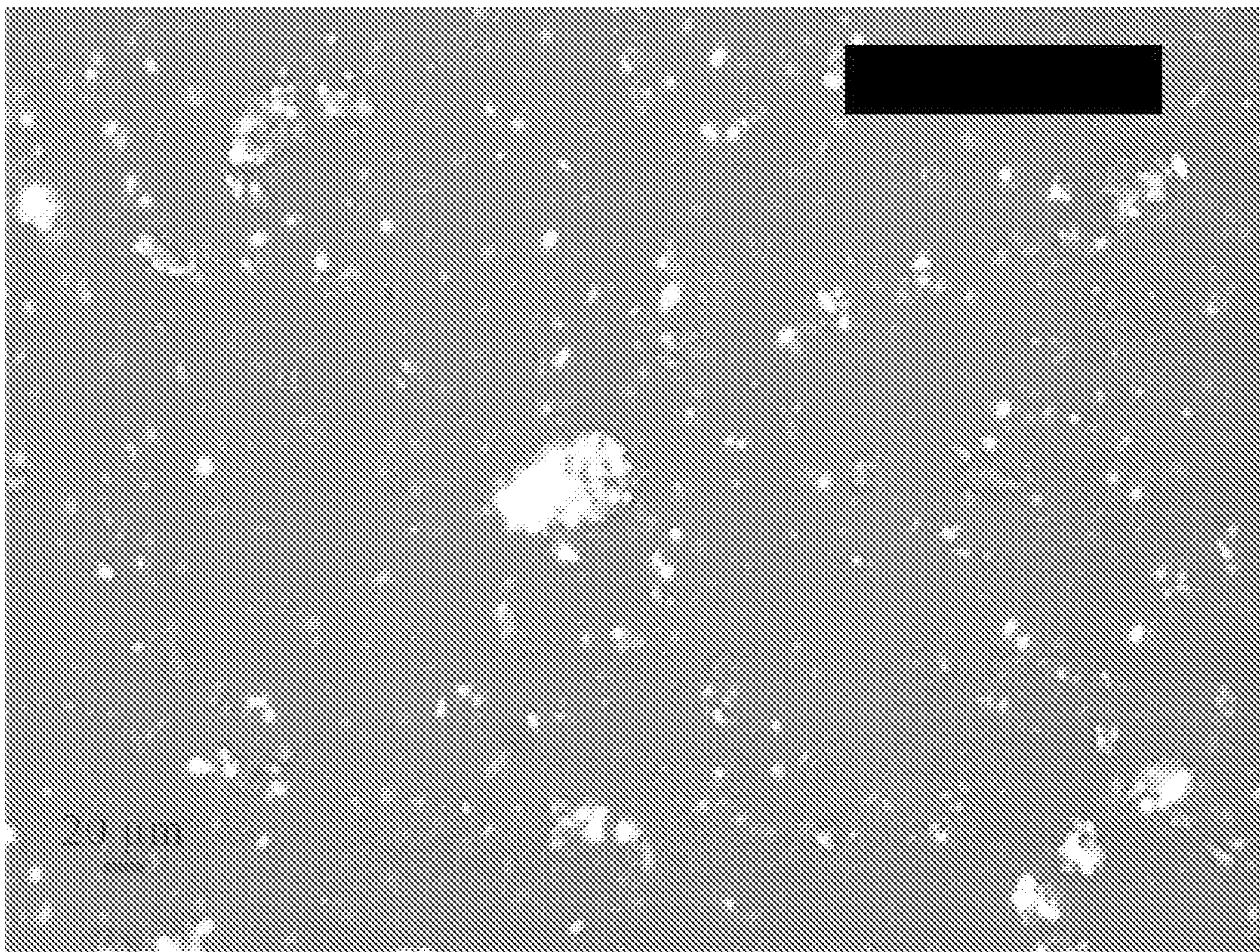


Figure 61

1

CRYSTAL FORMS OF AMINO LIPIDS

RELATED APPLICATIONS

This application is a U.S. National Phase application, filed under U.S.C. § 371, of International Application No. PCT/US2018/022740, filed Mar. 15, 2018, which claims priority to, and the benefit of, U.S. Provisional Application No. 62/471,908, filed Mar. 15, 2017; the entire content of which is incorporated herein by reference.

TECHNICAL FIELD

This disclosure relates to solid crystalline forms of each of three compounds: (1) heptadecan-9-yl 8-((2-hydroxyethyl)amino)octanoate ("Compound 1"), (2) heptadecan-9-yl 8-((2-hydroxyethyl)(6-oxo-6-(undecyloxy)hexyl)amino)octanoate ("Compound 2"), and (3) heptadecan-9-yl 8-((2-hydroxyethyl)(8-(nonyloxy)-8-oxooctyl)amino)octanoate ("Compound 3"), and related compositions and methods. This disclosure also relates to solid crystalline forms of (6Z,9Z,28Z,31Z)-heptatriaconta-6,9,28,31-tetraen-19-yl 4-(dimethylamino)butanoate ("MC3"), and related compositions and methods.

BACKGROUND

The effective targeted delivery of biologically active substances such as small molecule drugs, proteins, and nucleic acids represents a continuing medical challenge. In particular, the delivery of nucleic acids to cells is made difficult by the relative instability and low cell permeability of such species. Thus, there exists a need to develop methods and compositions to facilitate the delivery of therapeutic and/or prophylactics such as nucleic acids to cells.

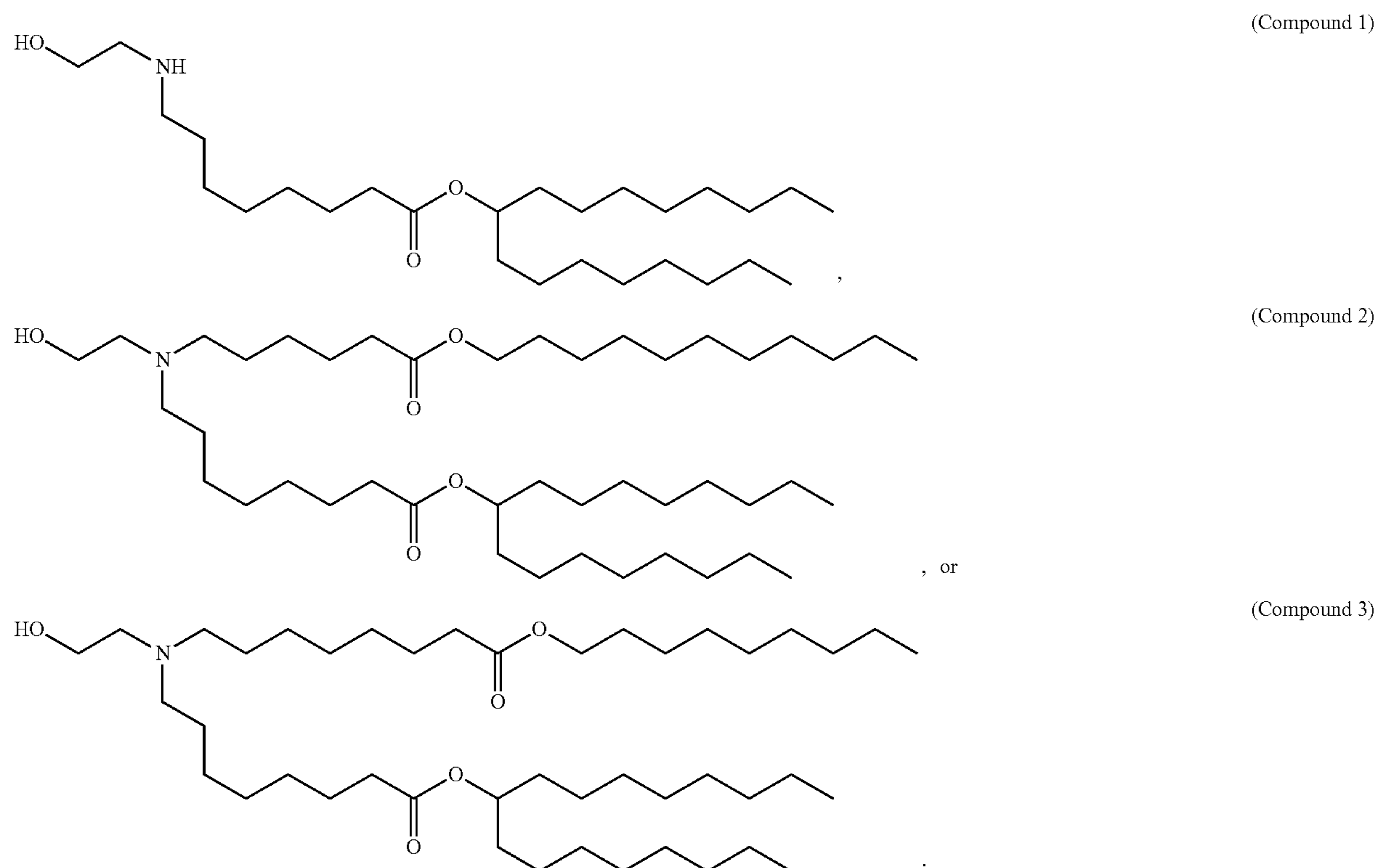
2

Lipid-containing nanoparticle compositions, liposomes, and lipoplexes have proven effective as transport vehicles into cells and/or intracellular compartments for biologically active substances such as small molecule drugs, proteins, and nucleic acids. Such compositions generally include one or more "cationic" and/or amino (ionizable) lipids, phospholipids including polyunsaturated lipids, structural lipids (e.g., sterols), and/or lipids containing polyethylene glycol (PEG lipids). Cationic and/or ionizable lipids include, for example, amine-containing lipids that can be readily protonated. Though a variety of such lipid-containing nanoparticle compositions have been demonstrated, improvements in safety, efficacy, and specificity are still lacking. In addition, the physical and chemical properties of lipid materials often present challenges relating to the practice of making and using lipid-containing nanoparticles for drug delivery.

SUMMARY

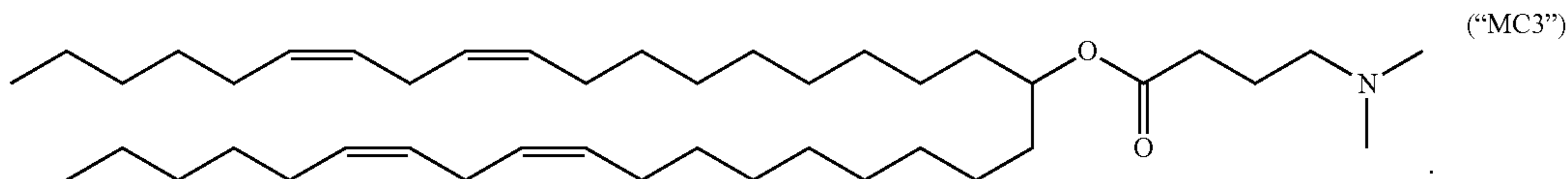
Long-chain amino lipids are usually viscous oils at room temperature. Solid forms of these lipids are desirable for e.g., improving handling, improving stability (such as storage stability) and/or control of physical/chemical properties, simplifying purification process, simplifying large-scale production process and/or increasing accuracy in measurements and characterization of lipids.

Accordingly, provided herein are novel solid forms (e.g., crystalline forms) of each of three compounds (1) heptadecan-9-yl 8-((2-hydroxyethyl)amino)octanoate ("Compound 1"), (2) heptadecan-9-yl 8-((2-hydroxyethyl)(6-oxo-6-(undecyloxy)hexyl)amino)octanoate ("Compound 2"), and (3) heptadecan-9-yl 8-((2-hydroxyethyl)(8-(nonyloxy)-8-oxooctyl)amino)octanoate ("Compound 3"), the structure of each of which is provided below:



3

In another aspect, provided herein are novel solid forms (e.g., crystalline forms) of (6Z,9Z,28Z,31Z)-heptatriaconta-6,9,28,31-tetraen-19-yl 4-(dimethylamino)butanoate (“MC3”), the structure of which is provided below:



In one aspect, disclosed herein is salt or cocrystal of heptadecan-9-yl 8-((2-hydroxyethyl)amino)octanoate (“Compound 1”), heptadecan-9-yl 8-((2-hydroxyethyl)(6-oxo-6-(undecyloxy)hexyl)amino)octanoate (“Compound 2”), or heptadecan-9-yl 8-((2-hydroxyethyl)(8-(nonyloxy)-8-oxooctyl)amino)octanoate (“Compound 3”). In another aspect, the salt or cocrystal of Compound 1, 2, or 3 has a melting point of about 50° C. or greater (e.g., about 60° C., about 70° C. or greater). In another aspect, the salt or cocrystal of Compound 3 has a melting point of about 270° C. or greater (e.g., about 280° C., about 290° C. or greater). For example, the salt or cocrystal of Compound 1, 2, or 3 is formed between Compound 1, 2, or 3 and a cofomer compound (e.g., an acid).

In one aspect, disclosed herein is a salt or cocrystal of (6Z,9Z,28Z,31Z)-heptatriaconta-6,9,28,31-tetraen-19-yl 4-(dimethylamino)butanoate (“MC3”). In another aspect, the salt or cocrystal of MC3 has a melting point of about 150° C. or greater (e.g., about 160° C., about 170° C., about 180° C. or greater, about 190° C. or greater). In another aspect, disclosed herein is a salt or cocrystal of (6Z,9Z,28Z,31Z)-heptatriaconta-6,9,28,31-tetraen-19-yl 4-(dimethylamino)butanoate (“MC3”). In another aspect, the salt or cocrystal of MC3 has a melting point of about 50° C. or greater (e.g., about 60° C., about 70° C., about 80° C. or greater). For example, the salt or cocrystal of MC3 is formed between MC3 and a cofomer compound (e.g., an acid).

In one aspect, this disclosure is directed to a salt or cocrystal of heptadecan-9-yl 8-((2-hydroxyethyl)amino)octanoate (“Compound 1”) and a compound (e.g., a cofomer compound) selected from the group consisting of 4-hydroxybenzoic acid, oxalic acid, trimellitic acid, orotic acid, trimesic acid, and sulfuric acid.

In another aspect, this disclosure is directed to a salt or cocrystal of heptadecan-9-yl 8-((2-hydroxyethyl)(6-oxo-6-(undecyloxy)hexyl)amino)octanoate (“Compound 2”) and a compound (e.g., a cofomer compound) selected from the group consisting of trimesic acid, (-)-2,3-dibenzoyl-L-tartaric acid, 4-acetamido benzoic acid, (+)-L-tartaric acid, and methanesulfonic acid.

In yet another aspect, this disclosure is directed to a salt or cocrystal of heptadecan-9-yl 8-((2-hydroxyethyl)(8-(nonyloxy)-8-oxooctyl)amino)octanoate (“Compound 3”) and trimesic acid.

In one aspect, this disclosure is directed to a salt or cocrystal of (6Z,9Z,28Z,31Z)-heptatriaconta-6,9,28,31-tetraen-19-yl 4-(dimethylamino)butanoate (“MC3”) and a compound selected from the group consisting of (+)-O,O-di-pivaloyl-D-tartaric acid (DPDT), (-)-O,O-di-pivaloyl-L-tartaric acid (DPLT), (+)-2,3-dibenzoyl-D-tartaric acid (DBDT), and trimesic acid. In one embodiment this disclosure is directed to a salt or cocrystal of (6Z,9Z,28Z,31Z)-heptatriaconta-6,9,28,31-tetraen-19-yl 4-(dimethylamino)butanoate (“MC3”) and trimesic acid.

4

The salts or cocrystals disclosed herein may comprise Compound 1 (or Compound 2 or 3) and the cofomer compound (e.g., an acid), within a ratio of from about 1:0.2 mol/mol (i.e., 5:1 mol/mol) to 1:5 mol/mol or from about

1:0.5 mol/mol (i.e., 2:1 mol/mol) to 1:2 mol/mol, or within the range of from 1:0.4 mol/mol (i.e., 2.5:1 mol/mol) to 1:1.1 mol/mol.

The salts or cocrystals disclosed herein may comprise (6Z,9Z,28Z,31Z)-heptatriaconta-6,9,28,31-tetraen-19-yl 4-(dimethylamino)butanoate (“MC3”) and the cofomer compound (e.g., an acid), within a ratio of from about 1:0.5 mol/mol (i.e., 2:1 mol/mol) to 1:2 mol/mol. For example the ratio is about 1:1.2 mol/mol, about 1:1.1 mol/mol, or about 1:1.5 mol/mol).

The salts or cocrystals disclosed herein may be anhydrous and/or essentially solvent-free form, or be in hydrate and/or solvate form. For example, 4-hydroxybenzoate of Compound 1 is anhydrous. For example, Compound 1 orotate may be anhydrous or in a hydrate or solvate form. For example, trimesate of MC3 may be anhydrous or in a hydrate or solvate form.

The salts or cocrystals disclosed herein may be non-hygroscopic. For example, the 4-hydroxybenzoate of Compound 1 is non-hygroscopic. For example, the trimesate of MC3 is non-hygroscopic.

It has been found that under suitable conditions some of the salts or cocrystals can be obtained in the form of different polymorphs. For example, 4-hydroxybenzoate of Compound 1 has at least two polymorphs, Polymorphs A and B. For example, orotate of Compound 1 has at least two polymorphs, Polymorphs A and B. For example, orotate of Compound 7 has at least two polymorphs, Polymorphs A and B. For example trimesate of Compound 3 has at least two polymorphs, Polymorphs A and B. For example, trimesate of MC3 has at least two polymorphs, Polymorphs A and B.

The polymorphs disclosed herein may be substantially pure, i.e., substantially free of impurities. Non-limiting examples of impurities include other polymorph forms, or residual organic and inorganic molecules such as related impurities (e.g., intermediates used to make the compounds), solvents, water or salts. As used herein “substantially pure” or “substantially free of impurities” means there is not a significant amount of impurities (e.g., other polymorph forms, or residual organic and inorganic molecules such as related impurities, solvents, water or salts) present in a sample of the salt, cocrystal, or polymorph. For example, a salt, cocrystal, or polymorph disclosed herein contains less than 10% weight by weight (wt/wt) total impurities, less than 5% wt/wt total impurities, less than 2% wt/wt total impurities, less than 1% wt/wt total impurities, less than 0.5% wt/wt total impurities, or not a detectable amount of impurities.

In one embodiment, Polymorph A of 4-hydroxybenzoate of Compound 1 is substantially free of impurities, meaning there is not a significant amount of impurities present in the sample of Polymorph A. In another embodiment, Polymorph A is a crystalline solid substantially free of Compound 1 (or

5

any of its amorphous salt forms). In yet another embodiment, Polymorph A is a crystalline solid substantially free of other polymorphs of 4-hydroxybenzoate of Compound 1 and substantially free of amorphous Compound 1 (or any of its amorphous salt forms). For example, Polymorph A is a crystalline solid substantially free of Polymorph B of 4-hydroxybenzoate of Compound 1 and substantially free of amorphous Compound 1 (or any of its amorphous salt forms). The skilled artisan understands that a solid sample of Polymorph A may also include other polymorphs (e.g., Polymorph B), and/or amorphous Compound 1 (or any of its amorphous salt forms).

Polymorph A of 4-hydroxybenzoate of Compound 1 can be defined according to its X-ray powder diffraction pattern. Accordingly, in one embodiment, Polymorph A exhibits an X-ray powder diffraction pattern obtained using Cu K α radiation, having two, three, or more characteristic peaks expressed in degrees 2-theta (± 0.2) selected from the group consisting of 4.5, 6.8, 9.1, and 11.4. In one embodiment, Polymorph A exhibits an X-ray powder diffraction pattern obtained using Cu K α radiation, having peaks with 2-theta values substantially in accordance with FIG. 1. In another embodiment, Polymorph A exhibits an X-ray powder diffraction pattern obtained using Cu K α radiation, having peaks with 2-theta values substantially in accordance with Table I.

Polymorph A of 4-hydroxybenzoate of Compound 1 can also be defined according to its differential scanning calorimetry thermogram. In one embodiment, the polymorph exhibits a differential scanning calorimetry thermogram showing a primary endotherm expressed in units of $^{\circ}$ C. at a temperature of $103 \pm 2^{\circ}$ C. and a second primary endotherm expressed in units of $^{\circ}$ C. at a temperature of $68 \pm 2^{\circ}$ C. In another embodiment, Polymorph A exhibits a differential scanning calorimetry thermogram substantially in accordance with the lower curve shown in FIG. 3.

In one embodiment, Polymorph B of Compound 1 orotate is substantially free of impurities (e.g., phase or form impurities), meaning there is not a significant amount of impurities present in the sample of Polymorph B. In another embodiment, Polymorph B is a crystalline solid substantially free of amorphous Compound 1 (or any of its amorphous salt forms). In yet another embodiment, Polymorph B is a crystalline solid substantially free of other polymorphs of Compound 1 orotate and substantially free of amorphous Compound 1 (or any of its amorphous salt forms). For example, Polymorph B is a crystalline solid substantially free of Polymorph A of Compound 1 orotate and substantially free of amorphous Compound 1 (or any of its amorphous salt forms). The skilled artisan understands that a solid sample of Polymorph B of Compound 1 orotate may also include other polymorphs (e.g., Polymorph A), and/or amorphous Compound 1 (or any of its amorphous salt forms).

Polymorph B of Compound 1 orotate can be defined according to its X-ray powder diffraction pattern. Accordingly, in one embodiment, Polymorph B exhibits an X-ray powder diffraction pattern obtained using Cu K α radiation, having two, three, four, or more characteristic peaks expressed in degrees 2-theta (± 0.2) selected from the group consisting of 5.1, 7.5, 10.1, 12.7, 15.2, and 17.8. In one embodiment, Polymorph B exhibits an X-ray powder diffraction pattern obtained using Cu K α radiation, having peaks with 2-theta values substantially in accordance with FIG. 18, upper profile. In another embodiment, Polymorph B exhibits an X-ray powder diffraction pattern obtained

6

using Cu K α radiation, having peaks with 2-theta values substantially in accordance with Table III.

In one embodiment, Polymorph B of trimesate of Compound 3 is substantially free of impurities, meaning there is not a significant amount of impurities present in the sample of Polymorph B. In another embodiment, Polymorph B is a crystalline solid substantially free of Compound 3 (or any of its amorphous salt forms). In yet another embodiment, Polymorph B is a crystalline solid substantially free of other polymorphs of trimesate of Compound 3 and substantially free of amorphous trimesate of Compound 3 (or any of its amorphous salt forms). For example Polymorph B is a crystalline solid substantially free of Polymorph A of trimesate of Compound 3 and substantially free of amorphous trimesate of Compound 3 (or any of its amorphous salt forms). The skilled artisan understands that a solid sample of Polymorph B may also include other polymorphs (e.g., Polymorph A) and/or amorphous Compound 3 (or any of its amorphous salt forms).

Polymorph B of Compound 3 trimesate can be defined according to its X-ray powder diffraction pattern. Accordingly, Polymorph B of Compound 3 trimesate exhibits an X-ray powder diffraction pattern obtained using Cu K α radiation, having two, three, four or more characteristic peaks expressed in degrees 2-theta (± 0.4) at 6.2, 10.8, 16.5, and 26.7. In one embodiment, Polymorph B exhibits an X-ray powder diffraction pattern obtained using Cu K α radiation, having peaks with 2-theta values substantially in accordance with FIG. 48. In another embodiment, Polymorph B exhibits an X-ray powder diffraction pattern obtained using Cu K α radiation, having peaks with 2-theta values substantially in accordance with Table XII.

In other embodiments, Polymorph B of trimesate of Compound 3 is identifiable on the basis of a characteristic peak observed in a differential scanning calorimetry thermogram. In one embodiment, the polymorph exhibits a differential scanning calorimetry thermogram showing a characteristic melting endotherm peak expressed in units of $^{\circ}$ C. with an onset temperature of about $305 \pm 2^{\circ}$ C. In another embodiment, the polymorph exhibits a differential scanning calorimetry thermogram showing a second primary endotherm expressed in units of $^{\circ}$ C. at a temperature of $240 \pm 2^{\circ}$ C. In another embodiment, the polymorph exhibits a differential scanning calorimetry thermogram substantially in accordance with FIG. 49.

In one embodiment, Polymorph A of trimesate of MC3 is substantially free of impurities, meaning there is not a significant amount of impurities present in the sample of Polymorph A. In another embodiment, Polymorph A is a crystalline solid substantially free of MC3 (or any of its amorphous salt forms). In yet another embodiment, Polymorph A is a crystalline solid substantially free of other polymorphs of trimesate of MC3 and substantially free of amorphous MC3 (or any of its amorphous salt forms). For example, Polymorph A is a crystalline solid substantially free of Polymorph B of trimesate of MC3 and substantially free of amorphous MC3 (or any of its amorphous salt forms). The skilled artisan understands that a solid sample of Polymorph A may also include other polymorphs (e.g., Polymorph B), and/or amorphous MC3 (or any of its amorphous salt forms).

Polymorph A of MC3 trimesate can be defined according to its X-ray powder diffraction pattern. Accordingly, Polymorph A of MC3 trimesate exhibits an X-ray powder diffraction pattern obtained using Cu K α radiation, having two, three, four or more characteristic peaks expressed in degrees 2-theta (± 0.4) at 5.2, 7.8, 10.4, 18.3, 20.9, 23.6, or

26.2. In one embodiment, Polymorph A exhibits an X-ray powder diffraction pattern obtained using Cu K α radiation, having peaks with 2-theta values substantially in accordance with FIG. 52. In another embodiment, Polymorph A exhibits an X-ray powder diffraction pattern obtained using Cu K α radiation, having peaks with 2-theta values substantially in accordance with Table XIII.

Polymorph A of MC3 trimesate can also be defined according to its differential scanning calorimetry thermogram. In one embodiment, the polymorph exhibits a differential scanning calorimetry thermogram showing a primary endotherm expressed in units of ° C. at a temperature of 184+/-2° C. In one embodiment, the polymorph exhibits a differential scanning calorimetry thermogram showing a primary endotherm expressed in units of ° C. at a temperature of 186+/-2° C. and a second primary endotherm expressed in units of ° C. at a temperature of 90+/-2° C. In yet another embodiment, the polymorph exhibits a differential scanning calorimetry thermogram substantially in accordance with FIG. 53 or FIG. 54.

Polymorph B of MC3 trimesate can be defined according to its X-ray powder diffraction pattern. Accordingly, Polymorph B of MC3 trimesate exhibits an X-ray powder diffraction pattern obtained using Cu K α radiation, having two, three, four or more characteristic peaks expressed in degrees 2-theta (+/-0.4) at 4.8, 5.4, 7.2, 9.7, 12.1, 14.5, 17.0, 19.4, 21.9, 24.3, 26.8, 29.3, or 31.8. In one embodiment, Polymorph B exhibits an X-ray powder diffraction pattern obtained using Cu K α radiation, having peaks with 2-theta values substantially in accordance with FIG. 59. In another embodiment, Polymorph B exhibits an X-ray powder diffraction pattern obtained using Cu K α radiation, having peaks with 2-theta values substantially in accordance with Table XIV.

Polymorph B of MC3 trimesate can also be defined according to its differential scanning calorimetry thermogram. In one embodiment, the polymorph exhibits a differential scanning calorimetry thermogram showing a primary endotherm expressed in units of ° C. at a temperature of 187+/-2° C. In another embodiment, the polymorph exhibits a differential scanning calorimetry thermogram substantially in accordance with FIG. 60.

Another aspect of the disclosure relates to the preparation of the salt or cocrystal of heptadecan-9-yl 8-((2-hydroxyethyl)amino)octanoate ("Compound 1") and a compound selected from the group consisting of 4-hydroxybenzoic acid, oxalic acid, trimellitic acid, orotic acid, trimesic acid, and sulfuric acid.

Also provided herein is a method for preparing the salt or cocrystal of heptadecan-9-yl 8-((2-hydroxyethyl)(6-oxo-6-(undecyloxy)hexyl)amino)octanoate ("Compound 2") and a compound selected from the group consisting of trimesic acid, (-)-2,3-dibenzoyl-L-tartaric acid, 4-acetamido benzoic acid, (+)-L-tartaric acid, and methanesulfonic acid.

This disclosure also provides a method of preparing the salt or cocrystal of heptadecan-9-yl 8-((2-hydroxyethyl)(8-(nonyloxy)-8-oxooctyl)amino)octanoate ("Compound 3") and trimesic acid.

This disclosure also provides a method of preparing the salt or cocrystal of (6Z,9Z,28Z,31Z)-heptatriaconta-6,9,28,31-tetraen-19-yl 4-(dimethylamino)butanoate ("MC3") and trimesic acid.

In still another aspect, provided herein is a process of synthesizing Compound 2, Compound 3, or an analog thereof by reacting a salt or cocrystal of Compound 1 disclosed herein with a suitable electrophile, such as an ester substituted with a halogen (e.g., Br or I).

Also provided herein is a process of purifying Compound 1, 2, or 3 by forming a salt or cocrystal thereof disclosed herein to separate the salt or cocrystal thereof from the impurities. The method may further comprise neutralizing the salt or cocrystal to convert to Compound 1, 2, or 3 (i.e., a free base).

In one embodiment, the process of the present disclosure is advantageous as compared to other processes in that the process of the disclosure produces Compound 1, 2, or 3 or a salt or cocrystal thereof at a large scale and/or at a high purity, e.g., such that cumbersome purification (e.g., column chromatography, extraction, phase separation, distillation and solvent evaporation) is not needed. In one embodiment, the process of the present disclosure is able to process at least 100 g, 200 g, 500 g, or more (e.g., 1 kg, 2 kg, 5 kg, 10 kg, 20 kg, 50 kg, 100 kg, 200 kg, 500 kg, or 1000 kg or more) Compound 1, 2, or 3 or a salt or cocrystal thereof. In one embodiment, the process of the present disclosure is able to produce Compound 1, 2, or 3 or a salt or cocrystal thereof at least at a purity of at least 75%, 80%, 85%, 90%, 95%, 96%, 97%, 98%, 99%, or 99.5%, or higher. In one embodiment, the process of the present disclosure is able to produce Compound 1, 2, or 3 or a salt or cocrystal thereof with little or no impurity. In one embodiment, the impurity produced in the process of the present disclosure, even if produced, is easy to be separated from Compound 1, 2, or 3 or a salt or cocrystal thereof, without cumbersome purification (e.g., column chromatography, extraction, phase separation, distillation and solvent evaporation).

Unless otherwise defined, all technical and scientific terms used herein have the same meaning as commonly understood by one of ordinary skill in the art to which this disclosure belongs. In the specification, the singular forms also include the plural unless the context clearly dictates otherwise. Although methods and materials similar or equivalent to those described herein can be used in the practice or testing of the present invention, suitable methods and materials are described below. In the case of conflict, the present specification, including definitions, will control. In addition, the materials, methods and examples are illustrative only and are not intended to be limiting.

Other features and advantages of the invention will be apparent from the following drawings, detailed description and claims.

BRIEF DESCRIPTION OF THE DRAWINGS

FIG. 1 depicts a representative X-ray powder diffraction (XRPD) pattern overlay of heptadecan-9-yl 8-((2-hydroxyethyl)amino)octanoate 4-hydroxybenzoate Polymorph A batches, i.e., 100 mg and 10 mg batches or batches Nos. 1 and 2.

FIG. 2 depicts a ¹H NMR spectrum of heptadecan-9-yl 8-((2-hydroxyethyl)amino)octanoate 4-hydroxybenzoate Polymorph A, batch No. 2.

FIG. 3 depicts thermo-gravimetric analysis (TGA) and differential scanning calorimetry (DSC) data for heptadecan-9-yl 8-((2-hydroxyethyl)amino)octanoate 4-hydroxybenzoate Polymorph A, batch No. 2.

FIG. 4 depicts cyclic DSC data for heptadecan-9-yl 8-((2-hydroxyethyl)amino)octanoate 4-hydroxybenzoate Polymorph A, batch No. 2.

FIG. 5 depicts a representative XRPD pattern overlay of heptadecan-9-yl 8-((2-hydroxyethyl)amino)octanoate 4-hydroxybenzoate Polymorph A (i.e., Type A in the figure), batch No. 2, before and after heating.

FIG. 6 depicts TGA and DSC data for heptadecan-9-yl 8-((2-hydroxyethyl)amino)octanoate 4-hydroxybenzoate Polymorph A, batch No. 1.

FIG. 7 depicts variable temperature X-ray powder diffraction (VT-XRPD) pattern overlay of heptadecan-9-yl 8-((2-hydroxyethyl)amino)octanoate 4-hydroxybenzoate Polymorph A batch No. 1, before and after heating. Type A ref. in this figure is heptadecan-9-yl 8-((2-hydroxyethyl)amino)octanoate 4-hydroxybenzoate Polymorph A, batch No. 2.

FIG. 8 depicts dynamic vapor sorption (DVS) data at 25° C. for heptadecan-9-yl 8-((2-hydroxyethyl)amino)octanoate 4-hydroxybenzoate Polymorph A, batch No. 1.

FIG. 9 depicts an XRPD pattern overlay of heptadecan-9-yl 8-((2-hydroxyethyl)amino)octanoate 4-hydroxybenzoate Polymorph A, batch No. 1, before and after DVS.

FIG. 10 depicts a polarized light microscopy (PLM) image for heptadecan-9-yl 8-((2-hydroxyethyl)amino)octanoate 4-hydroxybenzoate Polymorph A, batch No. 1.

FIG. 11 depicts a representative XRPD pattern overlay of heptadecan-9-yl 8-((2-hydroxyethyl)amino)octanoate trimellitate Polymorph A batches, i.e., 100 mg and 10 mg batches or batches Nos. 1 and 2.

FIG. 12 depicts an ¹H NMR spectrum of heptadecan-9-yl 8-((2-hydroxyethyl)amino)octanoate trimellitate Polymorph A, batch No. 2.

FIG. 13 depicts TGA and DSC data for heptadecan-9-yl 8-((2-hydroxyethyl)amino)octanoate trimellitate Polymorph A, batch No. 1.

FIG. 14 depicts a VT-XRPD pattern overlay of heptadecan-9-yl 8-((2-hydroxyethyl)amino)octanoate trimellitate Polymorph A batch No. 1, before and after heating.

FIG. 15 depicts DVS data at 25° C. for heptadecan-9-yl 8-((2-hydroxyethyl)amino)octanoate trimellitate Polymorph A, batch No. 1.

FIG. 16 depicts an XRPD pattern overlay of heptadecan-9-yl 8-((2-hydroxyethyl)amino)octanoate trimellitate Polymorph A, batch No. 1, before and after DVS.

FIG. 17 depicts a polarized light microscopy (PLM) image for heptadecan-9-yl 8-((2-hydroxyethyl)amino)octanoate trimellitate Polymorph A, batch No. 1.

FIG. 18 depicts a representative XRPD pattern overlay of heptadecan-9-yl 8-((2-hydroxyethyl)amino)octanoate orotate Polymorphs A and B.

FIG. 19 depicts an ¹H NMR spectrum of heptadecan-9-yl 8-((2-hydroxyethyl)amino)octanoate orotate Polymorph A.

FIG. 20 depicts TGA and DSC data for heptadecan-9-yl 8-((2-hydroxyethyl)amino)octanoate orotate Polymorph A.

FIG. 21 depicts a VT-XRPD pattern overlay of heptadecan-9-yl 8-((2-hydroxyethyl)amino)octanoate orotate Polymorph A, before and after heating.

FIG. 22 depicts heating-cooling DSC curve for heptadecan-9-yl 8-((2-hydroxyethyl)amino)octanoate orotate Polymorph A.

FIG. 23 depicts TGA and DSC data for heptadecan-9-yl 8-((2-hydroxyethyl)amino)octanoate orotate Polymorphs B.

FIG. 24 depicts cyclic DSC data for heptadecan-9-yl 8-((2-hydroxyethyl)amino)octanoate orotate Polymorphs B.

FIG. 25 depicts an XRPD pattern overlay of heptadecan-9-yl 8-((2-hydroxyethyl)amino)octanoate orotate Polymorph B, before and after cyclic DSC.

FIG. 26 depicts DVS data at 25° C. for heptadecan-9-yl 8-((2-hydroxyethyl)amino)octanoate orotate Polymorphs B.

FIG. 27 depicts an XRPD pattern overlay of heptadecan-9-yl 8-((2-hydroxyethyl)amino)octanoate orotate Polymorph B, before and after DVS.

FIG. 28 depicts a PLM image of heptadecan-9-yl 8-((2-hydroxyethyl)amino)octanoate orotate Polymorph B.

FIG. 29 depicts a PLM image of heptadecan-9-yl 8-((2-hydroxyethyl)amino)octanoate sulfate Polymorph A.

FIG. 30 depicts an XRPD pattern of heptadecan-9-yl 8-((2-hydroxyethyl)amino)octanoate sulfate Polymorph A.

FIG. 31 depicts TGA and DSC data of heptadecan-9-yl 8-((2-hydroxyethyl)amino)octanoate sulfate Polymorph A.

FIG. 32 depicts an XRPD pattern of heptadecan-9-yl 8-((2-hydroxyethyl)amino)octanoate trimesate Polymorph A.

FIG. 33 depicts an ¹H NMR overlay of heptadecan-9-yl 8-((2-hydroxyethyl)amino)octanoate trimesate and freebase.

FIG. 34 depicts TGA data of heptadecan-9-yl 8-((2-hydroxyethyl)amino)octanoate.

FIG. 35 depicts cyclic DSC data of heptadecan-9-yl 8-((2-hydroxyethyl)amino)octanoate (heating/cooling rate: 10° C./min).

FIG. 36 depicts an XRPD pattern overlay of heptadecan-9-yl 8-((2-hydroxyethyl)(6-oxo-6-(undecyloxy)hexyl)amino)octanoate dibenzoyl-L-tartrate Polymorph A and the corresponding acid, dibenzoyl-L-tartaric acid.

FIG. 37 depicts TGA and DSC data for heptadecan-9-yl 8-((2-hydroxyethyl)(6-oxo-6-(undecyloxy)hexyl)amino)octanoate dibenzoyl-L-tartrate Polymorph A.

FIG. 38 depicts an XRPD pattern overlay of heptadecan-9-yl 8-((2-hydroxyethyl)(6-oxo-6-(undecyloxy)hexyl)amino)octanoate trimesate Polymorph A and the corresponding acid, trimesic acid.

FIG. 39 depicts TGA and DSC data for heptadecan-9-yl 8-((2-hydroxyethyl)(6-oxo-6-(undecyloxy)hexyl)amino)octanoate trimesate Polymorph A.

FIG. 40 depicts an XRPD pattern overlay of heptadecan-9-yl 8-((2-hydroxyethyl)(6-oxo-6-(undecyloxy)hexyl)amino)octanoate L-tartrate Polymorph A and the corresponding acid, L-tartaric acid.

FIG. 41 depicts TGA and DSC data for heptadecan-9-yl 8-((2-hydroxyethyl)(6-oxo-6-(undecyloxy)hexyl)amino)octanoate L-tartrate Polymorph A.

FIG. 42 depicts an XRPD pattern of heptadecan-9-yl 8-((2-hydroxyethyl)(6-oxo-6-(undecyloxy)hexyl)amino)octanoate mesylate Polymorph A.

FIG. 43 depicts TGA and DSC data for heptadecan-9-yl 8-((2-hydroxyethyl)(6-oxo-6-(undecyloxy)hexyl)amino)octanoate mesylate Polymorph A.

FIG. 44 depicts an XRPD pattern overlay of heptadecan-9-yl 8-((2-hydroxyethyl)(6-oxo-6-(undecyloxy)hexyl)amino)octanoate 4-acetamido benzoate Polymorph A and the corresponding acid, 4-acetamido benzoic acid.

FIG. 45 depicts TGA and DSC data for heptadecan-9-yl 8-((2-hydroxyethyl)(6-oxo-6-(undecyloxy)hexyl)amino)octanoate 4-acetamido benzoate Polymorph A.

FIG. 46 depicts an XRPD pattern overlay of heptadecan-9-yl 8-((2-hydroxyethyl)(8-(nonyloxy)-8-oxooctyl)amino)octanoate trimesate Polymorph A and the corresponding acid, trimesic acid.

FIG. 47 depicts TGA and DSC data for heptadecan-9-yl 8-((2-hydroxyethyl)(8-(nonyloxy)-8-oxooctyl)amino)octanoate trimesate Polymorph A.

FIG. 48 depicts an XRPD pattern of heptadecan-9-yl 8-((2-hydroxyethyl)(8-(nonyloxy)-8-oxooctyl)amino)octanoate trimesate Polymorph B.

FIG. 49 depicts TGA and DSC data for heptadecan-9-yl 8-((2-hydroxyethyl)(8-(nonyloxy)-8-oxooctyl)amino)octanoate trimesate Polymorph B.

11

FIG. 50 depicts an ^1H NMR overlay of heptadecan-9-yl 8-((2-hydroxyethyl)(8-(nonyloxy)-8-oxooctyl)amino)octanoate trimesate Polymorph B and freebase.

FIG. 51 is a polarized light microscopy (PLM) image of heptadecan-9-yl 8-((2-hydroxyethyl)(8-(nonyloxy)-8-oxooctyl)amino)octanoate trimesate Polymorph B.

FIG. 52 is an XRPD pattern of (6Z,9Z,28Z,31Z)-heptatriaconta-6,9,28,31-tetraen-19-yl 4-(dimethylamino)butanoate trimesate Type A polymorph.

FIG. 53 depicts TGA and DSC data for (6Z,9Z,28Z,31Z)-heptatriaconta-6,9,28,31-tetraen-19-yl 4-(dimethylamino)butanoate trimesate Type A polymorph prepared with cyclohexane.

FIG. 54 depicts TGA and DSC data for (6Z,9Z,28Z,31Z)-heptatriaconta-6,9,28,31-tetraen-19-yl 4-(dimethylamino)butanoate trimesate Type A polymorph prepared with EtOAc.

FIG. 55 is a polarized light microscopy (PLM) image of (6Z,9Z,28Z,31Z)-heptatriaconta-6,9,28,31-tetraen-19-yl 4-(dimethylamino)butanoate trimesate Type A polymorph prepared with cyclohexane.

FIG. 56 is a polarized light microscopy (PLM) image of (6Z,9Z,28Z,31Z)-heptatriaconta-6,9,28,31-tetraen-19-yl 4-(dimethylamino)butanoate trimesate Type A polymorph prepared with EtOAc.

FIG. 57 depicts DVS data at 25° C. for (6Z,9Z,28Z,31Z)-heptatriaconta-6,9,28,31-tetraen-19-yl 4-(dimethylamino)butanoate trimesate Type A polymorphs before and after DVS.

FIG. 58 is an XRPD pattern overlay of (6Z,9Z,28Z,31Z)-heptatriaconta-6,9,28,31-tetraen-19-yl 4-(dimethylamino)

12

FIG. 59 is an XRPD pattern of (6Z,9Z,28Z,31Z)-heptatriaconta-6,9,28,31-tetraen-19-yl 4-(dimethylamino)butanoate trimesate Type B polymorph.

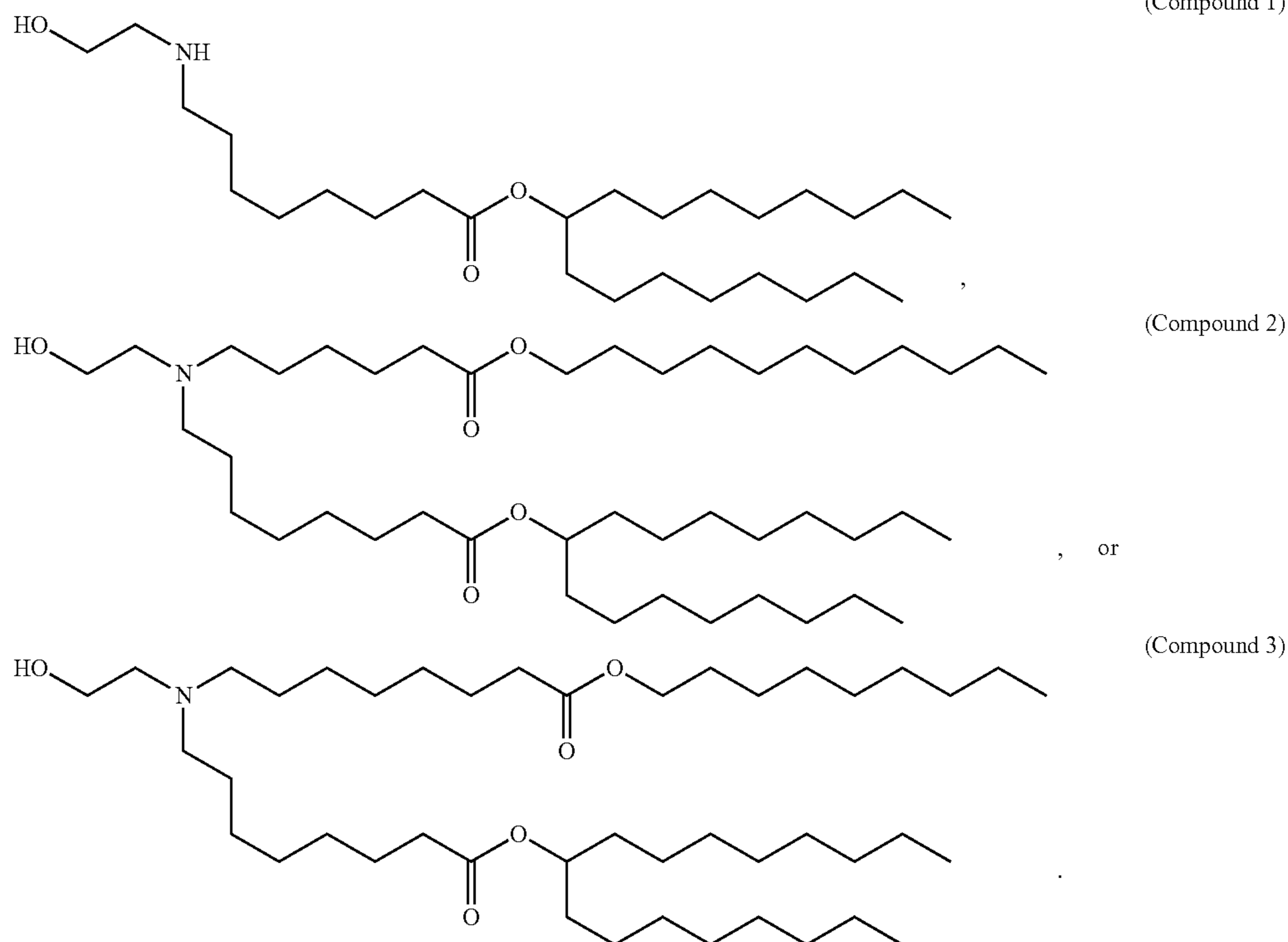
FIG. 60 depicts TGA and DSC data for (6Z,9Z,28Z,31Z)-heptatriaconta-6,9,28,31-tetraen-19-yl 4-(dimethylamino)butanoate trimesate Type B.

FIG. 61 is a polarized light microscopy (PLM) image of (6Z,9Z,28Z,31Z)-heptatriaconta-6,9,28,31-tetraen-19-yl 4-(dimethylamino)butanoate trimesate Type B polymorph.

DETAILED DESCRIPTION

The solid form (e.g., crystal state) of a compound may be important when the compound is used for pharmaceutical purposes. Compared with an amorphous solid or viscous oil, the physical properties of a crystalline compound are generally enhanced. These properties change from one solid form to another, which may impact its suitability for pharmaceutical use. In addition, different solid forms of a crystalline compound may incorporate different types and/or different amounts of impurities. Different solid forms of a compound may also have different chemical stability upon exposure to heat, light and/or moisture (e.g., atmospheric moisture) over a period of time, or different rates of dissolution. Long-chain amino lipids are usually oils at room temperature. Solid forms of these lipids are desirable for e.g., improving handling, improving stability (such as storage stability), simplifying purification process, simplifying large-scale production process and/or increasing accuracy in measurements and characterization of lipids.

Provided herein are novel solid forms (e.g., crystalline forms) of each of Compound 1, Compound 2, and Compound 3, the structure of each of which is provided below:

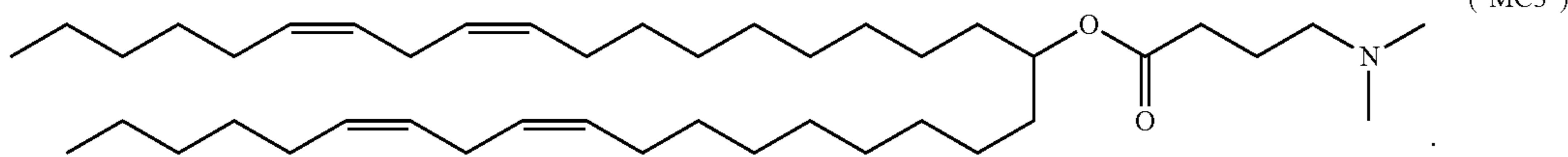


butanoate trimesate Type A polymorphs before and after DVS.

In another aspect, provided herein are novel solid forms (e.g., crystalline forms) of (6Z,9Z,28Z,31Z)-heptatriaconta-

13

6,9,28,31-tetraen-19-yl 4-(dimethylamino)butanoate (“MC3”), the structure of which is provided below:



10

In one aspect, disclosed herein is salt or cocrystal of Compound 1, 2, or 3, which has a melting point of about 50° C. or greater (e.g., about 60° C., about 70° C. or greater). For example, the salt or cocrystal of Compound 1, 2, or 3 is formed between Compound 1, 2, or 3 and a cofomer compound (e.g., an acid). In another aspect, the salt or cocrystal of Compound 3 has a melting point of about 270° C. or greater (e.g., about 280° C., about 290° C. or greater).

As used herein, “Compound 1” refers to heptadecan-9-yl 8-((2-hydroxyethyl)amino)octanoate; “Compound 2” refers to heptadecan-9-yl 8-((2-hydroxyethyl)(6-oxo-6-(undecyloxy)hexyl)amino)octanoate; and “Compound 3” refers to heptadecan-9-yl 8-((2-hydroxyethyl)(8-(nonyloxy)-8-oxooctyl)amino)octanoate. Compound 1 can be used as a starting material for the synthesis of Compound 2 or 3.

As used herein, “MC 3” refers to (6Z,9Z,28Z,31Z)-heptatriaconta-6,9,28,31-tetraen-19-yl 4-(dimethylamino)butanoate.

In one aspect, this disclosure is directed to a salt or cocrystal of Compound 1 and a compound selected from the group consisting of 4-hydroxybenzoic acid, oxalic acid, trimellitic acid, orotic acid, trimesic acid, and sulfuric acid. For example, the compound is 4-hydroxybenzoic acid. For example, the compound is oxalic acid.

Also described herein are polymorphic forms of a salt or cocrystal of Compound 1, e.g., Polymorphs A and B of 4-hydroxybenzoate of Compound 1, or Polymorphs A and B of orotate of Compound 1.

In one aspect, this disclosure is directed to a salt or cocrystal of (6Z,9Z,28Z,31Z)-heptatriaconta-6,9,28,31-tetraen-19-yl 4-(dimethylamino)butanoate (“MC3”). In another aspect, the salt or cocrystal of MC3 has a melting point of about 150° C. or greater (e.g., about 160° C., about 170° C., about 180° C. or greater, about 190° C. or greater). In another aspect, disclosed herein is a salt or cocrystal of (6Z,9Z,28Z,31Z)-heptatriaconta-6,9,28,31-tetraen-19-yl 4-(dimethylamino)butanoate (“MC3”). In another aspect, the salt or cocrystal of MC3 has a melting point of about 50° C. or greater (e.g., about 60° C., about 70° C., about 80° C. or greater). For example, the salt or cocrystal of MC3 is formed between MC3 and a cofomer compound (e.g., an acid).

The ability of a substance to exist in more than one crystal form is defined as polymorphism; the different crystal forms of a particular substance are referred to as “polymorphs” of one another. In general, polymorphism is affected by the ability of a molecule of a substance (or its salt, cocrystal, or hydrate) to change its conformation or to form different intermolecular or intra-molecular interactions, (e.g., different hydrogen bond configurations), which is reflected in different atomic arrangements in the crystal lattices of different polymorphs. In contrast, the overall external form of a substance is known as “morphology,” which refers to the external shape of the crystal and the planes present, without reference to the internal structure. A particular crystalline polymorph can display different morphology

14

based on different conditions, such as, for example, growth rate, stirring, and the presence of impurities.

The different polymorphs of a substance may possess different energies of the crystal lattice and, thus, in solid state they can show different physical properties such as form, density, melting point, color, stability, solubility, dissolution rate, etc., which can, in turn, effect the stability, dissolution rate and/or bioavailability of a given polymorph and its suitability for use as a pharmaceutical and in pharmaceutical compositions.

Polymorph A of 4-hydroxybenzoate of Compound 1 has a number of advantageous physical properties over its free base form, as well as other salts of the free base. In particular, Polymorph A of 4-hydroxybenzoate of Compound 1 has low hygroscopicity compared to other salt forms of Compound 1. More particularly, Polymorph A of 4-hydroxybenzoate of Compound 1 has low hygroscopicity compared to Polymorph A of Compound 1 trimellitate and Polymorph B of Compound 1 orotate (see, e.g., Table 1-2). Crystal forms that are highly hygroscopic may also be unstable, as the compound’s dissolution rate (and other physico-chemical properties) may change as it is stored in settings with varying humidity. Also, hygroscopicity can impact large-scale handling and manufacturing of a compound, as it can be difficult to determine the true weight of a hygroscopic agent when using it for reactions or when preparing a pharmaceutical composition comprising that agent. For example, in large scale medicinal formulating preparations, highly hygroscopic compounds can result in batch manufacturing inconsistency creating clinical and/or prescribing difficulties. For example, when Compound 1 is used as a starting material for the synthesis of Compound 2 or 3, Polymorph A of 4-hydroxybenzoate of Compound 1 has a low hygroscopicity compared to other salt forms of Compound 1, and as such, it may be stored over appreciable periods or conditions (e.g., relative humidity conditions), and not suffer from weight changes that would be detrimental for consistent production of Compound 2 or 3.

In certain embodiments, Polymorph A of 4-hydroxybenzoate of Compound 1 is identifiable on the basis of characteristic peaks in an X-ray powder diffraction analysis. X-ray powder diffraction pattern, also referred to as XRPD pattern, is a scientific technique involving the scattering of x-rays by crystal atoms, producing a diffraction pattern that yields information about the structure of the crystal. In certain embodiments, Polymorph A of 4-hydroxybenzoate of Compound 1 exhibits an X-ray powder diffraction (XRPD) pattern obtained using Cu K α radiation, having from two (2) to seven (7) characteristic peaks expressed in degrees 2-theta at 4.5, 6.8, 9.1, 11.4, 13.7, 18.3, 20.1, and 20.6.

The skilled artisan recognizes that some variation is associated with 2-theta measurements in XRPD. Typically, 2-theta values may vary from ± 0.1 to ± 0.2 . Such slight variation can be caused, for example, by sample preparation, instrument configurations and other experimental factors. The skilled artisan appreciates that such variation in values are greatest with low 2-theta values, and least with high 2-theta values. The skilled artisan recognizes that different

instruments may provide substantially the same XRPD pattern, even though the 2-theta values vary slightly. Moreover, the skilled artisan appreciates that the same instrument may provide substantially the same XRPD pattern for the same or different samples even though the XRPD of the respectively collected XRPD patterns vary slightly in the 2-theta values.

The skilled artisan also appreciates that XRPD patterns of the same sample (taken on the same or different instruments) may exhibit variations in peak intensity at the different 2-theta values. The skilled artisan also appreciates that XRPD patterns of different samples of the same polymorph (taken on the same or different instruments) may also exhibit variations in peak intensity at the different 2-theta values. XRPD patterns can be substantially the same pattern even though they have corresponding 2-theta signals that vary in their peak intensities.

In one embodiment, Polymorph A of 4-hydroxybenzoate of Compound 1 exhibits an X-ray powder diffraction pattern obtained using Cu K α radiation, having two or more characteristic peaks expressed in degrees 2-theta (+/-0.2) selected from the group consisting of 4.5, 6.8, 9.1, and 11.4. In another embodiment, Polymorph A of 4-hydroxybenzoate of Compound 1 exhibits an X-ray powder diffraction pattern obtained using Cu K α radiation, having three or more characteristic peaks expressed in degrees 2-theta (+/-0.2) selected from the group consisting of 4.5, 6.8, 9.1, 11.4, and 13.7. In another embodiment, Polymorph A of 4-hydroxybenzoate of Compound 1 exhibits an X-ray powder diffraction pattern obtained using Cu K α radiation, having four or more characteristic peaks expressed in degrees 2-theta (+/-0.2) selected from the group consisting of 4.5, 6.8, 9.1, 11.4, and 13.7. In another embodiment, Polymorph A of 4-hydroxybenzoate of Compound 1 exhibits an X-ray powder diffraction pattern obtained using Cu K α radiation, having characteristic peaks expressed in degrees 2-theta (+/-0.2) at 4.5, 6.8, 9.1, 11.4, 13.7, 18.3, 20.1, and 20.6. In one embodiment, Polymorph A of 4-hydroxybenzoate of Compound 1 exhibits an X-ray powder diffraction pattern obtained using Cu K α radiation, having two, three, four, or more characteristic peaks expressed in degrees 2-theta (+/-0.2) selected from the group consisting of 4.5, 6.8, 9.1, 11.4, and 13.7.

In a particular embodiment, Polymorph A of 4-hydroxybenzoate of Compound 1 exhibits an X-ray powder diffraction pattern obtained using Cu K α radiation, having at least eight characteristic peaks expressed in degrees 2-theta (+/-0.2), selected from the group consisting of 4.5, 6.8, 9.1, 11.4, 13.7, 16.0, 18.3, 20.1, and 20.6. In another particular embodiment, Polymorph A of 4-hydroxybenzoate of Compound 1 exhibits an X-ray powder diffraction pattern obtained using Cu K α radiation, having at least nine characteristic peaks expressed in degrees 2-theta (+/-0.2), selected from the group consisting of 4.5, 6.8, 9.1, 11.4, 13.7, 16.0, 16.6, 18.3, 20.1, and 20.6. In a further embodiment, Polymorph A of 4-hydroxybenzoate of Compound 1 exhibits an X-ray powder diffraction pattern obtained using Cu K α radiation, having at least ten characteristic peaks expressed in degrees 2-theta (+/-0.2), selected from the group consisting of 4.5, 6.8, 9.1, 11.4, 13.7, 16.0, 16.6, 18.3, 20.1, 20.6, and 21.5. In one embodiment, Polymorph A exhibits an X-ray powder diffraction pattern obtained using Cu K α radiation, having peaks with 2-theta values substantially in accordance with FIG. 1. In another embodiment, Polymorph A exhibits an X-ray powder diffraction pattern obtained using Cu K α radiation, having peaks with 2-theta values substantially in accordance with Table I below.

TABLE I

Peak	Position [$^{\circ}$ 2Th.]
1.	4.5
2.	6.8
3.	9.1
4.	11.4
5.	13.7
6.	16.0
7.	16.6
8.	18.3
9.	20.1
10.	20.6
11.	21.5
12.	23.8
13.	24.9
14.	25.8

In other embodiments, Polymorph A of 4-hydroxybenzoate of Compound 1 is identifiable on the basis of a characteristic peak observed in a differential scanning calorimetry thermogram. Differential scanning calorimetry, or DSC, is a thermoanalytical technique in which the difference in the amount of heat required to increase the temperature of a sample and reference is measured as a function of temperature. In one embodiment, Polymorph A of 4-hydroxybenzoate of Compound 1 exhibits a differential scanning calorimetry thermogram showing a characteristic primary endotherm peak expressed in units of $^{\circ}$ C. with an onset temperature of about 103+1-2 $^{\circ}$ C. In another embodiment, Polymorph A of 4-hydroxybenzoate of Compound 1 exhibits a differential scanning calorimetry thermogram showing a characteristic second primary endotherm expressed in units of $^{\circ}$ C. with an onset temperature of about 68+/-2 $^{\circ}$ C. In another embodiment, Polymorph A of 4-hydroxybenzoate of Compound 1 exhibits a differential scanning calorimetry thermogram substantially in accordance with the lower curve shown in FIG. 3.

In another embodiment, provided herein is Polymorph A of 4-hydroxybenzoate of Compound 1, wherein the solid form undergoes a weight increase of less than 1.5% (e.g., less than 1%, or less than 0.6%) upon increasing relative humidity from 5.0% to 95.0% at e.g., 25 $^{\circ}$ C. In another embodiment, Polymorph A of 4-hydroxybenzoate of Compound 1 is characterized as having a dynamic vapor sorption profile that is substantially in accordance with FIG. 8.

In one embodiment, Polymorph A of 4-hydroxybenzoate of Compound 1 is substantially free of impurities, meaning there is not a significant amount of impurities present in the sample of Polymorph A. In another embodiment, Polymorph A is a crystalline solid substantially free of amorphous Compound 1 (or any of its amorphous salt forms). In yet another embodiment, Polymorph A is a crystalline solid substantially free of other polymorphs of 4-hydroxybenzoate of Compound 1 and substantially free of amorphous Compound 1 (or any of its amorphous salt forms). For example, Polymorph A is a crystalline solid substantially free of Polymorph B of 4-hydroxybenzoate of Compound 1 and substantially free of amorphous Compound 1 (or any of its amorphous salt forms). The skilled artisan understands that a solid sample of Polymorph A may also include other polymorphs (e.g., Polymorph A), and/or amorphous Compound 1 (or any of its amorphous salt forms).

As used herein, the term "substantially free of amorphous Compound 1" means that the compound contains no significant amount of amorphous Compound 1 (or any of its amorphous salt forms). In another embodiment, a sample of a salt or cocrystal of Compound 1 comprises Polymorph A

of 4-hydroxybenzoate of Compound 1 substantially free of other polymorphs (e.g., Polymorph B of 4-hydroxybenzoate of Compound 1). As used herein, the term “substantially free of other polymorphs” means that a sample of crystalline Compound 1 4-hydroxybenzoate contains no significant amount of other polymorphs (e.g., Polymorph B). In certain embodiments, at least about 90% by weight of a sample is Polymorph A, with only 10% being other polymorphs (e.g., Polymorph B) and/or amorphous Compound 1 (or any of its amorphous salt forms). In certain embodiments, at least about 95% by weight of a sample is Polymorph A, with only 5% being other polymorphs (e.g., Polymorph B) and/or amorphous Compound 1 (or any of its amorphous salt forms). In still other embodiments, at least about 98% by weight of a sample is Polymorph A, with only 2% by weight being other polymorphs (e.g., Polymorph B) and/or amorphous Compound 1 (or any of its amorphous salt forms). In still other embodiments, at least about 99% by weight of a sample is Polymorph A, with only 1% by weight being other polymorphs (e.g., Polymorph B) and/or amorphous Compound 1 (or any of its amorphous salt forms). In still other embodiments, at least about 99.5% by weight of a sample is Polymorph A, with only 0.5% by weight being other polymorphs (e.g., Polymorph B) and/or amorphous Compound 1 (or any of its amorphous salt forms). In still other embodiments, at least about 99.9% by weight of a sample is Polymorph A, with only 0.1% by weight being other polymorphs (e.g., Polymorph B) and/or amorphous Compound 1 (or any of its amorphous salt forms).

In certain embodiments, a sample of a salt or cocrystal of Compound 1 (e.g., Compound 1 oxalate or 4-hydroxybenzoate) may contain impurities. Non-limiting examples of impurities include other polymorph forms, or residual organic and inorganic molecules such as related impurities (e.g., intermediates used to make Compound 1 or by-products, e.g., heptadecan-9-yl 8-bromooctanoate and di(heptadecan-9-yl) 8,8'-((2-hydroxyethyl)azanediyl)dioc-tanoate), solvents, water or salts. In one embodiment, a sample of a salt or cocrystal of Compound 1, e.g., oxalate or 4-hydroxybenzoate Polymorph A is substantially free from impurities, meaning that no significant amount of impurities are present. In another embodiment, a sample of the salt or cocrystal of Compound 1 contains less than 10% weight by weight (wt/wt) total impurities. In another embodiment, a sample of the salt or cocrystal of Compound 1 contains less than 5% wt/wt total impurities. In another embodiment, a sample of the salt or cocrystal of Compound 1 contains less than 2% wt/wt total impurities. In another embodiment, a sample of the salt or cocrystal of Compound 1 contains less than 1% wt/wt total impurities. In yet another embodiment, a sample of the salt or cocrystal of Compound 1 contains less than 0.1% wt/wt total impurities. In yet another embodiment, a sample of the salt or cocrystal of Compound 1 does not contain a detectable amount of impurities.

Also disclosed herein are Polymorphs A and B of Compound 1 orotate. In a particular embodiment, Polymorph A of Compound 1 orotate exhibits an X-ray powder diffraction pattern obtained using Cu K α radiation, having two, three, four, or more characteristic peaks expressed in degrees 2-theta (+/-0.2) selected from the group consisting of 5.3, 10.7, 13.3, 16.1, and 18.7. In one embodiment, Polymorph A exhibits an X-ray powder diffraction pattern obtained using Cu K α radiation, having peaks with 2-theta values substantially in accordance with FIG. 18, lower profile. In another embodiment, Polymorph A exhibits an X-ray pow-

der diffraction pattern obtained using Cu K α radiation, having peaks with 2-theta values substantially in accordance with Table II below.

TABLE II

Peak	Position [$^{\circ}$ 2Th.]
1.	5.3
2.	10.7
3.	13.3
4.	16.1
5.	18.7
6.	24.3
7.	26.9

Polymorph B of Compound 1 orotate can be defined according to its X-ray powder diffraction pattern. Accordingly, in one embodiment, Polymorph B exhibits an X-ray powder diffraction pattern obtained using Cu K α radiation, having two, three, four, or more characteristic peaks expressed in degrees 2-theta (+/-0.2) selected from the group consisting of 5.1, 7.5, 10.1, 12.7, 15.2, and 17.8. In one embodiment, Polymorph B exhibits an X-ray powder diffraction pattern obtained using Cu K α radiation, having peaks with 2-theta values substantially in accordance with FIG. 18, upper profile. In another embodiment, Polymorph B exhibits an X-ray powder diffraction pattern obtained using Cu K α radiation, having peaks with 2-theta values substantially in accordance with Table III.

TABLE III

Peak	Position [$^{\circ}$ 2Th.]
1.	5.1
2.	7.5
3.	10.1
4.	12.7
5.	15.2
6.	17.8
7.	20.2
8.	25.5
9.	28.2

In yet another embodiment, this disclosure provides Polymorph A of Compound 1 trimesate. In a particular embodiment, Polymorph A of Compound 1 trimesate exhibits an X-ray powder diffraction pattern obtained using Cu K α radiation, having two, three, four, or more characteristic peaks expressed in degrees 2-theta (+/-0.2) selected from the group consisting of 3.3, 5.3, 6.7, 7.9, 10.5, 18.5, 21.3, 23.9, and 26.5. In one embodiment, Polymorph A exhibits an X-ray powder diffraction pattern obtained using Cu K α radiation, having peaks with 2-theta values substantially in accordance with FIG. 32. In another embodiment, Polymorph A exhibits an X-ray powder diffraction pattern obtained using Cu K α radiation, having peaks with 2-theta values substantially in accordance with Table IV below.

TABLE IV

Peak	Position [$^{\circ}$ 2Th.]
1.	3.3
2.	5.3
3.	6.7
4.	7.9
5.	10.5
6.	13.6
7.	18.5

TABLE IV-continued

Peak	Position [$^{\circ}$ 2Th.]
8.	21.3
9.	23.9
10.	26.5
11.	29.1

This disclosure also provides Polymorph A of Compound 1 trimellitate. In a particular embodiment, Polymorph A of Compound 1 trimellitate exhibits an X-ray powder diffraction pattern obtained using Cu K α radiation, having two, three, four, or more characteristic peaks expressed in degrees 2-theta (+/-0.2) selected from the group consisting of 4.6, 6.8, 9.2, 11.5, 23.1, and 25.4. In one embodiment, Polymorph A exhibits an X-ray powder diffraction pattern obtained using Cu K α radiation, having peaks with 2-theta values substantially in accordance with FIG. 11. In another embodiment, Polymorph A exhibits an X-ray powder diffraction pattern obtained using Cu K α radiation, having peaks with 2-theta values substantially in accordance with Table V below.

TABLE V

Peak	Position [$^{\circ}$ 2Th.]
1.	4.6
2.	6.8
3.	9.2
4.	11.5
5.	23.1
6.	25.4
7.	27.7

Also provided herein is Polymorph A of Compound 1 sulfate. In a particular embodiment, Polymorph A of Compound 1 sulfate exhibits an X-ray powder diffraction pattern obtained using Cu K α radiation, having two, three, four, or more characteristic peaks expressed in degrees 2-theta (+/-0.2) selected from the group consisting of 4.0, 11.8, 21.4, 21.8, and 22.8. In one embodiment, Polymorph A exhibits an X-ray powder diffraction pattern obtained using Cu K α radiation, having peaks with 2-theta values substantially in accordance with FIG. 30. In another embodiment, Polymorph A exhibits an X-ray powder diffraction pattern obtained using Cu K α radiation, having peaks with 2-theta values substantially in accordance with Table VI below.

TABLE VI

Peak	Position [$^{\circ}$ 2Th.]
1.	4.0
2.	11.4
3.	11.8
4.	19.8
5.	21.4
6.	21.8
7.	22.8

In another aspect, this disclosure is directed to a salt or cocrystal of heptadecan-9-yl 8-((2-hydroxyethyl)(6-oxo-6-(undecyloxy)hexyl)amino)octanoate ("Compound 2") and a compound selected from the group consisting of trimesic acid, (-)-2,3-dibenzoyl-L-tartaric acid, 4-acetamido benzoic acid, (+)-L-tartaric acid, and methanesulfonic acid.

In one embodiment, this disclosure also provides Polymorph A of Compound 2 trimesate. In a particular embodiment, Polymorph A of Compound 2 trimesate exhibits an

X-ray powder diffraction pattern obtained using Cu K α radiation, having two, three, four, or more characteristic peaks expressed in degrees 2-theta (+/-0.2) selected from the group consisting of 3.4, 6.8, 10.2, 20.5, and 23.8. In one embodiment, Polymorph A exhibits an X-ray powder diffraction pattern obtained using Cu K α radiation, having peaks with 2-theta values substantially in accordance with FIG. 38. In another embodiment, Polymorph A exhibits an X-ray powder diffraction pattern obtained using Cu K α radiation, having peaks with 2-theta values substantially in accordance with Table VII below.

TABLE VII

Peak	Position [$^{\circ}$ 2Th.]
1.	3.4
2.	6.8
3.	10.2
4.	20.5
5.	23.8

In another embodiment, this disclosure also provides Polymorph A of Compound 2 dibenzoyl-L-tartrate. In a particular embodiment, Polymorph A of Compound 2 dibenzoyl-L-tartrate exhibits an X-ray powder diffraction pattern obtained using Cu K α radiation, having two characteristic peaks expressed in degrees 2-theta (+/-0.2) at 6.1 and 9.1. In one embodiment, Polymorph A exhibits an X-ray powder diffraction pattern obtained using Cu K α radiation, having peaks with 2-theta values substantially in accordance with FIG. 36, upper profile. In another embodiment, Polymorph A exhibits an X-ray powder diffraction pattern obtained using Cu K α radiation, having peaks with 2-theta values substantially in accordance with Table VIII below.

TABLE VIII

Peak	Pos. [$^{\circ}$ 2Th.]
1	6.1
2	9.1

In yet another embodiment, this disclosure also provides Polymorph A of Compound 2 L-tartrate. In a particular embodiment, Polymorph A of Compound 2 L-tartrate exhibits an X-ray powder diffraction pattern obtained using Cu K α radiation, having two characteristic peaks expressed in degrees 2-theta (+/-0.2) at 5.4 and 8.1. In one embodiment, Polymorph A exhibits an X-ray powder diffraction pattern obtained using Cu K α radiation, having peaks with 2-theta values substantially in accordance with FIG. 40, upper profile. In another embodiment, Polymorph A exhibits an X-ray powder diffraction pattern obtained using Cu K α radiation, having peaks with 2-theta values substantially in accordance with Table IX below.

TABLE IX

Peak	Position [$^{\circ}$ 2Th.]
1	5.4
2	8.1

In yet another embodiment, this disclosure also provides Polymorph A of Compound 2 mesylate. In a particular embodiment, Polymorph A of Compound 2 mesylate exhibits an X-ray powder diffraction pattern obtained using Cu K α radiation, having two, three, or four characteristic peaks

21

expressed in degrees 2-theta (+/-0.2) selected from the group consisting of 4.0, 11.4, 11.8, and 19.8. In one embodiment, Polymorph A exhibits an X-ray powder diffraction pattern obtained using Cu K α radiation, having peaks with 2-theta values substantially in accordance with FIG. 42. In another embodiment, Polymorph A exhibits an X-ray powder diffraction pattern obtained using Cu K α radiation, having peaks with 2-theta values substantially in accordance with Table X below.

TABLE X

Peak	Position [$^{\circ}$ 2Th.]
1.	4.0
2.	11.4
3.	11.8
4.	19.8
5.	27.9
6.	36.0

In yet another aspect, this disclosure is directed to a salt or cocrystal of heptadecan-9-yl 8-((2-hydroxyethyl)(8-(nonyloxy)-8-oxooctyl)amino)octanoate ("Compound 3") and trimesic acid.

In one embodiment, this disclosure also provides Polymorph A of Compound 3 trimesate. In a particular embodiment, Polymorph A of Compound 3 trimesate exhibits an X-ray powder diffraction pattern obtained using Cu K α radiation, having two, three, four or more characteristic peaks expressed in degrees 2-theta (+/-0.4) selected from the group consisting of 3.5, 6.8, 10.4, 18.9 and 20.9. In one embodiment, Polymorph A exhibits an X-ray powder diffraction pattern obtained using Cu K α radiation, having peaks with 2-theta values substantially in accordance with FIG. 46. In another embodiment, Polymorph A exhibits an X-ray powder diffraction pattern obtained using Cu K α radiation, having peaks with 2-theta values substantially in accordance with Table XI below.

TABLE XI

Peak	Position [$^{\circ}$ 2Th.]
1.	3.5
2.	6.8
3.	10.4
4.	18.9
5.	20.9
6.	24.3
7.	27.5

In one embodiment, this disclosure also provides Polymorph B of Compound 3 trimesate. In a particular embodiment, Polymorph B of Compound 3 trimesate exhibits an X-ray powder diffraction pattern obtained using Cu K α radiation, comprising two, three, or more characteristic peaks expressed in degrees 2-theta (+/-0.2) selected from the group consisting of 6.2, 10.8, 16.5, and 26.7. In another embodiment, Polymorph B of Compound 3 trimesate exhibits an X-ray powder diffraction pattern obtained using Cu K α radiation, having characteristic peaks expressed in degrees 2-theta (+/-0.2) at 6.2, 10.8, 16.5, and 26.7.

In a further embodiment, Polymorph B of Compound 3 trimesate exhibits an X-ray powder diffraction pattern obtained using Cu K α radiation, having at least five characteristic peaks expressed in degrees 2-theta (+/-0.2), selected from the group consisting of 6.2, 10.8, 12.4, 16.5, 18.7, 22.5, and 26.7. In one embodiment, Polymorph B of Compound 3 trimesate exhibits an X-ray powder diffraction

22

obtained using Cu K α radiation, pattern having at least six characteristic peaks expressed in degrees 2-theta (+/-0.2), selected from the group consisting of 6.2, 10.8, 12.4, 16.5, 18.7, 22.5, and 26.7.

In a particular embodiment, Polymorph B of Compound 3 trimesate exhibits an X-ray powder diffraction pattern obtained using Cu K α radiation, having two, three, four, or more characteristic peaks expressed in degrees 2-theta (+/-0.4) selected from the group consisting of 6.2, 10.8, 12.4, 16.5, 18.7, 22.5 and 26.7. In one embodiment, Polymorph B exhibits an X-ray powder diffraction pattern obtained using Cu K α radiation, having peaks with 2-theta values substantially in accordance with FIG. 48. In another embodiment, Polymorph B exhibits an X-ray powder diffraction obtained using Cu K α radiation, pattern having peaks with 2-theta values substantially in accordance with Table XII below.

TABLE XII

Peak	Position [$^{\circ}$ 2Th.]
1.	6.2
2.	10.8
3.	12.4
4.	16.5
5.	18.7
6.	22.5
7.	26.7

In other embodiments, Polymorph B of trimesate of Compound 3 is identifiable on the basis of a characteristic peak observed in a differential scanning calorimetry thermogram. In one embodiment, Polymorph B of trimesate of Compound 3 exhibits a differential scanning calorimetry thermogram showing a characteristic melting endotherm peak expressed in units of $^{\circ}$ C. with an onset temperature of about 305+/-2 $^{\circ}$ C. In another embodiment, Polymorph A of trimesate of Compound 3 exhibits a differential scanning calorimetry thermogram showing a second primary endotherm expressed in units of $^{\circ}$ C. at a temperature of 240+/-2 $^{\circ}$ C. In another embodiment, Polymorph B of trimesate of Compound 3 exhibits a differential scanning calorimetry thermogram substantially in accordance with FIG. 49.

In one embodiment, Polymorph A of trimesate of Compound 3 is substantially free of impurities, meaning there is not a significant amount of impurities present in the sample of Polymorph A. In another embodiment, Polymorph A is a crystalline solid substantially free of amorphous Compound 3 (or any of its amorphous salt forms). In yet another embodiment, Polymorph A is a crystalline solid substantially free of other polymorphs of 4-hydroxybenzoate of Compound 3 and substantially free of amorphous Compound 3 (or any of its amorphous salt forms). For example, Polymorph A is a crystalline solid substantially free of Polymorph B of trimesate of Compound 3 and substantially free of amorphous Compound 3 (or any of its amorphous salt forms). The skilled artisan understands that a solid sample of Polymorph B may also include other polymorphs (e.g., Polymorph A), and/or amorphous Compound 3 (or any of its amorphous salt forms).

In another embodiment, a sample of a salt or cocrystal of Compound 3 comprises Polymorph A of trimesate of Compound 3 substantially free of other polymorphs (e.g., Polymorph B of trimesate of Compound 3). As used herein, the term "substantially free of other polymorphs" means that a sample of crystalline Compound 3 trimesate contains no significant amount of other polymorphs (e.g., Polymorph B). In certain embodiments, at least about 90% by weight of a

sample is Polymorph A, with only 10% being other polymorphs (e.g., Polymorph B) and/or amorphous Compound 3 (or any of its amorphous salt forms). In certain embodiments, at least about 95% by weight of a sample is Polymorph A, with only 5% being other polymorphs (e.g., Polymorph B) and/or amorphous Compound 3 (or any of its amorphous salt forms). In still other embodiments, at least about 98% by weight of a sample is Polymorph A, with only 2% by weight being other polymorphs (e.g., Polymorph B) and/or amorphous Compound 3 (or any of its amorphous salt forms). In still other embodiments, at least about 99% by weight of a sample is Polymorph A, with only 1% by weight being other polymorphs (e.g., Polymorph B) and/or amorphous Compound 3 (or any of its amorphous salt forms). In still other embodiments, at least about 99.5% by weight of a sample is Polymorph A, with only 0.5% by weight being other polymorphs (e.g., Polymorph B) and/or amorphous Compound 3 (or any of its amorphous salt forms). In still other embodiments, at least about 99.9% by weight of a sample is Polymorph A, with only 0.1% by weight being other polymorphs (e.g., Polymorph B) and/or amorphous Compound 3 (or any of its amorphous salt forms).

In certain embodiments, a sample of a salt or cocrystal of Compound 3 (e.g., Compound 3 trimesate) may contain impurities. Non-limiting examples of impurities include other polymorph forms, or residual organic and inorganic molecules such as related impurities (e.g., intermediates used to make Compound 3 or by-products), solvents, water or salts. In one embodiment, a sample of a salt or cocrystal of Compound 3, e.g., trimesate Polymorph A is substantially free from impurities, meaning that no significant amount of impurities are present. In another embodiment, a sample of the salt or cocrystal of Compound 3 contains less than 10% weight by weight (wt/wt) total impurities. In another embodiment, a sample of the salt or cocrystal of Compound 3 contains less than 5% wt/wt total impurities. In another embodiment, a sample of the salt or cocrystal of Compound 3 contains less than 2% wt/wt total impurities. In another embodiment, a sample of the salt or cocrystal of Compound 3 contains less than 1% wt/wt total impurities. In yet another embodiment, a sample of the salt or cocrystal of Compound 3 contains less than 0.1% wt/wt total impurities. In yet another embodiment, a sample of the salt or cocrystal of Compound 3 does not contain a detectable amount of impurities.

In one embodiment, this disclosure also provides Polymorph A of MC3 trimesate. In one embodiment, Polymorph A of MC3 trimesate exhibits an X-ray powder diffraction pattern obtained using Cu K α radiation, comprising two, three, or more characteristic peaks expressed in degrees 2-theta (+/-0.2) selected from the group consisting of 5.2, 7.8, 20.9, and 23.6. In another embodiment, Polymorph A of MC3 trimesate exhibits an X-ray powder diffraction pattern obtained using Cu K α radiation, having two, three, four, or more characteristic peaks expressed in degrees 2-theta (+/-0.2) selected from the group consisting of 5.2, 7.8, 10.4, 20.9, and 23.6. In a further embodiment, Polymorph A of MC3 trimesate exhibits an X-ray powder diffraction pattern obtained using Cu K α radiation, having characteristic peaks expressed in degrees 2-theta (+/-0.2) at 5.2, 7.8, 10.4, 18.3, 20.9, 23.6, and 26.2.

In one embodiment, Polymorph A of MC3 trimesate exhibits an X-ray powder diffraction pattern obtained using Cu K α radiation, having at least seven characteristic peaks expressed in degrees 2-theta (+/-0.2), selected from the group consisting of 5.2, 7.8, 9.7, 10.4, 18.3, 20.9, 23.6, and 26.2. In another embodiment, Polymorph A of MC3 trime-

ate exhibits an X-ray powder diffraction pattern obtained using Cu K α radiation, having at least nine characteristic peaks expressed in degrees 2-theta (+/-0.2), selected from the group consisting of 5.2, 7.8, 9.7, 10.4, 11.5, 13.0, 18.3, 20.9, 23.6, and 26.2.

In a particular embodiment, Polymorph A of MC3 trimesate exhibits an X-ray powder diffraction pattern obtained using Cu K α radiation, having two, three, four or more characteristic peaks expressed in degrees 2-theta (+/-0.2) selected from the group consisting of 5.2, 7.8, 10.4, 18.3, 20.9, 23.6, and 26.2. In one embodiment, Polymorph A exhibits an X-ray powder diffraction pattern obtained using Cu K α radiation, having peaks with 2-theta values substantially in accordance with FIG. 52. In another embodiment, Polymorph A exhibits an X-ray powder diffraction pattern obtained using Cu K α radiation, having peaks with 2-theta values substantially in accordance with Table XIII below.

TABLE XIII

Peak	Position [$^{\circ}$ 2Th.]
1.	5.2
2.	7.8
3.	9.7
4.	10.4
5.	11.5
6.	13.0
7.	18.3
8.	20.9
9.	23.6
10.	26.2

In other embodiments, Polymorph A of trimesate of MC3 is identifiable on the basis of a characteristic peak observed in a differential scanning calorimetry thermogram. In one embodiment, Polymorph A of trimesate of MC3 exhibits a differential scanning calorimetry thermogram showing a characteristic melting endotherm peak expressed in units of $^{\circ}$ C. with an onset temperature of about 184+/-2 $^{\circ}$ C. In another embodiment, Polymorph A of trimesate of MC3 exhibits a differential scanning calorimetry thermogram substantially in accordance with the lower curve shown in FIG. 53. In another embodiment, Polymorph A of trimesate of MC3 exhibits a differential scanning calorimetry thermogram showing a characteristic melting endotherm peak expressed in units of $^{\circ}$ C. with an onset temperature of about 186+/-2 $^{\circ}$ C. In another embodiment, Polymorph A of trimesate of MC3 exhibits a differential scanning calorimetry thermogram showing a second primary endotherm expressed in units of $^{\circ}$ C. at a temperature of 90+/-2 $^{\circ}$ C. In another embodiment, Polymorph A of trimesate of MC3 exhibits a differential scanning calorimetry thermogram substantially in accordance with FIG. 54.

In another embodiment, provided herein is Polymorph A of trimesate of MC3, wherein the solid form undergoes a weight increase of less than 1.0% (e.g., less than 0.5%, or less than 0.3%) upon increasing relative humidity from 5.0% to 95.0% at e.g., 25 $^{\circ}$ C. In another embodiment, Polymorph A of trimesate of MC3 is characterized as having a dynamic vapor sorption profile that is substantially in accordance with FIG. 57.

In one embodiment, Polymorph A of trimesate of MC3 is substantially free of impurities, meaning there is not a significant amount of impurities present in the sample of Polymorph A. In another embodiment, Polymorph A is a crystalline solid substantially free of amorphous MC3 (or any of its amorphous salt forms). In yet another embodiment, Polymorph A is a crystalline solid substantially free of

other polymorphs of trimesate of MC3 and substantially free of amorphous MC3 (or any of its amorphous salt forms). For example, Polymorph A is a crystalline solid substantially free of Polymorph B of trimesate of MC3 and substantially free of amorphous MC3 (or any of its amorphous salt forms). The skilled artisan understands that a solid sample of Polymorph A may also include other polymorphs (e.g., Polymorph B), and/or amorphous MC3 (or any of its amorphous salt forms).

As used herein, the term “substantially free of amorphous MC3” means that the compound contains no significant amount of amorphous MC3 (or any of its amorphous salt forms). In another embodiment, a sample of a salt or cocrystal of MC3 comprises Polymorph A of trimesate of MC3 substantially free of other polymorphs (e.g., Polymorph B of trimesate of MC3). As used herein, the term “substantially free of other polymorphs” means that a sample of crystalline MC3 trimesate contains no significant amount of other polymorphs (e.g., Polymorph B). In certain embodiments, at least about 90% by weight of a sample is Polymorph A, with only 10% being other polymorphs (e.g., Polymorph B) and/or amorphous MC3 (or any of its amorphous salt forms). In certain embodiments, at least about 95% by weight of a sample is Polymorph A, with only 5% being other polymorphs (e.g., Polymorph B) and/or amorphous MC3 (or any of its amorphous salt forms). In still other embodiments, at least about 98% by weight of a sample is Polymorph A, with only 2% by weight being other polymorphs (e.g., Polymorph B) and/or amorphous MC3 (or any of its amorphous salt forms). In still other embodiments, at least about 99% by weight of a sample is Polymorph A, with only 1% by weight being other polymorphs (e.g., Polymorph B) and/or amorphous MC3 (or any of its amorphous salt forms). In still other embodiments, at least about 99.5% by weight of a sample is Polymorph A, with only 0.5% by weight being other polymorphs (e.g., Polymorph B) and/or amorphous MC3 (or any of its amorphous salt forms). In still other embodiments, at least about 99.9% by weight of a sample is Polymorph A, with only 0.1% by weight being other polymorphs (e.g., Polymorph B) and/or amorphous MC3 (or any of its amorphous salt forms).

In certain embodiments, a sample of a salt or cocrystal of MC3 (e.g., MC3 trimesate) may contain impurities. Non-limiting examples of impurities include other polymorph forms, or residual organic and inorganic molecules such as related impurities (e.g., intermediates used to make MC3 or by-products), solvents, water or salts. In one embodiment, a sample of a salt or cocrystal of MC3, e.g., trimesate Polymorph A is substantially free from impurities, meaning that no significant amount of impurities are present. In another embodiment, a sample of the salt or cocrystal of MC3 contains less than 10% weight by weight (wt/wt) total impurities. In another embodiment, a sample of the salt or cocrystal of MC3 contains less than 5% wt/wt total impurities. In another embodiment, a sample of the salt or cocrystal of MC3 contains less than 2% wt/wt total impurities. In another embodiment, a sample of the salt or cocrystal of MC3 contains less than 1% wt/wt total impurities. In yet another embodiment, a sample of the salt or cocrystal of MC3 contains less than 0.1% wt/wt total impurities. In yet another embodiment, a sample of the salt or cocrystal of MC3 does not contain a detectable amount of impurities.

In one embodiment, this disclosure also provides Polymorph B of MC3 trimesate. In one embodiment, Polymorph B of MC3 trimesate exhibits an X-ray powder diffraction pattern obtained using Cu K α radiation, having two, three,

four or more characteristic peaks expressed in degrees 2-theta (+/-0.2) selected from the group consisting of (+/-0.2) at 4.8, 19.4, 24.3, and 26.8. In a further embodiment, Polymorph B of MC3 trimesate exhibits an X-ray powder diffraction pattern obtained using Cu K α radiation, having characteristic peaks expressed in degrees 2-theta (+/-0.2) at 4.8, 5.4, 7.2, 9.7, 19.4, 24.3, 26.8, and 29.3.

In one embodiment, Polymorph B of MC3 trimesate exhibits an X-ray powder diffraction pattern obtained using Cu K α radiation, having at least seven characteristic peaks expressed in degrees 2-theta (+/-0.2), selected from the group consisting of 4.8, 5.4, 7.2, 9.7, 12.1, 19.4, 21.9, 24.3, 26.8, 29.3, and 31.8. In another embodiment, Polymorph B of MC3 trimesate exhibits an X-ray powder diffraction pattern obtained using Cu K α radiation, having at least nine characteristic peaks expressed in degrees 2-theta (+/-0.2), selected from the group consisting 4.8, 5.4, 7.2, 9.7, 12.1, 14.5, 17.0, 19.4, 21.9, 24.3, 26.8, and 29.3.

In a particular embodiment, Polymorph B of MC3 trimesate exhibits an X-ray powder diffraction pattern obtained using Cu K α radiation, having two, three, four or more characteristic peaks expressed in degrees 2-theta (+/-0.2) selected from the group consisting of 4.8, 5.4, 7.2, 9.7, 19.4, 24.3, 26.8, and 29.3. In one embodiment, Polymorph B exhibits an X-ray powder diffraction pattern obtained using Cu K α radiation, having peaks with 2-theta values substantially in accordance with FIG. 59. In another embodiment, Polymorph B exhibits an X-ray powder diffraction pattern obtained using Cu K α radiation, having peaks with 2-theta values substantially in accordance with Table XIV below.

TABLE XIV

Peak	Position [$^{\circ}$ 2Th.]
1.	4.8
2.	5.4
3.	7.2
4.	9.7
5.	12.1
6.	14.5
7.	17.0
8.	19.4
9.	21.9
10.	24.3
11.	26.8
12.	29.3
13.	31.8

In other embodiments, Polymorph B of trimesate of MC3 is identifiable on the basis of a characteristic peak observed in a differential scanning calorimetry thermogram. In one embodiment, Polymorph B of trimesate of MC3 exhibits a differential scanning calorimetry thermogram showing a characteristic melting endotherm peak expressed in units of $^{\circ}$ C. with an onset temperature of about 187+/-2 $^{\circ}$ C. In another embodiment, Polymorph B of trimesate of MC3 exhibits a differential scanning calorimetry thermogram substantially in accordance with FIG. 60.

In one embodiment, Polymorph B of trimesate of MC3 is substantially free of impurities, meaning there is not a significant amount of impurities present in the sample of Polymorph B. In another embodiment, Polymorph B is a crystalline solid substantially free of amorphous MC3 (or any of its amorphous salt forms). In yet another embodiment, Polymorph B is a crystalline solid substantially free of other polymorphs of trimesate of MC3 and substantially free of amorphous trimesate of MC3 (or any of its amorphous salt forms). For example, Polymorph B is a crystalline solid

27

substantially free of Polymorph A of trimesate of MC3 and substantially free of amorphous trimesate of MC3 (or any of its amorphous salt forms). The skilled artisan understands that a solid sample of Polymorph B may also include other polymorphs (e.g., Polymorph A), and/or amorphous MC3 (or any of its amorphous salt forms). As used herein, the term “substantially free of amorphous MC3” means that the compound contains no significant amount of amorphous MC3 (or any of its amorphous salt forms).

In another embodiment, a sample of a salt or cocrystal of MC3 comprises Polymorph B of trimesate of MC3 substantially free of other polymorphs (e.g., Polymorph A of trimesate of MC3).

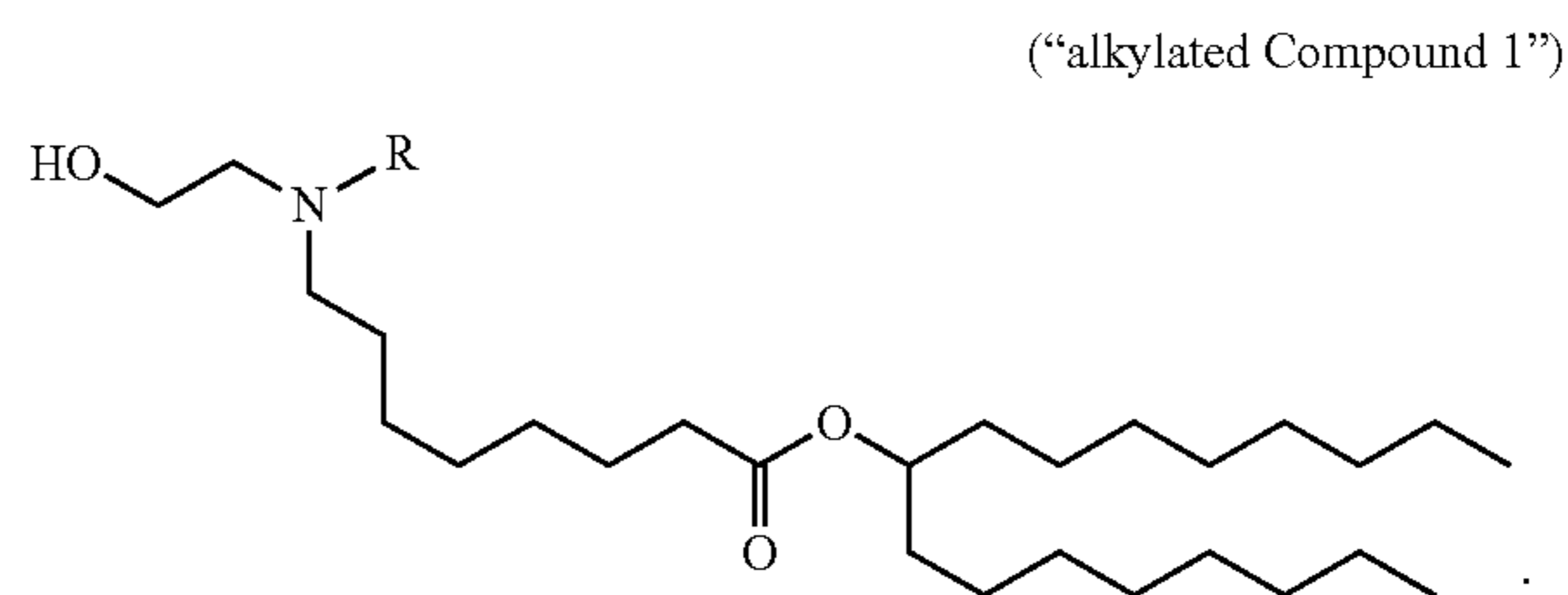
As used herein, the term “substantially free of other polymorphs” means that a sample of crystalline MC3 trimesate contains no significant amount of other polymorphs (e.g., Polymorph A). In certain embodiments, at least about 90% by weight of a sample is Polymorph B, with only 10% being other polymorphs (e.g., Polymorph A) and/or amorphous MC3 (or any of its amorphous salt forms). In certain embodiments, at least about 95% by weight of a sample is Polymorph B, with only 5% being other polymorphs (e.g., Polymorph A) and/or amorphous MC3 (or any of its amorphous salt forms). In still other embodiments, at least about 98% by weight of a sample is Polymorph B, with only 2% by weight being other polymorphs (e.g., Polymorph A) and/or amorphous MC3 (or any of its amorphous salt forms). In still other embodiments, at least about 99% by weight of a sample is Polymorph B, with only 1% by weight being other polymorphs (e.g., Polymorph A) and/or amorphous MC3 (or any of its amorphous salt forms). In still other embodiments, at least about 99.5% by weight of a sample is Polymorph B, with only 0.5% by weight being other polymorphs (e.g., Polymorph A) and/or amorphous MC3 (or any of its amorphous salt forms). In still other embodiments, at least about 99.9% by weight of a sample is Polymorph B, with only 0.1% by weight being other polymorphs (e.g., Polymorph A) and/or amorphous MC3 (or any of its amorphous salt forms).

In certain embodiments, a sample of a salt or cocrystal of MC3 (e.g., MC3 trimesate) may contain impurities. Non-limiting examples of impurities include other polymorph forms, or residual organic and inorganic molecules such as related impurities (e.g., intermediates used to make MC3 or by-products), solvents, water or salts. In one embodiment, a sample of a salt or cocrystal of MC3, e.g., trimesate Polymorph B is substantially free from impurities, meaning that no significant amount of impurities are present. In another embodiment, a sample of the salt or cocrystal of MC3 contains less than 10% weight by weight (wt/wt) total impurities. In another embodiment, a sample of the salt or cocrystal of MC3 contains less than 5% wt/wt total impurities. In another embodiment, a sample of the salt or cocrystal of MC3 contains less than 2% wt/wt total impurities. In another embodiment, a sample of the salt or cocrystal of MC3 contains less than 1% wt/wt total impurities. In yet another embodiment, a sample of the salt or cocrystal of MC3 contains less than 0.1% wt/wt total impurities.

Also disclosed herein is a salt or cocrystal of an alkylated Compound 1 (structure of which is shown below, wherein R is an alkyl having, e.g., 1-20 carbon atoms) and a cofomer compound such as those disclosed herein, e.g., 4-hydroxybenzoic acid, oxalic acid, trimellitic acid, orotic acid, trimesic acid, sulfuric acid, (-)-2,3-dibenzoyl-L-tartaric acid, 4-acetamido benzoic acid, (+)-L-tartaric acid, and methanesulfonic acid. For example, the salt or cocrystal of an

28

alkylated Compound 1 has a melting point of about 50° C. or greater (e.g., about 60° C., 70° C., or greater).



The salts or cocrystals disclosed herein may comprise Compound 1 (or Compound 2 or 3) and the cofomer compound (e.g., an acid), within a ratio from 1:0.2 mol/mol to 1:5 mol/mol or from about 1:0.5 mol/mol to 1:2 mol/mol, or from 1:0.4 mol/mol to 1:1.1 mol/mol. For example, the molar ratio is about 1:1 mol/mol.

The salts or cocrystals disclosed herein may comprise (6Z,9Z,28Z,31Z)-heptatriaconta-6,9,28,31-tetraen-19-yl 4-(dimethylamino)butanoate (“MC3”) and the cofomer compound (e.g., an acid), within a ratio from 1:0.5 mol/mol (i.e., 2:1 mol/mol) to 1:2 mol/mol.

The salts or cocrystals disclosed herein may be anhydrous and/or essentially solvent-free form, or be in hydrate and/or solvate form. For example, 4-hydroxybenzoate of Compound 1 is anhydrous. For example, Compound 1 orotate may be anhydrous or in a hydrate or solvate form.

Preparation of Salts or Cocrystals and Polymorphs Thereof

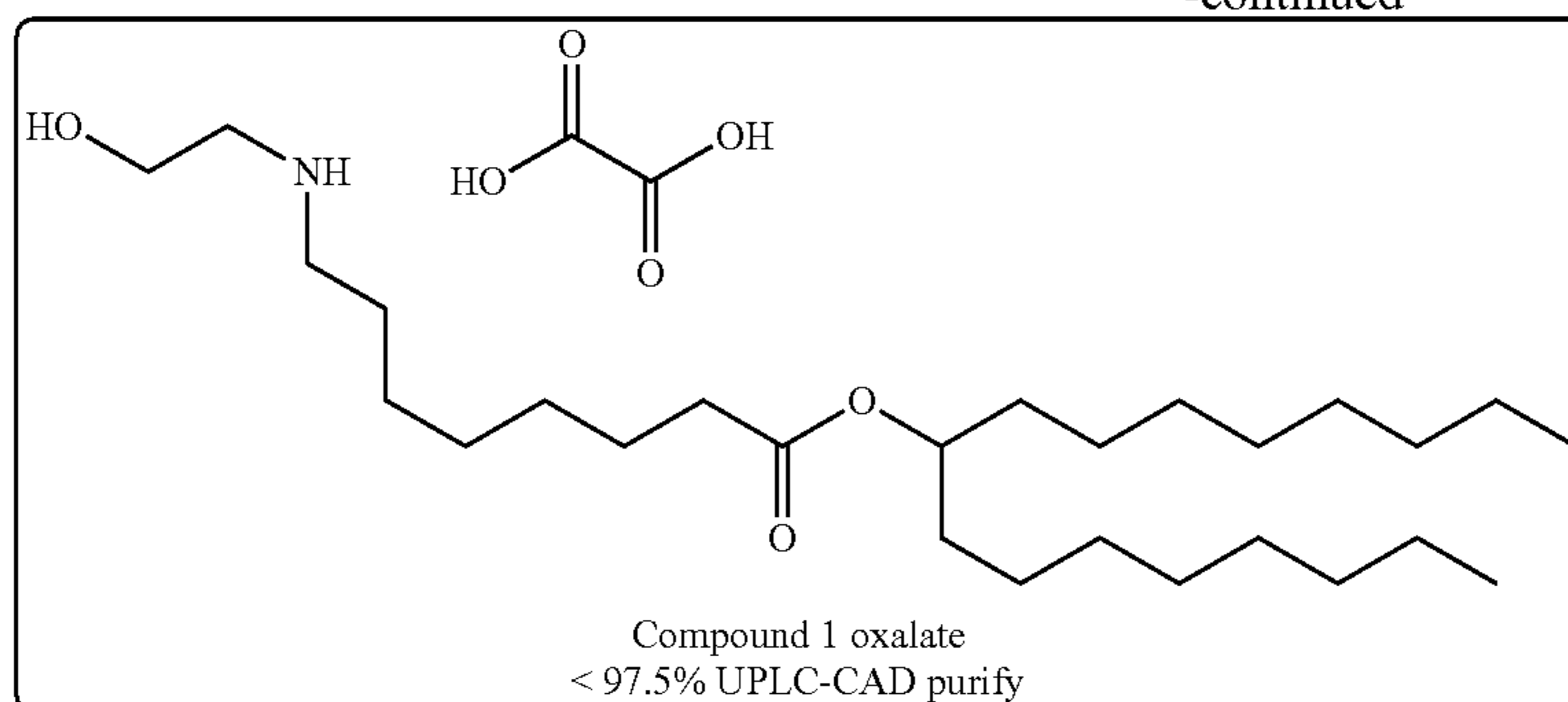
General techniques for making polymorphs are understood by the skilled artisan. Conventionally, a salt form or cocrystal is prepared by combining in solution the free base compound and a cofomer (e.g., an acid cofomer) containing the anion of the salt form desired, and then isolating the solid salt or cocrystal product from the reaction solution (e.g., by crystallization, precipitation, evaporation, etc.). Other salt-forming or cocrystallization techniques may be employed.

In one aspect, provided herein is a method of preparing a salt or cocrystal of Compound 1 by combining Compound 1 with a compound selected from the group consisting of 4-hydroxybenzoic acid, oxalic acid, trimellitic acid, orotic acid, trimesic acid, and sulfuric acid. In one embodiment, the method comprises the steps: a) dissolving Compound 1 in a solvent to obtain a solution; b) combining the cofomer compound with the solution; c) precipitating or crystallizing the salt or cocrystal from the solution; and d) collecting the salt or cocrystal. In one embodiment, the solvent used in step a) is n-heptane, ethyl acetate, or cyclohexane. In one embodiment, step c) is carried out substantively free of evaporation to obtain 4-hydroxybenzoate, trimellitate, orotate, and trimesate of Compound 1. In another embodiment, step c) is carried out by slow evaporation, at e.g., 5° C., to obtain, e.g., sulfate of Compound 1. In some embodiments, the molar ratio of Compound 1 and the compound is about 1:1.

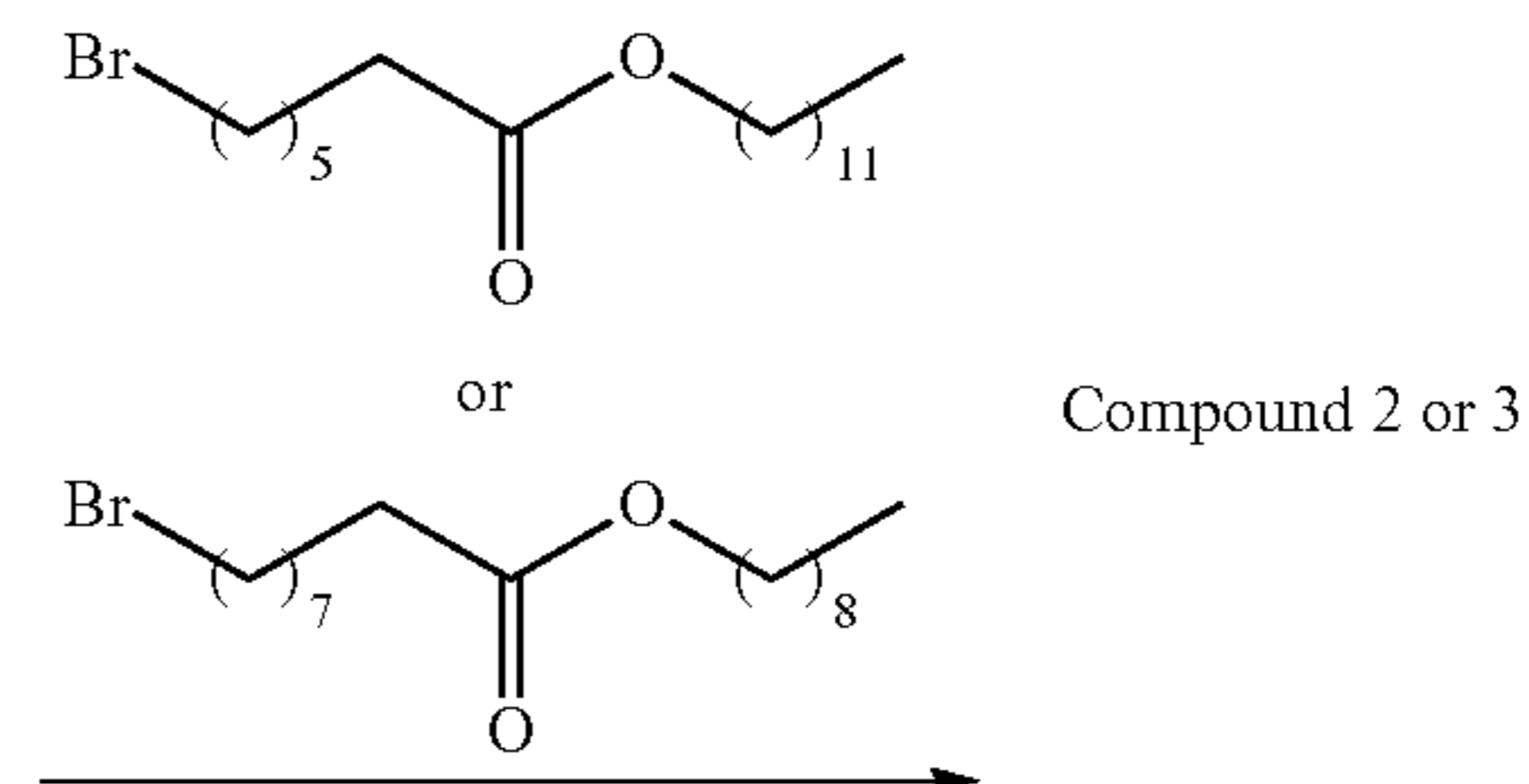
Also provided herein is a method for preparing a salt or cocrystal of Compound 2 by combining Compound 2 with a compound selected from the group consisting of trimesic acid, (-)-2,3-dibenzoyl-L-tartaric acid, 4-acetamido benzoic acid, (+)-L-tartaric acid, and methanesulfonic acid. In one embodiment, the method comprises the steps: a) dissolving

31

-continued



32



In the scheme above, Compound 1 is oil and it is hard to purify it, e.g., by separating it from a and b, and other by-products. Compound 1 oxalate is a crystal, thus is easy to separate from a, b, and/or other by-products. Forming a salt or cocrystal of Compound 1, e.g., oxalate, improves purification. Also, Compound 1 oxalate can be used to synthesize Compound 2 or 3 without converting back to Compound 1 (i.e., neutralization).

A process for synthesizing MC3 is described in Jayaraman, M.; Maximizing the Potency of siRNA Lipid Nanoparticles for Hepatic Gene Silencing In Vivo, *Angew. Chem. Int. Ed.* 2012, 51, 8529-8533, which is incorporated herein by reference in its entirety. MC3 corresponds to compound 16 in this article.

In one embodiment, the process of the present disclosure is advantageous as compared to other processes in that the process of the disclosure produces Compound 1, 2, or 3 or a salt or cocrystal thereof at a large scale and/or at a high purity, e.g., such that cumbersome purification (e.g., column chromatography, extraction, phase separation, distillation and solvent evaporation) is not needed. In one embodiment, the process of the present disclosure is able to process at least 100 g, 200 g, 500 g or more (e.g., 1 kg, 2 kg, 5 kg, 10 kg, 20 kg, 50 kg, 100 kg, 200 kg, 500 kg, or 1000 kg or more) Compound 1, 2, or 3 or a salt or cocrystal thereof without the need to scale up. In one embodiment, the process of the present disclosure is able to produce Compound 1, 2, or 3 or a salt or cocrystal thereof at least at a purity of at least 75%, 80%, 85%, 90%, 95%, 96%, 97%, 98%, 99%, or 99.5%, or higher. In one embodiment, the process of the present disclosure is able to produce Compound 1, 2, or 3 or a salt or cocrystal thereof with little or none impurity. In one embodiment, the impurity produced in the process of the present disclosure, even if produced, is easy to be separated from Compound 1, 2, or 3 or a salt or cocrystal thereof, without cumbersome purification (e.g., column chromatography, extraction, phase separation, distillation and solvent evaporation).

All percentages and ratios used herein, unless otherwise indicated, are by weight (i.e., weight by weight or wt/wt). Other features and advantages of the present invention are apparent from the different examples. The provided examples illustrate different components and methodology useful in practicing the present invention. The examples do

not limit the claimed invention. Based on the present disclosure the skilled artisan can identify and employ other components and methodology useful for practicing the present invention.

EXAMPLES

X-Ray Powder Diffraction

XRPD was performed with PANalytical Empyrean, X'Pert3, and Bruker D2 X-ray powder diffractometers. The parameters used are listed in the table below.

Parameters	XRPD		
Model	Empyrean	X' Pert3	Bruker D2
X-Ray wavelength	Cu, $\text{K}\alpha$, $\text{K}\alpha_1$ (\AA): 1.540598, $\text{K}\alpha_2$ (\AA): 1.544426 $\text{K}\alpha_2/\text{K}\alpha_1$ intensity ratio: 0.50		
X-Ray tube setting	45 kV, 40 mA		30 kV, 10 mA
Divergence slit	Automatic	1/8°	0.6 mm
Scan mode	Continuous		
Scan range ($^{\circ}2$ -theta)	3-40		
Scan step time (s)	17.8	46.7	0.1
Step size ($^{\circ}2$ -theta)	0.0167	0.0263	0.0201
Scan speed ($^{\circ}/\text{min}$)	5 min 30 s	5 min 04 s	3 min 27 s

TGA/DSC

TGA data were collected using a TA Q500/Q5000 TGA from TA Instruments. DSC was performed using a TA Q200/Q2000 DSC from TA Instruments. Detailed parameters used are listed in the following table.

Parameters	TGA	DSC
Method	Ramp	
Sample pan	Aluminum or platinum, open	Aluminum or platinum, crimped
Temperature	RT—desired temperature; or -60°C .—desired temperature; or RT-350° C.	—desired temperature; or RT-300° C.
Heating rate	10° C./min	
Purge gas	N ₂	

HPLC

Agilent 1100 or Agilent 1100/1260 HPLC was utilized to analyze purity, with the detailed method listed in the table below.

HPLC	Agilent 1100 with DAD Detector	Agilent 1100/1260
Column	Agilent Eclipse Plus C18, 150 × 4.6 mm, 5 μm	Agilent ZORBAX SB-Phenyl, 150 × 4.6 mm, 3.5 μm
Mobile phase	A: 0.1% TFA in H ₂ O B: 0.1% TFA in Acetonitrile	

-continued

	Time (min)	% B	Time (min)	% B
Gradient table	0.0	30	0.0	10
	15.0	100	4.0	80
	22.0	100	6.0	80
	22.1	30	6.10	10
	25.0	30	8.0	10
Run time	25.0 min		8.0 min	
Post time	0.0 min		0.0 min	
Flow rate	0.8 mL/min		1.0 mL/min	
Injection volume	5 μ L		10 μ L	
Column temperature		40° C.		
Sample temperature		RT		
Diluent	MeOH		EtOH	
Detector	ELSD	Grace 3300	Detector wavelength	
	Temperature	50° C.	UV at 210 nm, reference 500 nm	
	Flow	2 L/min		
	Gain	1		

Agilent 1100/1260 HPLC with Halo C18 column was utilized for purity and concentration measurements of MC3 free base, with the detailed method listed in the table below.

Parameter	Condition
Column	Halo C18, 100 \times 4.6 mm, 2.7 μ m
Mobile phase	A: 20% NH ₄ HCO ₃ (10 mM) + 40% MeOH + 40% THF B: 20% IPA + 40% MeOH + 40% THF
	Time (min) % B
Gradient table	0.00 0
	30.00 40
	35.00 50
	35.01 0
	40.00 0
Run time	40.0 min
Post time	0.0 min
Flow rate	10 mL/min
Injection volume	10 μ L
Detector wavelength	UV at 207 nm, reference 500 nm
Column temperature	40° C.
Sample temperature	RT
Diluent	EtOH

Dynamic Vapor Sorption

DVS was measured on via a SMS (Surface Measurement Systems) DVS Intrinsic. The relative humidity at 25° C. were calibrated against deliquescence point of LiCl, Mg(NO₃)₂ and KCl. Actual parameters for DVS test are listed in the table below.

Parameters	DVS
Temperature	25° C.
Sample size	10~20 mg
Gas and flow rate	N ₂ , 200 mL/min
dm/dt	0.002%/min
Min. dm/dt stability duration	10 min
Max. equilibrium time	180 min

-continued

Parameters	DVS
RH range	0%RH-95%RH
RH step size	10% (0% RH-90% RH, 90% RH-0% RH) 5% (90% RH-95% RH, 95% RH-90% RH)

¹H NMR spectrum was collected on Bruker 400M NMR Spectrometer using DMSO-d₆ as solvent.

Polarized light microscopic (PLM) images were captured on Axio Lab A1 upright microscope at room temperature.

Example 1: Salts or Cocrystals of Compound 1

Preparation

Compound 1 freebase is an oil at ambient conditions. As per the results in FIGS. 34 and 35, the freebase showed minor weight loss of 1.1% before 200° C. in TGA, and possible crystallization and melting signals in cyclic DSC, suggesting the existence of a crystalline form which melts around 17° C. (peak). Purity of the material was determined to be 99.95 area % by HPLC with ELSD detector.

To identify a crystalline salt form or cocrystal of Compound 1, screening was performed under 96 conditions using 32 acids and three solvent systems. Compound 1 freebase was dispersed in selected solvent with a 1.5-mL glass vial and corresponding salt former was added with a molar charge ratio of 1:1. The mixtures of freebase and the cofomer compound (e.g., an acid) were first transferred to temperature cycling from 50° C. to 5° C. for two cycles (heating rate of 4.5° C./min, cooling rate of 0.1° C./min) and then stirred at 5° C. to induce precipitation. If the samples were still clear, they would be subjected to evaporation at different temperatures (5° C. or RT) to dryness. Resulted solids were isolated and analyzed.

Isolated crystal solids were characterized by X-ray powder diffraction (XRPD), thermo-gravimetric analysis (TGA) and differential scanning calorimetry (DSC), with proton nuclear magnetic resonance (¹H NMR) to confirm the freebase chemical structure and also potential co-existence with some organic acids. Exemplary data from the initial findings are summarized in Table 1.

TABLE 1

	n-Heptane	EtOAc	Cyclohexane
1 Hexanoic acid	Amorphous*	Amorphous*	Oil**
2 Fumaric acid	Acid + two extra peaks	Acid + two extra peaks*	Acid + two extra peaks
3 Adipic acid	Amorphous*	Amorphous*	Acid + one extra peak**
4 Suberic acid	Amorphous*	Acid*	Oil**
5 Cinnamic acid	Amorphous*	Amorphous*	Oil**
6 Benzoic acid, 4-acetamido	Acid	Two peaks*	Acid
7 (S)-Mandelic acid	Two peaks*	Two peaks*	Oil**
8 (-)-O,O-Di-pivaloyl-L-tartaric acid	Amorphous*	Amorphous*	Oil**
9 Terephthalic acid	Acid	Acid	Acid
10 Trimesic acid	Amorphous	Trimesate Polymorph A	Oil**
11 Citric acid	Two peaks*	Amorphous*	Two peaks**
12 Succinic acid	Two peaks*	Two peaks*	Two peaks**
13 Malonic acid	Amorphous*	Amorphous*	Oil**
14 (+)-Camphor-10-sulfonic acid	Amorphous*	Amorphous*	Oil**
15 Nicotinic acid	Amorphous*	Acid*	Oil**
16 (+)-L-tartaric acid	Two peaks	Two peaks*	Oil**
17 p-Toluenesulfonic acid	Amorphous*	Two peaks*	Oil**
18 Hydrochloric acid	Amorphous*	Amorphous*	Amorphous**
19 Sulfuric acid	Sulfate Polymorph A*	Amorphous*	Oil**
20 Phosphoric acid	Two peaks*	Amorphous*	Oil**
20 Acetic acid	Amorphous*	Amorphous*	Oil**
21 Methanesulfonic acid	Amorphous*	Amorphous*	Oil**
22 Sebacic acid	Sebacic acid	Sebacic acid*	Sebacic acid*
23 Benzoic acid	Amorphous*	Amorphous*	Amorphous*
24 1,2,4-Trimellitic acid	Trimellitate Polymorph A	Trimellitate Polymorph A	Trimellitate Polymorph A
25 Phthalic acid	Oil*	Oil*	Oil*
26 Isophthalic acid	Isophthalic acid	Isophthalic acid	Isophthalic acid
27 Orotic acid	Orotate Polymorph A	Orotate Polymorph A	Orotate Polymorph A
28 4-Hydroxybenzoic acid	4-Hydroxybenzoate Polymorph A	4-Hydroxybenzoate Polymorph A	4-Hydroxybenzoate Polymorph A
29 (-)-Dibenzoyl-L-tartaric acid	Weakly crystalline	Amorphous*	Weakly crystalline
30 2,5-Dihydroxybenzoic acid	Oil*	Oil*	2,5-Dihydroxybenzoic acid
31 2-Hydroxy benzoic acid	Oil**	Oil**	Oil**
32 3-Hydroxy benzoic acid	Oil**	Oil**	Oil**

*clear solutions obtained after 5° C. stirring were transferred to 5° C. evaporation.

**clear solutions obtained after 5° C. stirring were slow evaporated at RT.

Among them, five crystalline hits were discovered, including 4-hydroxybenzoate, trimellitate, orotate, trimesate

45

and sulfate. Table 2 summarizes the properties of certain polymorphs of the salts or cocrystals.

TABLE 2

	4-Hydroxybenzoate	Trimellitate	Orotate	
	Polymorph A	Polymorph A	Polymorph A	Polymorph B
Appearance	White powder	Wax-like solid	Wax-like solid	
Solid form	Anhydrate	Hydrate	Anhydrate/Hydrate	Hydrate/solvate
Crystallinity	High	Medium	Medium	
Purity, area %	99.96	99.97	—	99.97
TGA weight loss, %	0.7-1.7	1.5-3.4	4.0	4.0
DSC endotherm, ° C. (onset)	66.8, 101.8 (batch 1) 68.2, 103.5 (batch 2)	78.3, 137.1 (batch 1) 80.0*, 137.1 (batch 2)	78.8*, 85.1*, 176.3*	83.5*
Hygroscopicity (form change after DVS)	Non-hygroscopic (no)	Slightly hygroscopic (no)	—	Hygroscopic (convert to orotate Polymorph A)

*peak temperature.

—: no data available.

Three crystalline polymorphs of Compound 1 (4-hydroxybenzoate Polymorph A, trimellitate Polymorph A and orotate Polymorph B) were prepared to larger scale for further investigation, with the detailed procedure shown below:

1. About 100 mg of freebase Compound 1 was added into a 3-mL glass vial;
2. Add corresponding acids (molar charge ratio is 1:1) into the vial;
3. Add 0.5 mL of solvent and transfer the suspension to temperature cycling from 50° C. to 5° C. (cooling rate of 0.1° C./min, two cycles) with magnetic stirring.
4. Centrifuge to isolate solids and vacuum dry at RT.

Characterization of 4-hydroxybenzoate

Two batches of 4-hydroxybenzoate Polymorph A (or Type A) (batch Nos. 1 and 2) were prepared by slurry in n-heptane and showed high crystallinity as characterized by XRPD in FIG. 1. The ¹H NMR of sample (batch No. 2) was collected with spectrum shown in FIG. 2. Besides freebase, a certain amount of 4-hydroxybenzoic acid was detected in ¹H NMR (signals around 6.7 and 7.7 ppm), indicating the possibility of salt formation.

As indicated by the TGA and DSC data in FIG. 3, sample (batch No. 2) showed a weight loss of 0.7% up to 140° C. and two sharp endothermic peaks at 68.2° C. and 103.5° C. (onset temperature) before decomposition. Based on the negligible weight loss in TGA, 4-hydroxybenzoate Polymorph A was considered to be an anhydrous form. In addition, the two sharp endothermic signals in DSC curve implied the possible existence of another anhydrous form at higher temperature.

As evidenced by heating experiments in FIG. 5 and VT-XRPD results in FIGS. 6 and 7, form change (new form assigned as 4-hydroxybenzoate Polymorph B) was observed after heating sample (batch No. 1) to 83° C. (over the first endotherm in DSC) in VT-XRPD test and no form change was observed after heating sample (batch No. 2) over the first endotherm and cooling back to RT. Considering results of heating experiments and thermal signals in cyclic DSC (FIG. 4), 4-hydroxybenzoate Polymorphs A and B are possibly enantiotropically related and Polymorph A is more stable at lower temperature (RT).

Further evaluation on hygroscopicity of 4-hydroxybenzoate Polymorph A was conducted via DVS isotherm collection at 25° C. Results in FIGS. 8 and 9 showed that sample (batch No. 1) is non-hygroscopic with no form change before and after DVS test. Moreover, sample (batch No. 1) showed aggregation of small particles (<10 μm) in PLM image (FIG. 10) and a purity of 99.96 area % determined by HPLC (Table 3).

TABLE 3

# Peak	Time (min)	RRT	Area (mAU*S)	Area (%)
1	16.58	1.00	2070.9	99.96
2	16.99	1.02	0.8	0.04

Characterization of Trimellitate

Trimellitate Polymorph A samples (batch Nos. 1 and 2) were prepared by reactive crystallization in EtOAc with XRPD patterns shown in FIG. 11. The ¹H NMR spectrum was collected for sample (batch No. 2) and is shown in FIG. 12. Compared to freebase, a certain amount of trimellitic acid was detected (signals between 8.0 and 9.0 ppm), indicating the salt formation.

As per the TGA and DSC data in FIG. 13, sample (batch No. 1) showed a weight loss of 3.4% up to 110° C. and two endothermic peaks at 78.3° C. and 137.1° C. (onset temperature) before decomposition. As demonstrated by VT-XRPD results in FIG. 14, extra diffraction peaks appeared after 20 minutes of N₂ flow, and new form was observed at 90° C., which converted back to trimellitate Polymorph A after being heated and exposed to ambient condition, suggesting that Polymorph A is a hydrated form.

Further evaluation on hygroscopicity of trimellitate Polymorph A was performed via DVS isotherm collection at 25° C. Results in FIGS. 15 and 16 showed that sample (batch No. 1) is slightly hygroscopic with no form change before and after DVS test. Platform observed in DVS plot (FIG. 15) also indicated that Polymorph A is a hydrated form. Moreover, sample (batch No. 1) showed irregular particles (<10 μm) in PLM image (FIG. 17) and a purity of 99.97 area % determined by HPLC (Table 4).

TABLE 4

# Peak	Time (min)	RRT	Area (mAU*S)	Area (%)
1	16.62	1.00	1404.2	99.97
2	16.99	1.02	0.5	0.03

Characterization of Orotate

Orotate Polymorph A and Polymorph B were generated via reactive crystallization in EtOAc with XRPD patterns shown in FIG. 18. The ¹H NMR spectrum of Polymorph A was collected and is shown in FIG. 19. In addition to freebase, a certain amount of orotic acid was detected (signal at 5.7 ppm).

As per the TGA and DSC data in FIG. 20, Polymorph A sample showed a weight loss of 4.0% up to 110° C. and endothermic peaks at 78.8, 85.1 and 176.3° C. (peak temperature) before decomposition. Results of heating experiments in FIG. 21 showed that no form change was observed after heating Polymorph A sample over the first two endothermic signals and cooling back to RT, suggesting Polymorph A is anhydrous or a hydrated form which can rapidly absorb water at ambient conditions after de-hydration. In addition, as evidenced by the heating-cooling DSC curve of Polymorph A in FIG. 22, endothermic and exothermic signals with similar enthalpy were observed at 170~175° C. and 80~90° C., suggesting the possible form transition and the existence of anhydrate form at higher temperature.

TGA and DSC data of Polymorph B in FIG. 23 showed a weight loss of 4.0% up to 110° C. and endothermic peak at 78.1° C. (onset) before decomposition. After cyclic DSC between 25° C. and 130° C., Polymorph B converted to Polymorph A with data illustrated in FIG. 24 and FIG. 25, indicating Polymorph B is a hydrated or solvate form. DVS test of Polymorph B sample showed that it is slightly hygroscopic and converted to Polymorph A after DVS test, with data displayed in FIG. 26 and FIG. 27. Also, Polymorph B sample showed irregular particles in PLM image (FIG. 28) and a purity of 99.97 area % detected by HPLC (Table 5).

TABLE 5

# Peak	Time (min)	RRT	Area (mAU*S)	Area (%)
1	16.62	1.00	1464.2	99.97
2	17.00	1.02	0.5	0.03

Characterization of Sulfate

Sulfate Polymorph A was generated by slow evaporation at 5° C. in n-heptane. Needle like crystals were observed during evaporation (FIG. 29), which was further isolated for XRPD, TGA and DSC tests. Results in FIGS. 30 and 31 showed that the sample is crystalline with continuous weight loss and multiple endotherms.

Characterization of Trimesate

Trimesate Polymorph A was generated from reactive crystallization in EtOAc system and XRPD pattern is shown in FIG. 32. ¹H NMR results in FIG. 33 showed obvious signal of trimesic acid besides chemical shifts of freebase. Characterization of Oxalate

Compound 1 Oxalate was generated from recrystallization. A purity of >97.5 area % detected by UPLC-CAD.

Example 2: Salts or Cocrystals of Compound 2

Preparation

Compound 2 freebase showed minor weight loss of 1.6% before reaching 200° C. in TGA. No obvious glass transition signal was observed and multiple endothermic peaks were observed with temperature elevated from -60 to 35° C. Two

endothermic signals at -47.7 and -34.0° C. (onset) were observed during temperature elevated from -60 to 35° C.

Similar to the process described in Example 1, to identify a crystalline salt form or cocrystal of Compound 2, screening was performed under 93 conditions using 31 acids and three solvent systems. 0.3 mL stock solutions of Compound 2 freebase (~50 mg/mL) was dispersed in selected solvent and corresponding salt former was added with a molar charge ratio of 1:1. The mixtures of freebase and the coformer compound (e.g., an acid) were first transferred to temperature cycling from 50° C. to 5° C. for three cycles (heating rate of 4.5° C./min, cooling rate of 0.1° C./min) and then stored at 5° C. before analysis. If the samples were still clear, they would be subjected to slow evaporation at 5° C. to dryness. Resulted solids were isolated and analyzed.

Isolated crystal solids were characterized by X-ray powder diffraction (XRPD), thermo-gravimetric analysis (TGA) and differential scanning calorimetry (DSC), with proton nuclear magnetic resonance (¹H NMR) to confirm the freebase chemical structure and also potential co-existence with some organic acids. Exemplary data from the initial findings are summarized in Table 6.

TABLE 6

#	Acid	Solvent		
		n-Heptane	Cyclohexane	EtOAc
1	Trimesic acid	Trimesate Polymorph A	Trimesate Polymorph A	Gel
2	Trimellitic acid	Amorphous + acid	Amorphous	Gel
3	(-)-2,3-Dibenzoyl-L-tartaric acid	Dibenzoyl-L-tartrate Polymorph A	Dibenzoyl-L-tartrate Polymorph A*	Dibenzoyl-L-tartrate Polymorph A*
4	Fumaric acid	Amorphous + two peaks	Acid	Gel
5	Terephthalic acid	Acid	Acid	Gel
6	Phthalic acid	Gel	Gel	Gel
7	Isophthalic acid	Acid	Acid	Gel
8	Benzoic acid	Gel	Gel	Gel
9	Cinnamic acid	Gel	Gel	Gel
10	4-Hydroxy benzoic acid	Amorphous	Gel	Gel
11	Salicylic acid	Gel	Gel	Gel
12	Adipic acid	Acid	Gel	Gel
13	Suberic acid	Acid	Acid	Gel
14	Sebacic acid	Gel	Acid	Acid
15	4-Acetamido benzoic acid	4-Acetamido benzoate Polymorph A + acid	Acid	Acid
16	S-(+)-Mandelic	Gel	Gel	Gel
17	Orotic acid	Gel	Acid	Acid
18	Hexanoic acid	Gel	Gel	Gel
19	Citric acid	Gel	Gel	Gel
20	Acetic acid	Gel	Gel	Gel
21	Succinic acid	Acid	Acid	Gel
22	Malonic acid	Gel	Gel	Gel
23	(+)-Camphor-10-sulfonic acid	Gel	Gel	Gel
24	Nicotinic acid	Acid	Acid	Acid
25	(+)-L-tartaric acid	L-Tartrate Polymorph A*	Gel	L-Tartrate Polymorph A*
26	Hydrochloric acid	Gel	Gel	Gel
27	Sulfuric acid	Gel	Gel	Gel
28	Phosphoric acid	Gel	Gel	Gel
29	Methanesulfonic acid	Mesylate Polymorph A*	Mesylate Polymorph A*	Gel
30	p-Toluene sulfonic acid	Gel	Gel	Gel
31	2,5-Dihydroxybenzoic acid	Gel	Gel	Gel

*solids obtained after 5° C. evaporation.

Characterization of Dibenzoyl-L-tartrate

Compound 2 dibenzoyl-L-tartrate Polymorph A was prepared by combining Compound 2 freebase with (-)-2,3-dibenzoyl-L-tartaric acid in n-heptane and showed crystallinity as characterized by XRPD in FIG. 36. The TGA/DSC data as shown in FIG. 37 indicate a weight loss of 30.5% up to 100° C. and broad endothermic signals before decomposition.

Characterization of Trimesate

Compound 2 trimesate Polymorph A was prepared by combining Compound 2 freebase with trimesic acid in n-heptane and showed crystallinity as characterized by XRPD in FIG. 38. The TGA/DSC data as shown in FIG. 39 indicate a weight loss of 0.8% up to 150° C. and multiple endothermic signals before decomposition.

Characterization of L-tartrate

Compound 2 L-tartrate Polymorph A was prepared by combining Compound 2 freebase with L-tartaric acid in n-heptane and showed crystallinity as characterized by XRPD in FIG. 40. The TGA/DSC data as shown in FIG. 41 indicate a weight loss of 4.0% up to 100° C. and multiple endothermic signals before decomposition.

Characterization of Mesylate

Compound 2 mesylate Polymorph A was prepared by combining Compound 2 freebase with methanesulfonic acid in n-heptane and showed crystallinity as characterized by XRPD in FIG. 42. The TGA/DSC data as shown in FIG. 43 indicate a weight loss of 5.9% up to 100° C. and irregular signals in the DSC curve.

Characterization of 4-acetamido Benzoate

Compound 2 4-acetamido benzoate Polymorph A was prepared by combining Compound 2 freebase with 4-acetamido benzoic acid in n-heptane and showed crystallinity as characterized by XRPD in FIG. 44. The TGA/DSC data as shown in FIG. 45 indicate a weight loss of 0.02% up to 150° C. and multiple endothermic signals before decomposition.

Example 3: Salts or Cocrystals of Compound 3

Preparation

Compound 3 freebase, as characterized via modulated DSC (mDSC), exhibits no glass transition signal. A weight loss of 1.2% was observed up to 200° C., and endotherms were observed at -44.1° C. and -29.9° C. (peak).

Similar to the process described in Example 1 or 2, to identify a crystalline salt form or cocrystal of Compound 3, screening was performed under 93 conditions using 31 acids and three solvent systems. 0.5 mL stock solutions of Compound 3 freebase (~40 mg/mL) was dispersed in selected solvent and corresponding salt former was added with a molar charge ratio of 1:1. The mixtures of freebase and the cofomer compound (e.g., an acid) were first transferred to temperature cycling from 50° C. to 5° C. for three cycles (heating rate of 4.5° C./min, cooling rate of 0.1° C./min) and then stored at 5° C. before analysis. If the samples were still clear, they would be subjected to slow evaporation at 5° C. to obtain gels. Resulting solids were isolated and analyzed.

Isolated crystal solids were characterized by X-ray powder diffraction (XRPD), thermo-gravimetric analysis (TGA) and differential scanning calorimetry (DSC), with proton nuclear magnetic resonance (¹H NMR) to confirm the free-base chemical structure and also potential co-existence with some organic acids. Exemplary data from the initial findings are summarized in Table 7.

TABLE 7

#	Acid	Solvent		
		n-Heptane	EtOAc	Toluene
1	Trimesic acid	Trimesate Type A	Acid	Trimesate Type A
2	Trimellitic acid	Acid	Acid	Acid
3	(-)-2,3-Dibenzoyl-L-tartaric acid	Gel	Gel	Gel
4	Fumaric acid	Gel	Gel	Gel
5	Terephthalic acid	Gel	Gel	Gel
6	Phthalic acid	Gel	Gel	Gel
7	Isophthalic acid	Acid	Acid	Acid
8	Benzoic acid	Gel	Gel	Gel
9	Cinnamic acid	Gel	Gel	Gel
10	4-Hydroxy benzoic acid	Gel	Gel	Gel
11	Salicylic acid	Gel	Gel	Gel
12	Adipic acid	Acid	Acid	Acid
13	Suberic acid	Acid	Gel	Acid
14	Sebacic acid	Acid	Acid	Acid
15	4-Acetamido benzoic acid	Acid	Acid	Acid
16	S-(+)-Mandelic acid	Gel	Gel	Gel
17	Orotic acid	Acid	Acid	Acid
18	Hexanoic acid	Gel	Gel	Gel
19	Citric acid	Gel	Gel	Gel
20	Acetic acid	Gel	Gel	Gel
21	Succinic acid	Acid	Gel	Gel
22	Malonic acid	Gel	Gel	Gel
23	(+)-Camphor-10-sulfonic acid	Gel	Gel	Gel
24	Nicotinic acid	Acid	Acid	Acid
25	(+)-L-tartaric acid	Gel	Gel	Gel
26	Hydrochloric acid	Gel	Gel	Gel
27	Sulfuric acid	Gel	Gel	Gel
28	Phosphoric acid	Gel	Gel	Gel
29	Methanesulfonic acid	Gel	Gel	Gel
30	p-Toluene sulfonic acid	Gel	Gel	Gel
31	2,5-Dihydroxybenzoic acid	Gel	Gel	Gel

Characterization of Trimesate

Compound 3 trimesate Polymorph A was prepared by combining Compound 3 freebase with trimesic acid in n-heptane and showed crystallinity as characterized by XRPD in FIG. 46. The TGA/DSC data as shown in FIG. 47 indicate a weight loss of 0.9% up to 200° C. and three endothermic peaks at 49.4° C., 100.2° C. and 129.2° C. (peak temperature) before decomposition. Polymorph B was obtained via temperature cycling in EtOH/n-heptane (1:19, v/v) from 50° C. to 5° C. with molar charge ratio (compound 3:trimesic acid) at 1:1, and showed crystallinity as characterized by XRPD in FIG. 48. The TGA/DSC data as shown in FIG. 49 indicate a weight loss of 5.4% up to 200° C. and two endothermic peaks at 239.9° C. and 257.5° C. before decomposition at 304.6° C. An ¹H NMR spectrum was collected using (CD₃)₂SO as the test solvent, and signals of trimesic acid and compound 3 were observed. See FIG. 50.

Example 4: Salts or Co-Crystals of MC3

Only one crystalline salt of MC3 (O,O-Dibenzoyl-L-Tartrate, abbreviated as "DBLT" hereafter) has been previously identified, and only one polymorph, Type A, has been discovered for the DBLT salt. An onset temperature of 69.8° C. in DSC analysis indicated a low melting point, however, not as low as the free base which is oil-like at room temperature. The crude free base has an HPLC purity of 88.6 area % and was used in the synthesis of the DBLT salt. Impurities are not rejected by the salt formation and the purity of the crystallized salt was found to be the same as the crude free base. Additional salt screening experiments were performed to identify new crystalline salts.

An oil-like MC3 free base with an HPLC purity of 97.6 area % ("purified free base") was used in the salt screening. A total of 24 acids and three solvent systems were screened. Crystalline salt hits were obtained with (+)-O,O-di-pivaloyl-D-tartaric acid (DPDT), (-)-O,O-di-pivaloyl-L-tartaric acid (DPLT), and trimesic acid.

Solvent Screening

A solvent screening was performed by reaction of free base and DPDT, DPLT and trimesic acid in 17 selected solvents to improve crystallinity and facilitate salt isolation and re-preparation. The X-ray powder diffraction (XRPD) results showed that crystalline trimesate Type A and B were obtained in ketones, esters and some other selected solvents from slurry at room temperature. For DPDT and DPLT salts, no suitable anti-solvent was found, only clear solutions were obtained during the solvent screening.

Based on the screening results, attempts were made to re-prepare trimesate Type A and B, but only trimesate Type A was successfully prepared at a 100-mg scale. Both polymorphs were further characterized using thermogravimetric analysis (TGA), differential scanning calorimetry (DSC), polarizing microscopy (PLM), dynamic vapor sorption (DVS), and HPLC. The characterization results of trimesate samples are summarized in Table 8. As the results show, trimesate Type A is anhydrous and non-hygroscopic.

TABLE 8

Salt form	Trimesate Type A		Trimesate Type B
	Prepared solvent	EtOAc	Cyclohexane
Scale, mg	100	100	10
Molar ratio (acid/FB) ^a	1.2	1.1	1.5
Speculated form ^b	Anhydrate	Anhydrate	N/A
HPLC purity (area %)	98.3	99.4 ^c	93.7
Weight loss (%)	1.9	0.3	8.0
Endotherm (° C., onset)	186.4	183.8	186.8
Hygroscopicity/purity decrease	Non-hygroscopic	N/A	N/A
Morphology	Aggregated of small particles (<20 μm)		
Appearance of solution in preparation	Suspension	Wax/emulsus	Wax/emulsus

N/A: not applicable or data not collected in this study.

^athe molar ratio (acid/FB) was determined by HPLC/IC.

^bresults speculated based on the preliminary thermal analysis data.

^caverage value of three sampling (100.0 area %, 99.34 area %, and 98.74 area %), suggesting the sample is inhomogeneous.

Hygroscopicity concluded using the water uptake up to 80% RH at 25° C.: <0.2% for non-hygroscopic.

Salt Screening

A total of 41 screening experiments were designed based on the free base pKa>8 and the solubility of MC3. Crystalline hits of trimesate (Type A), DPDT and DPLT salts were obtained.

In the 1st tier experiments, about 10 mg of MC3 free base and the corresponding acid were mixed, at a 1:1 molar ratio, into a 1.5-mL glass vial and 0.5 mL of n-heptane were then added. The mixtures were stirred at room temperature for about two days. If clear solutions were obtained, the samples were cooled at 5° C. or left to evaporate to induce solid formation. All the obtained solids were isolated by centrifugation and vacuum dried at room temperature for about 5 hours before being analyzed by X-Ray Powder Diffraction (XRPD). As summarized in Table 9, amorphous salts or acids were found under most of the conditions while potential crystalline forms were obtained with DPDT, DPLT, and trimesic acid.

To enhance the chance of crystallization during the 2nd tier screening, the concentration of free base was increased from 20 to 50 mg/mL when using the acids that yielded solutions in the 1st tier screening. Also, isopropyl alcohol/n-heptane (3:97, v/v) was used with those acids which

yielded crystalline acid in the 1st tier screening. As summarized in Table 10, no new crystalline hit was obtained.

Six more acids with structures closely related to trimesic acid were screened. The free base and the acids were mixed, at a 1:1 molar ratio, in EtOAc (free base loading 50 mg/mL) and the suspensions were then shaken at room temperature for about three days. The results are summarized in Table 11.

TABLE 9

No. Acid	Solid form	No. Acid	Solid form
1 Hexanoic acid	Amorphous ^a	10 (R)-(-)-Mandelic acid	Amorphous ^a
2 Fumaric acid	Acid	11 Benzyloxy lactic acid	Amorphous ^a
3 Adipic acid	Amorphous	12 (+)-O,O-Di-pivaloyl-D-tartaric acid	DPDT salt Type A ^a
4 Suberic acid	Acid	13 (-)-O,O-Di-pivaloyl-L-tartaric acid	DPLT salt Type A ^a
5 Sebacic acid	Acid	14 Terephthalic acid	Acid
6 Alginic acid	Amorphous ^a	15 Trimesic acid	Acid + new peaks ^c
7 Cinnamic acid	Amorphous ^a	16 4-Hydroxy benzoic acid	Acid
8 Benzoic acid, 4-acetamido	Acid	17 2-(4-Hydroxybenzoyl)-benzoic acid	Amorphous ^a

TABLE 9-continued

No. Acid	Solid form	No. Acid	Solid form
9 (S)-(+)-Mandelic acid	Amorphous ^a	18 (+)-2,3-Dibenzoyl-D-tartaric acid	DBDT salt Type A ^b

^aclear solution was observed after slurry at room temperature (RT) and 5° C., which was then transferred to slow evaporate at RT.

^bobtained in a previous experiment with no obvious purity improvement.

^cnew peaks conformed to trimesate Type A.

TABLE 10

No.	Acid	Solvent	Solid form
1	Hexanoic acid	n-Heptane	N/A
2	Alginic acid		N/A
3	Cinnamic acid		N/A
4	(S)-(+)-Mandelic acid		N/A
5	R)-(-)-Mandelic acid		N/A
6	Benzyloxy lactic acid		N/A
7	(+)-O,O-Di-pivaloyl-D-tartaric acid		N/A

TABLE 10-continued

No.	Acid	Solvent	Solid form
8	(-)-O,O-Di-pivaloyl-L-tartaric acid		N/A
9	2-(4-Hydroxybenzoyl)-benzoic acid		N/A
10	Fumaric acid	IPA/H ₂ O	Acid
11	Adipic acid	(3:97, v/v)	Amorphous
12	Suberic acid		Acid
13	Sebacic acid		Acid
14	Benzoic acid, 4-acetamido		Acid
15	Terephthalic acid		Acid
16	Trimesic acid		Acid
17	4-Hydroxy benzoic acid		Acid
—	—	—	—

N/A: clear solution was observed after slurry at RT and 5° C..

TABLE 11

No.	Acid	Solvent	Solid form
1	1,2,4-Trimellitic acid	EtOAc	Amorphous
2	Phthalic acid		Amorphous
3	Isophthalic acid		Amorphous
4	Terephthalic acid		Acid
5	Orotic acid		Acid + new peaks*
6	1,2,3-Benzene tricarboxylic acid		Amorphous

*only amorphous was observed in the re-preparation experiment.

Optimization of Solvent Systems

A solvent screening was performed to select an optimal solvent system for re-preparation of the salt hits and to improve crystallinity. The free base was mixed in a 1:1 molar ratio, with DPDT, DPLT, and trimesic acid in 17 selected solvents. Trimesate Type A and B polymorphs were isolated from slurries in several solvents (see Table 12). DPDT and DPLT salts were not obtained as solids from any solvent. In addition, the samples containing tetrahydrofuran (THF)/H₂O, THF, cyclohexane and 1,4-dioxane were freeze-dried, but no crystalline solid was obtained.

TABLE 12

Form	Acid			
	Solvent	DPDT	DPLT	Trimesic acid
1	Acetone	N/A*	N/A*	Trimesate Type A
2	Methyl isobutyl ketone (MIBK)	N/A	N/A	Trimesate Type A
3	Methyl ethyl ketone (MEK)	N/A	N/A	Trimesate Type A
4	CH ₂ Cl ₂	N/A	N/A	Acid
5	Methyl tert-butyl ether (MTBE)	N/A	N/A	Trimesate Type A
6	2-Methyl tetrahydrofuran (2-MeTHF)	N/A	N/A	N/A
7	Tetrahydrofuran (THF)	N/A*	N/A*	N/A
8	Anisole	N/A	N/A	Trimesate Type A
9	1,4-Dioxane	N/A*	N/A*	N/A
10	EtOAc	N/A	N/A	Trimesate Type A
11	Isopropyl acetate (IPAc)	N/A	N/A	Trimesate Type A
12	Acetonitrile (CAN)	N/A*	N/A*	N/A
13	MeOH	N/A*	N/A*	N/A
14	Isopropyl alcohol (IPA)	N/A*	N/A*	N/A
15	Cyclohexane	N/A	N/A	Trimesate Type A
16	Xylene	N/A	N/A	N/A
17	Toluene	N/A	N/A	Trimesate Type B

N/A: clear solution was obtained after slurry at RT and 5° C..

*about 0.2-0.3 mL of H₂O was added into the clear solution to induce precipitation and emulsion was obtained.

Preparation of Trimesate Polymorphs (100 mg Scale)

Heating and cooling experiments were carried out at 100-mg scale to improve crystal morphology and chemical purity. Trimesate Type A polymorph was successfully re-prepared in cyclohexane and EtOAc following the procedure detailed below.

Preparation of Trimesate Type A Polymorph:

A 5 mL vial was charged with 100.0 mg of the free base (97.6 area %) and 30 mg of trimesic acid and 2 mL of cyclohexane or EtOAc, were added. The suspension was stirred at room temperature for about 0.5 h. The solution was continued to be stirred while being heated and cooled between 5° C. and 50° C. for two cycles with a 4.5° C./min heating rate and a 0.1° C./min cooling rate. The resulting solid was isolated by centrifugation and dried under vacuum at room temperature for 2 hours before characterization.

Preparation of Trimesate Type B Polymorph:

About 10 mg of free base and trimesic acid were mixed, at a 1:1 molar ratio, in a 1.5-mL glass vial. n-Heptane (0.5 mL) was added. The mixtures were magnetically stirred at RT for about two days. If clear solutions were obtained, the samples were cooled at 5° C. or left to evaporate to induce solid formation. All the obtained solids were isolated by centrifugation and vacuum dried at RT for about 5 hours before being analyzed by XRPD.

Characterization of Trimesate Polymorphs

Both trimesate Type A (100-mg scale) and Type B (10-mg scale) were characterized, and results are summarized in Table 8.

The XRPD pattern of polymorph A is shown in FIG. 52. TGA/DSC curves of trimesate Type A polymorph prepared with cyclohexane, displayed in FIG. 53, shows a weight loss of 0.3% before 120° C. and a sharp melting endotherm at 183.8° C. (onset temperature). The TGA/DSC curves of trimesate Type A polymorph prepared with EtOAc displayed in FIG. 54, shows a weight loss of 1.9% before 120° C. and a sharp melting endotherm at 186.4° C. (onset temperature). Agglomerate and small particles (<20 μm) were observed in the trimesate Type A polymorphs. See FIGS. 55 and 56. The XRPD pattern of trimesate Type B polymorph is shown in FIG. 59. TGA/DSC curves displayed in FIG. 60 show a weight loss of 8.0% before 150° C. and a sharp melting endotherm at 186.8° C. (onset temperature). As shown in FIG. 61, agglomerate particles with small size (<20 μm) are observed in trimesate Type B sample.

As the DVS result shows, the trimesate Type A polymorph is non-hygroscopic. See FIG. 57. The hygroscopicity of free base (crude and pure) was determined as well. The crude free base was slightly hygroscopic (0.27 and 0.24% water uptake at 80% relative humidity for the desorption and adsorption isotherms, respectively), but the pure free base was non-hygroscopic (0.17 and 0.14% water uptake at 80% relative humidity for the desorption and adsorption isotherms, respectively).

HPLC Purity of Trimesate Type A

Trimesate Type A samples were prepared according to the procedure described in the foregoing, using the crude free base (HPLC purity of 88.5 area %) or purified free base (HPLC purity of 97.6 area %) as starting material, and analyzed by HPLC. The results of the HPLC purity analysis for the samples prepared with crude and purified free base are summarized in Tables 13 and 14, respectively. No significant HPLC purity change was observed for both samples after the DVS experiment.

TABLE 13

Sample	Solvent/ scale (mg)	Imp 1 (RRT 0.08)	Imp 2 (RRT 0.50)	Imp 3 (RRT 0.51)	Imp 4 (RRT 0.52)	Imp 5 (RRT 0.53)	Imp 6 (RRT 0.90)
Free base	N/A	0.11	0.22	<0.05	0.34	0.44	1.74
Trimesate	EtOAc/100	<0.05	4.18	1.38	<0.05	<0.05	1.96
Type A	Cyclohexane/ 100	<0.05	<0.05	<0.05	<0.05	<0.05	1.91

Sample	Solvent/ scale (mg)	Imp 7 (RRT 0.91)	Imp 8 (RRT 0.99)	Imp 9 (RRT 1.04)	Imp 10 (RRT 1.06)	Imp 11 (RRT 1.14)	Area (%)
Free base	N/A	0.16	0.36	5.02	0.28	2.74	88.6
Trimesate	EtOAc/100	<0.05	<0.05	3.78	<0.05	3.31	85.38
Type A	Cyclohexane/ 100	<0.05	<0.05	4.45	<0.05	3.97	89.66

TABLE 14

Sample	Solvent/ scale (mg)	Imp 1 (RRT 0.58)	Imp 2 (RRT 1.04)	Imp 3 (RRT 1.14)	Area(%)
Free base	N/A	0.99	1.41	<0.05	97.60
Trimesate	EtOAc/100	<0.05	1.04	0.68	98.28
Type A	Cyclohexane/ 100	<0.05	<0.05	<0.05	100.00
		<0.05	1.26	<0.05	98.74 (av.)
		<0.05	0.66	<0.05	99.34

The entire disclosure of each of the patent documents and scientific articles referred to herein is incorporated by reference for all purposes.

The invention can be embodied in other specific forms without departing from the spirit or essential characteristics thereof. The foregoing embodiments are therefore to be considered in all respects illustrative rather than limiting on the invention described herein. Scope of the invention is thus indicated by the appended claims rather than by the foregoing description, and all changes that come within the meaning and range of equivalency of the claims are intended to be embraced therein.

The invention claimed is:

1. A salt or cocrystal of heptadecan-9-yl 8-((2-hydroxyethyl)(6-oxo-6-(undecyloxy)hexyl)amino)octanoate ("Compound 2").

2. The salt or cocrystal of claim 1, wherein the salt or cocrystal is a salt or cocrystal of Compound 2 and a compound selected from the group consisting of trimesic acid, (-)-2,3-dibenzoyl-L-tartaric acid, 4-acetamido benzoic acid, (+)-L-tartaric acid, and methanesulfonic acid.

3. The salt or cocrystal of claim 1, wherein the salt or cocrystal exhibits an X-ray powder diffraction pattern obtained using CuK α radiation having peaks with 2-theta values substantially in accordance with FIG. 36, 38, 40, 42, or 44.

4. The salt or cocrystal of claim 1, wherein the salt or cocrystal exhibits a differential scanning calorimetry thermogram substantially in accordance with the DSC profile shown in FIG. 37, 39, 41, 43, or 45.

5. The salt or cocrystal of claim 1, wherein said salt or cocrystal is substantially free of impurities.

6. The salt or cocrystal of claim 1, being an anhydrate, a solvate, or a hydrate.

7. The salt or cocrystal of claim 1, wherein the stoichiometry of Compound 2 and the compound selected from the group consisting of trimesic acid, (-)-2,3-dibenzoyl-L-tartaric acid, 4-acetamido benzoic acid, (+)-L-tartaric acid, and

methanesulfonic acid is within the range of from about 1:0.2 mol/mol to about 1:5 mol/mol.

8. The salt or cocrystal of claim 1, wherein the stoichiometry of Compound 2 and the compound selected from the group consisting of trimesic acid, (-)-2,3-dibenzoyl-L-tartaric acid, 4-acetamido benzoic acid, (+)-L-tartaric acid, and methanesulfonic acid is about 1:1 mol/mol.

9. The salt or cocrystal of claim 1, wherein the salt or cocrystal is a salt or cocrystal of Compound 2 and trimesic acid.

10. The salt or cocrystal of claim 9, wherein the salt or cocrystal exhibits an X-ray powder diffraction pattern obtained using CuK α radiation having peaks with 2-theta values substantially in accordance with FIG. 38.

11. The salt or cocrystal of claim 9, wherein the salt or cocrystal exhibits a differential scanning calorimetry thermogram substantially in accordance with the DSC profile shown in FIG. 39.

12. The salt or cocrystal of claim 9, wherein the salt or cocrystal exhibits an X-ray powder diffraction pattern obtained using CuK α radiation having two characteristic peaks expressed in degrees 2-theta (+/-0.2) selected from the group consisting of 3.4, 6.8, 10.2, 20.5, and 23.8.

13. The salt or cocrystal of claim 9, wherein the salt or cocrystal exhibits an X-ray powder diffraction pattern obtained using CuK α radiation having three characteristic peaks expressed in degrees 2-theta (+/-0.2) selected from the group consisting of 3.4, 6.8, 10.2, 20.5, and 23.8.

14. The salt or cocrystal of claim 9, wherein the salt or cocrystal exhibits an X-ray powder diffraction pattern obtained using CuK α radiation having four characteristic peaks expressed in degrees 2-theta (+/-0.2) selected from the group consisting of 3.4, 6.8, 10.2, 20.5, and 23.8.

15. The salt or cocrystal of claim 9, wherein the salt or cocrystal exhibits an X-ray powder diffraction pattern obtained using CuK α radiation having characteristic peaks expressed in degrees 2-theta (+/-0.2) at 3.4, 6.8, 10.2, 20.5, and 23.8.

16. The salt or cocrystal of claim 1, wherein the salt or cocrystal is a salt or cocrystal of Compound 2 and (-)-2,3-dibenzoyl-L-tartaric acid, and wherein the salt or cocrystal exhibits an X-ray powder diffraction pattern obtained using CuK α radiation having two characteristic peaks expressed in degrees 2-theta (+/-0.2) at 6.1 and 9.1.

17. The salt or cocrystal of claim 1, wherein the salt or cocrystal is a salt or cocrystal of Compound 2 and (+)-L-tartaric acid, and wherein the salt or cocrystal exhibits an X-ray powder diffraction pattern obtained using CuK α

radiation having two characteristic peaks expressed in degrees 2-theta (± 0.2) at 5.4 and 8.1.

18. The salt or cocrystal of claim 1, wherein the salt or cocrystal is a salt or cocrystal of Compound 2 and methanesulfonic acid, and wherein the salt or cocrystal exhibits an X-ray powder diffraction pattern obtained using $\text{CuK}\alpha$ radiation having two characteristic peaks expressed in degrees 2-theta (± 0.2) selected from the group consisting of 4.0, 11.4, 11.8, and 19.8.

19. The salt or cocrystal of claim 1, wherein the salt or cocrystal is a salt or cocrystal of Compound 2 and methanesulfonic acid, and wherein the salt or cocrystal exhibits an X-ray powder diffraction pattern obtained using $\text{CuK}\alpha$ radiation having three characteristic peaks expressed in degrees 2-theta (± 0.2) selected from the group consisting of 4.0, 11.4, 11.8, and 19.8.

20. The salt or cocrystal of claim 1, wherein the salt or cocrystal is a salt or cocrystal of Compound 2 and methanesulfonic acid, and wherein the salt or cocrystal exhibits an X-ray powder diffraction pattern obtained using $\text{CuK}\alpha$ radiation having four characteristic peaks expressed in degrees 2-theta (± 0.2) at 4.0, 11.4, 11.8, and 19.8.

* * * * *

UNITED STATES PATENT AND TRADEMARK OFFICE
CERTIFICATE OF CORRECTION

PATENT NO. : 11,203,569 B2
APPLICATION NO. : 16/493789
DATED : December 21, 2021
INVENTOR(S) : Almarsson et al.

Page 1 of 2

It is certified that error appears in the above-identified patent and that said Letters Patent is hereby corrected as shown below:

In the Claims

At Column 47, Claim number 3, Line number 51:
“The salt or cocrystal of claim 1, wherein said salt or”
Should read:
--The salt or cocrystal of claim 2, wherein said salt or--

At Column 47, Claim number 3, Line number 54:
“values substantially in accordance with FIG. 36, 38, 40, 42”
Should read:
--values substantially in accordance with Figure 36, 38, 40, 42--

At Column 47, Claim number 4, Line number 56:
“The salt or cocrystal of claim 1, wherein the salt or”
Should read:
--The salt or cocrystal of claim 2, wherein the salt or--

At Column 47, Claim number 4, Line number 59:
“shown in FIG. 37, 39, 41, 43, or 45.”
Should read:
--shown in Figure 37, 39, 41, 43, or 45.--

At Column 47, Claim number 7, Line number 64:
“The salt or cocrystal of claim 1, wherein the stoichi-”
Should read:
--The salt or cocrystal of claim 2, wherein the stoichi- --

At Column 48, Claim number 8, Line number 21:
“The salt or cocrystal of claim 1, wherein the stoichi-”

Signed and Sealed this
Fifteenth Day of March, 2022



Drew Hirshfeld
*Performing the Functions and Duties of the
Under Secretary of Commerce for Intellectual Property and
Director of the United States Patent and Trademark Office*

Should read:

--The salt or cocrystal of claim 2, wherein the stoichi--

At Column 48, Claim number 9, Line number 26:

“The salt or cocrystal of claim 1, wherein the salt or”

Should read:

--The salt or cocrystal of claim 2, wherein the salt or--

At Column 48, Claim number 10, Line number 33:

“values substantially in accordance with FIG. 38.”

Should read:

--values substantially in accordance with Figure 38.--

At Column 48, Claim number 11, Line number 37:

“shown in FIG. 39.”

Should read:

--shown in Figure 39.--

At Column 48, Claim number 16, Line number 58:

“The salt or cocrystal of claim 1, wherein the salt or”

Should read:

--The salt or cocrystal of claim 2, wherein the salt or--

At Column 48, Claim number 17, Line number 64:

“The salt or cocrystal of claim 1, wherein the salt or”

Should read:

--The salt or cocrystal of claim 2, wherein the salt or--

At Column 49, Claim number 18, Line number 3:

“The salt or cocrystal of claim 1, wherein the salt or”

Should read:

--The salt or cocrystal of claim 2, wherein the salt or--

At Column 49, Claim number 19, Line number 10:

“The salt or cocrystal of claim 1, wherein the salt or”

Should read:

--The salt or cocrystal of claim 2, wherein the salt or--

At Column 49, Claim number 20, Line number 17:

“The salt or cocrystal of claim 1, wherein the salt or”

Should read:

--The salt or cocrystal of claim 2, wherein the salt or--